# STUDY ON OPEN-CYCLE DESICCANT DEHUMIDIFICATION AND AIR CONDITIONING FOR DRYING OF AGRICULTURAL PRODUCTS

シャジア, ハニフ

# STUDY ON OPEN-CYCLE DESICCANT DEHUMIDIFICATION AND AIR CONDITIONING FOR DRYING OF AGRICULTURAL PRODUCTS

**SHAZIA HANIF**

**September 2018**

Department of Energy and Environmental Engineering
Interdisciplinary Graduate School of Engineering Sciences

**KYUSHU UNIVERSITY**

**JAPAN**

# STUDY ON OPEN-CYCLE DESICCANT DEHUMIDIFICATION AND AIR CONDITIONING FOR DRYING OF AGRICULTURAL PRODUCTS

A THESIS SUBMITTED IN PARTIAL FULFILLMENT OF THE REQUIREMENTS FOR THE AWARD OF THE DEGREE OF

**DOCTOR OF ENGINEERING (Dr. Eng.)**

By

**SHAZIA HANIF**

**September 2018**

Supervisor

**Prof. Takahiko Miyazaki**

Department of Energy and Environmental Engineering
Interdisciplinary Graduate School of Engineering Sciences

**KYUSHU UNIVERSITY**

**JAPAN**

# DECLARATION

I hereby declare that the work, which is being presented in the thesis entitled *"**Study on open-cycle desiccant dehumidification and air conditioning for drying of agricultural products**"* submitted in partial fulfillment of the requirements for the award of the degree of Doctor of Engineering (Dr. Eng.), Interdisciplinary Graduate School of Engineering Sciences, Kyushu University, Japan is an authentic record of my own research work.

The research work presented in the thesis has not been submitted by me for the award of any other degree in this or any other university.

**Shazia Hanif**

September 2018

# Acknowledgment

*ALLAH the Almighty never spoils any effort. Every piece of work is rewarded according to the nature of devotion. I invoke ALLAH' blessings, peace for His Holy Prophet "MUHAMMAD" (Peace Be Upon Him), the messenger of ALLAH, the most perfect and exalted among and of even born.*

*The work presented in this thesis was accomplished under the inspiring guidance and dynamic supervision of honorable* ***Prof. Takahiko Miyazaki*** *(Supervisor). I express my deepest sense of gratitude and indebtedness to him for his precious guidance and inspiration throughout this research work.*

*I am also beholden to* ***Research Prof. Shigeru Koyama*** *for his encouragement and valuable assistance.*

*I am also indebted to* ***Prof. Takahiko Miyazaki****,* ***Associate Prof. Osama Eljamal*** *and* ***Associate Prof. Hooman Farzaneh*** *for evaluating this work and for their valuable comments and questions.*

*I express my gratitude to* ***Dr. Muhammad Sultan*** *for his valuable assistance, encouragement and guidance in my research.*

*I am thankful to all of my laboratory members and staff for their help and cooperation.*

*I would also like to thanks* ***Schlumberger Foundation Faculty for the Future*** *for providing the scholarship and all the facilities required in this study.*

*I am grateful to all of my teachers, friends, well-wishers and colleagues for their kind support and motivation during this study.*

*I express my humble obligation to my affectionate and loving Parents, Brothers, Sisters and brother In-Laws for their love, inspiration and prayers for me. In particular, I am thankful and would like to express my high appreciation to my Father* ***Muhammad Hanif (Late)****, Mother* ***Hanifan Bibi****, Brothers* ***Dr. Muhammad Imran, Muhammad Irfan Zaib*** *and Sisters* ***Dr. Kousar Naeem****,* ***Aysha Imran*** *and* ***Sumaira Hanif*** *for all their prayers, motivation, and for everything they have done for me.*

*Finally, I dedicate my PhD thesis to my Father* ***Muhammad Hanif*** *who wished to see me as* ***Dr. Shazia Hanif*** *but left me alone during my PhD studies; Dear Dad! I love you and miss you forever.*

***Shazia Hanif***

# CONTENTS

# SUMMARY

High growth rate in world population has doubled the liability on agriculture sector to meet the challenges in food security. It is required to develop better genetics of the crop seeds as well as energy conservative drying system followed by safe storage. In drying process, air conditions, temperature and relative humidity affects the quality of the drying product. High temperature drying causes loss of nutrients and vitamin C, found in agricultural products. In addition to higher drying air temperature, higher humidity also affects the color and quality of the drying product. Due to the complex structure of biological product, convective drying mechanism complete in two phases, known as constant and falling-drying rate. During constant drying rate, water is removed from the surface of the product whereas during falling drying rate, water is removed from inside of the product. Usually, falling-drying rate is more energy intensive and sometime give rise to over dry or even burn the surface of the product. This problem is addressed with the development of drying system that creates more pressure deficit by dehumidification of air to increase the moisture carrying capacity of the air. In this regard desiccant drying system provides its best applicability for low temperature and quality drying. This study focuses on low-temperature drying of agricultural produce, steady state desiccant-drying, dynamics of adsorption-drying and comparison with conventional-drying system. In addition, to change in effective thermal conductivity at different relative humidity, attributed to change in heat transfer coefficient is also discussed. The key features of the study are highlighted as follows:

The need for drying agricultural produce, drying mechanism and the degradation factors are discussed in chapter one. While chapter two, accounts for the review of literature in detail about desiccant drying technologies including bed type, wheel type and liquid desiccant system. A brief review about some other drying technologies including; convective drying, freeze drying, microwave and vacuum drying is also indicated. Out of these technologies; freeze drying, microwave and vacuum drying are regarded as best as they maintain the good quality of the products. It is due the fact that these technologies ensure volumetric heating and fast drying while limiting shrinkage of the product. However, their

cost of energy is high, overall efficiency is low and it is difficult to control the product temperature in some cases. On the other hand, desiccant drying technology provides energy efficient system and also reduces thermal degradation. In addition, a brief review about hybrid drying with its potential to make significant progress in industrial drying is also mentioned. These systems (integration of desiccant and other drying technologies) give better solutions with special focus on the quality and quantity of drying product.

The chapter three illustrates the steady state investigation of desiccant drying system (DDS) for the drying of cereals grain at low temperature and lower humidity. The performance of two drying approaches with two desiccant materials i.e. silica gel and lithium chloride (LiCl) have been analyzed by a desiccant dehumidification model as presented in literature. Case-I deals with the drying of cereals grain without heating at various levels of humidity ratio of processed air. Whereas Case-II deals with the dehumidification of the ambient air at certain levels, then heating the processed air up to safe temperature limit. Case I results showed that, by increasing the regeneration temperature moisture, the carrying capacity of the air increases, however at the expense of elevated energy. In Case-I, drying air conditions found effective for seed drying as drying air temperature does not exceed the recommended drying temperature limit of the seed. Case-II gives more economical and energy saving drying solution as compared to Case I, however, it is suitable for commercial purpose drying, because temperature rises little higher than the safe limit.

In contrary to steady state, chapter four characterizes the drying kinetic of freshly harvested wheat grains in order to reduce the moisture to an optimum level. A comparison of desiccant drying has been made with the conventional method in terms of drying kinetics, allowable time for safe storage, the total time for drying cycle, and overall energy consumption. It has been found that the proposed desiccant drying system provides high drying rate and allows higher time for the safe storage. As the desiccants possess water adsorbing ability by means of vapor pressure deficit, therefore, the desiccant system successfully provided low-temperature drying which ensures the quality of wheat grains. It could be useful not only for domestic drying applications but also for industrial applications. Upon comparison with conventional drying methods, it has been found that the proposed drying system is not only useful for providing quick and low-temperature drying but also helps in overall energy saving. The performance index of desiccant drying system is found

higher than the conventional system at drying temperatures. Overall energy consumption required for desiccant system is less as compared to conventional drying energy at all drying temperatures. This Study has been very useful to develop a low-cost and sustainable drying technology for various agricultural products.

In chapter five, the effect of relative humidity on the effective thermal conductivity of the desiccant materials is demonstrated Change in effective thermal conductivity is attributed to the change in heat transfer coefficient, which influences the performance of the systems. Most of the adsorbents are porous in nature and therefore adsorption uptake is affected due to monolayer/multilayer configuration, that results into different ETC at different operating conditions i.e. temperature and relative humidity (RH). Consequently, present study, experimentally investigates the RH effect on the thermal conductivity of the commercially available zeolite-based adsorbents, which are commercially named as: AQSOA-Z02 (zeolite-1) and AQSOA-Z05 (zeolite-2). The study is useful for the researchers who are working in the field of adsorption cooling, air-conditioning and desalination. In this regard, an experimental setup was developed by which the ETC was measured at different levels of RH. According to the results, the ETC of oven dried zeolite-1 and zeolite-2 was 0.060 W m-1 K-1 and 0.066 W m-1 K-1, respectively. With the increase in RH, the numerical value of ETC increases up to 0.090 W m-1 K-1 for zeolite-1 and 0.089 W m-1 K-1 zeolite-2. Moreover, the empirical relation is proposed which can estimate ETC at different levels of RH for both adsorbents.

The present work concludes that desiccant drying should considered on top priority for drying of agricultural produce as DDS not only provides low temperature drying for temperature sensitive products but also reduce the total drying time. The basic principle is to create vapor pressure deficit between the product and environment hence accelerate the moisture removal. Present study illustrates the energy consumption for two different desiccant drying approaches i.e. latent load control and both latent and sensible load control. The choice of approach depends on the purpose of end use e.g. seed or commercial use. It is also concluded that the performance of desiccant system is affected by the change in relative humidity (RH). As change in RH causes to change in effective thermal conductivity (ETC) of the desiccant material attributed to change in heat transfer coefficient.

# LIST OF FIGURES

## Chapter 1



## Chapter 2

## Chapter 3

## Chapter 4



## Chapter 5

# LIST OF TABLES

# CHAPTER 1

# BACKGROUNG OF THE STUDY

# Chapter 1

# BACKGROUND OF THE STUDY

This chapter addresses the need of drying and storage of agricultural products as well as it describes the effect of temperature and relative humidity on the quality of the drying product. Due to the complex structure of biological product, drying mechanism; constant and falling drying rate are discussed concerning the energy consumption. Type of degradations and quality degradation parameters are explained in details as motivation towards the use of desiccant drying system.

## 1.1 Introduction

Increased in world population, doubled the liability on agriculture sector to ensure the physical, social and economic access to sufficient safe and nutritious food for all people. In order to feed the world's growing population and to meet the challenges in food security, it is required to develop a better genetics of the crop seeds and energy conservative drying system followed by safe storage. The basic purpose of the storage of agricultural produce is to make sure the availability for domestic, industrial and animal feed consumption, throughout the year. As at the time of harvest huge quantity of agricultural produce available which may last only for few weeks, that's why must be dried and stored carefully. It is important to mention that one of the basic purposes of storage is also to provide agricultural produce for export. As in a market during off-season the value of any surplus agricultural produce tends to rise.

Agricultural crops are harvested at higher moisture content than the safe storage level due to the disclosure of quantitative and qualitative losses. Therefore it is important to complete harvesting as soon as possible. Figure 1 represents the different factors directly or indirectly affect the total produce of harvested crop (Kumar and Kalita 2017). Initial growing crop has more moisture, it start decreasing as crop approaches to its maturity, but still it is higher than the safe storage level.

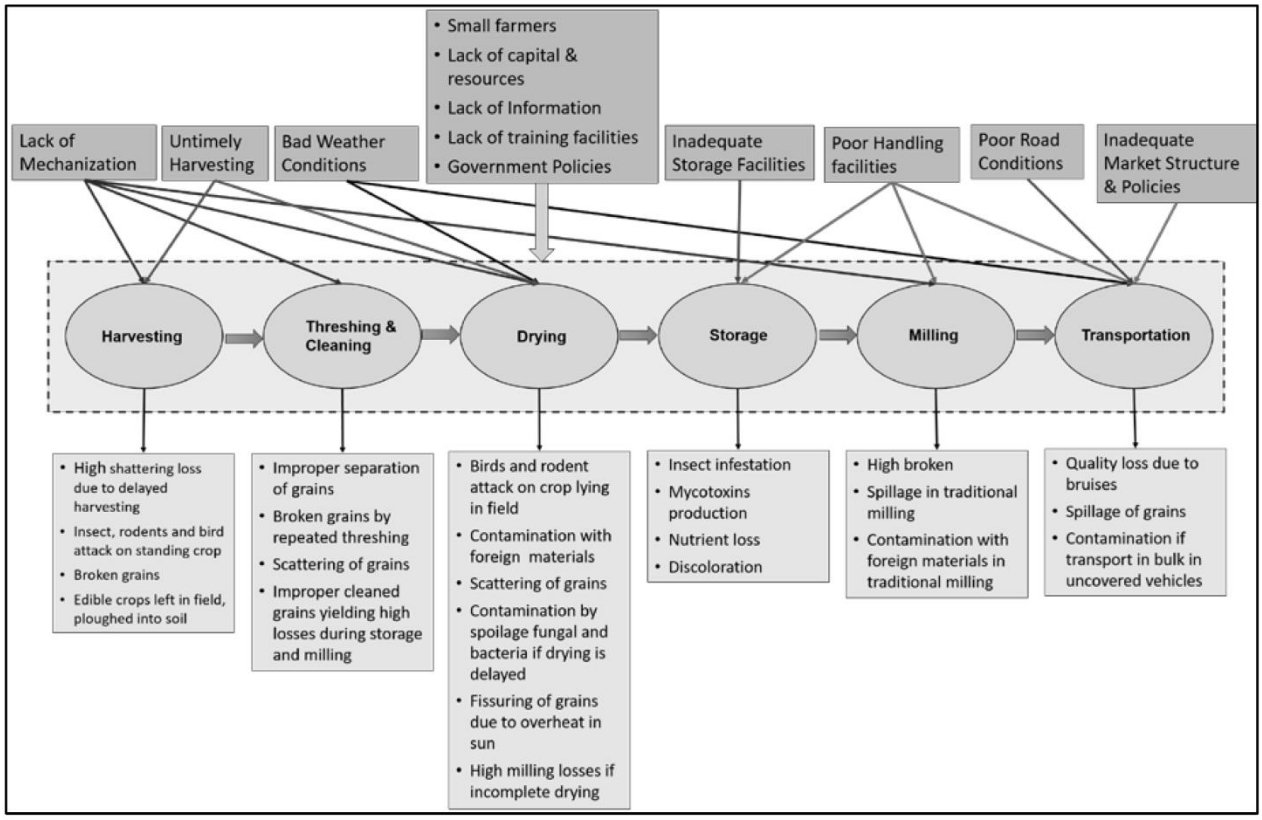


**Figure 1.1** Various factors and types of losses during the supply chain of cereal crops in developing countries (Kumar and Kalita 2017).

Different crops have different moisture content at various stages of maturity e.g. paddy, maize, sorghum, beans, groundnut and sunflower have moisture content 22-28, 23-28, 20-25, 30-40, 30-35 and 9-10 percentage, respectively. This moisture content starts to equilibrate with the environmental condition. One of the major factors affecting the successful storage of agricultural produce is the moisture content. As high moisture content activate the fungal and insect growth in the crop. The relative humidity also known as water activity is defined as the ratio of the partial pressure of water over the wet solid system to the equilibrium vapor pressure of water at the same temperature.

$$a_w = \frac{p}{p_w} = \frac{RH}{100} \tag{1.1}$$

where $a_w$, $p$ and $p_w$ are water activity, partial pressure of water and standard state partial vapor pressure of water, respicyively. Figure 1.2 represents the minimum water activity, for microbial growth and spore germination and deterioration rates as a function of water activity for food systems

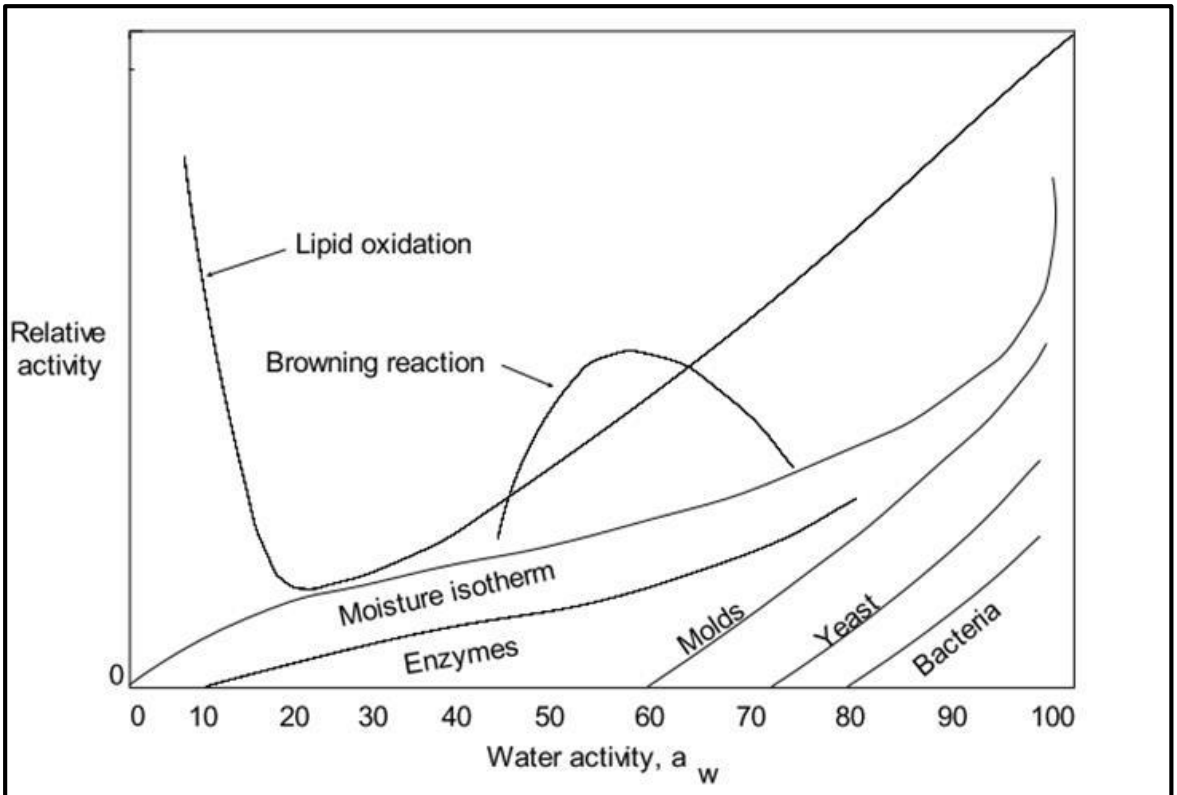


| Micro-organism | Water activity |
|---|---|
| Organisms producing slime on meat | 0.98 |
| *Pseudomonas, Bacillus cereus* spores | 0.97 |
| *B. subtilis, C. botulinum* spores | 0.95 |
| *C. botulinum, Salmonella* | 0.93 |
| Most bacteria | 0.91 |
| Most yeast | 0.88 |
| *Aspergillus niger* | 0.85 |
| Most molds | 0.80 |
| Halophilic bacteria | 0.75 |
| Xerophilic fungi | 0.65 |
| Osmophilic yeast | 0.62 |

**Figure 1.2** Water activity effect on spoilage of food (Sachin V.Jangam et al. 2010).

The other factor which effects the storage of agricultural produce is temperature, which is the product of respiration reaction. Another effect of higher temperature is to accelerate the activity of insect and fungal problems. With lower temperatures, the metabolic rate of insects and fungi decreases consequently spoilage decreases. By providing the aeration in storage helps to decrease the rate of respiration, thereby lengthening the storage life by lessening the possibility of germination. In general, under ideal condition, the shelf

life of a food product can be predicted based on microbial growth equations (Fu and Labuza, 1993)

$$N = N_0 \exp[k(t - t_L)] \quad (1.2)$$

$$t_s = \frac{\ln\left(\frac{N_S}{N_0}\right)}{k + t_L} \quad (1.3)$$

where $N_0$, $N$, $t$, $N_s$, $t_s$, $k$ and $t_L$ are the initial microbial load, microbial level at time t, microbial level at the end of shelf life, shelf life at constant temperature, specific growth rate and lag time at constant temperature, respectively. Therefore an efficient storage system helps to maintain the produce of crop as long as possible without any deterioration. The storage and handling methods should minimize losses, but must also be appropriate in relation to other factors, such as economies of scale, labor cost and availability, building costs and machinery cost.

## 1.2 Insights of drying

Drying is a key technology to preserve agricultural produce. It is a process by which the availability of off-season food products and their nutritional content is ensured All agricultural products are very complex materials and undergoes various physical and biochemical processes e.g. shrinkage due to loss of moisture during drying, change of temperature due to evaporation of moisture and high temperature drying, change in structure of cellular structure, quality loss due to heat sensitive nutrient compounds. Drying at low temperature will be preferable for obtaining dry products with high product quality, but the driving force for moisture migration is limited in such process.

Combine effect of temperature and water activity on microbial growth can be determined from equation (Davey, 1989).

$$ln\, k = C_0 + \frac{C_1}{T} + \frac{C_2}{T^2} + C_3 a_w + C_4 {a_w}^2 \quad (1.4)$$

where $C_0$ to $C_4$, are the five coefficients to be determined by multiple-linear regression. $a_w$ is the water activity and T is temperature.

The degradation of a nutrient during drying process can be can be expressed by: (Benali, 2004).

Degradation rate = $\frac{d[N]}{dt} = -k([N]_0 - [N]_x)$ (1.5)

$$k = k_0 exp^{\frac{-E_a}{RT}} \quad (1.6)$$

where $[N]_0$, $[N]_x$, $k$, $Ea$, $R$, and $T$ are the initial concentration of nutrient, final concentration of the nutrient, degradation rate constant, activation energy and universal gas constant, respectively.

In addition, the exchange of heat and mass with the surrounding airflow plays an important role in the drying kinetics, particularly for convective drying processes. The drying process becomes even more complex when the fruits are composite materials. The cereal grains have complex structure and composed of different layers as shown in Figure 1.3 that's why convective drying of cereals accomplished by two phase i.e. constant rate and falling rate period (Fournier and Guinebault 1995) Initially moisture at the top layer is removed and this is considered as the faster drying rate and uses a less amount of energy. In case of second phase, the interior moisture of the product migrates to the surface and then it is dried by passing through the hot air. The second phase is slower than first phase and consumes more energy. Belessiotis and Delyannis (2011) introduced one more process called third phase for hygroscopic material. However, not so many products go to this third phase.

To avoid the degradation and damage of the product, some products like (food, pharma and some high heat sensitive products) are not advisable to dry at high temperature. The drying time depend on the drying condition and the product nature.

## 1.3 Motivation of the study and originality

Drying conditions are very important regarding the quality of the drying product. Drying conditions may cause poor quality e.g. various degrees of browning, shrinkage, loss of nutrients, and so on. Mainly food stuff experience three types of degradation: physical, chemical and nutritional. In physical degradation, rehydration, solubility, texture and aroma loss are included. In chemical degradation browning reaction, lipid oxidation, color loss and gelatinization are included. However vitamin loss, protein loss and microbial survival, considered as nutritional degradation (Chou and Chua 2001). It is important to mention that, in dried product the concentration of nutrients increased as product loses its water content. Hence, dried food contains more carbohydrates, fats and proteins per unit weight as compared to fresh food.

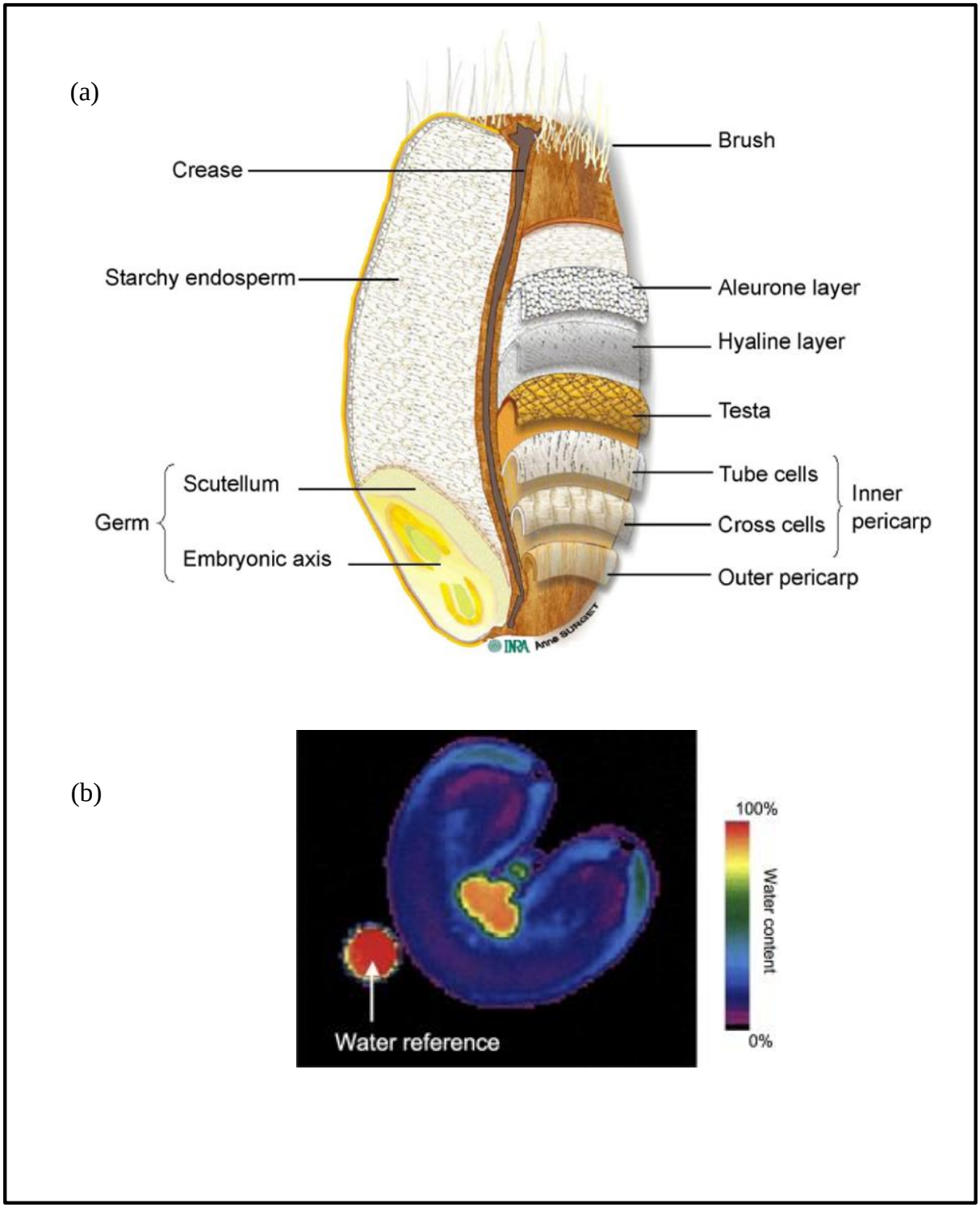


**Figure 1.3** (a) Wheat grain, showing component tissues (reprinted from (Saulnier et al. 2007); (b) Normalize magnetic resonance image (water density) of a median transverse slice of wheat grain (Saulnier et al. 2012).

All types of food stuff containing fractions of lipids, proteins and carbohydrates are very sensitive to temperature. These compounds are easily modified by high temperatures which results in degraded food quality. Many researcher work on hot air flow drying of rice (Hacihafizog et al., 2008), soybeans Hutchinson and Otten, 1983), green beans (Doymaz, 2005) and canola (Zare et al., 2009) showed that it is energy intensive process. In addition, hot airflow drying take long time and has low energy efficiency as it causes shrinkage of dried product which result in reduced moisture and heat transfer. Severe shrinkage also reduces bulk density and rehydration capacity. Another method is microwave drying which also has some drawbacks including uneven heating and textural damage of product (Zhang et al., 2006). Drying of agricultural product by adsorption technology by using desiccant drying system (DDS) is identified as a means of low temperature drying as well as improve energy efficiency suitable for heat sensitive products like food (Atuonwu et al., 2011a; Atuonwu et al., 2011b;). Desiccant drying is one of the quality and energy conservation drying technique. It has been used from ancient time in alternate layer of desiccant material and drying products (Watts et al., 1987). In addition to maintain the quality of product, the cost of production is another concern that motivates the researcher to adopt desiccant drying system. The quality of drying product is equally important as far as the drying process for the storage of agricultural products for certain period of time. As far quality is concerned, drying air conditions are very important. Temperature and humidity of the drying air influence the quality of product in term of nutrient conservation, color and surface texture (Rane et al., 2005). High temperature drying may result in irreversible biological or chemical degradation.

In addition to high temperature, high humidity also affects the quality of drying product. Drying at low temperature will be preferable for obtaining dry products with high product quality, but the driving force for moisture migration is limited in such process. Whereas desiccant drying system provide option of improved drying at low temperature.

A sound knowledge of equilibrium moisture content (EMC) and equilibrium relative humidity (ERH) is essential for making strategies regarding drying conditions. Figures 1.4 showed the equilibrium moisture contents (EMC) with relation to temperature and humidity ratio for wheat. The significance of humidity control can be seen Figure 1.4, thereby dehumidified air requires low drying temperature in order to achieve safe level EMC. However, in case of higher humidity ratio, higher drying air temperature is required to achieve optimum level of EMC e.g. 14% for wheat. The desiccant drying system has ability to dry the agricultural products at low temperature and low humidity ratio.

Many studies have been reported on desiccant materials for moisture adsorption equilibrium (Sultan et al., 2015) and adsorption rate (Sultan et al., 2016). On the other hand steady-state investigation of desiccant drying systems for agricultural applications has not been extensively studied in the literature for a particular produce. From the above prospective, drying chart will help to select the drying air conditions according to the different drying applications/stages.

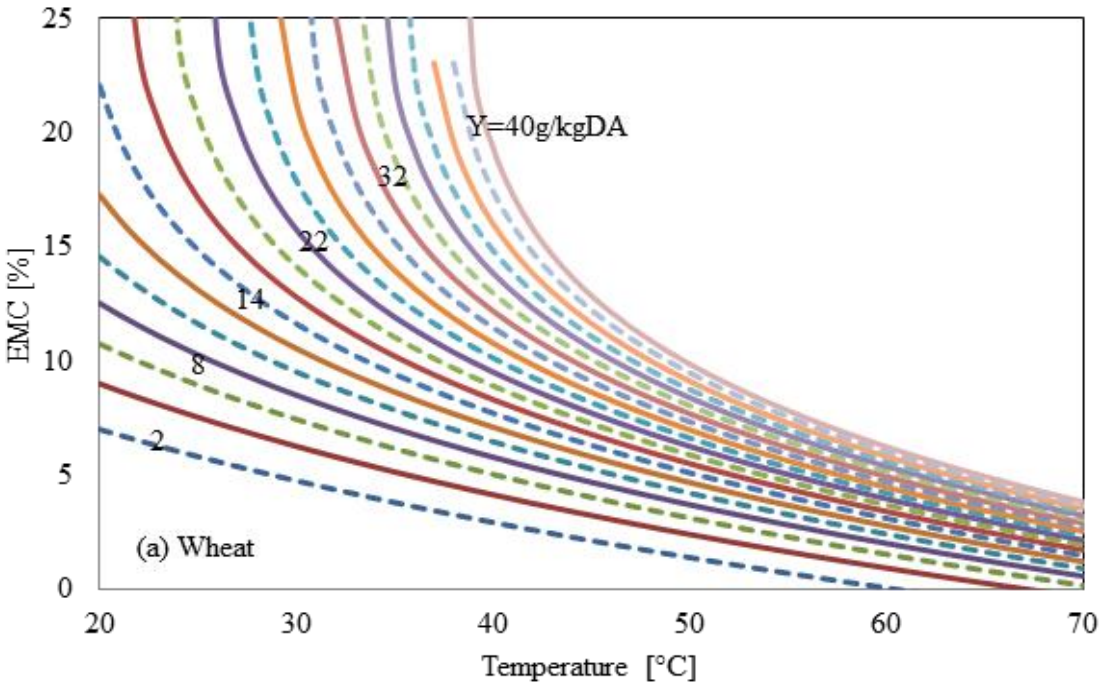


**Figure 1.4** Effect of temperature and humidity ratio on EMC for wheat.

## 1.4 Scope and objectives

The scope and objectives of the work presented in this thesis are as follows

- To investigate the steady state desiccant drying system for agricultural applications.
- To investigate the effect of latent load control of drying air for the drying of temperature sensitive agricultural produce.
- To investigate the combine effect of sensible and latent load control for the drying of agricultural products for commercial usage.
- Investigation of adsorption kinetics of desiccant drying for the drying of wheat.

- Comparison of desiccant drying and conventional hot air drying in term of allowable time for safe storage, total drying time and energy consumption.
- Investigation of the effect of relative humidity on the effective thermal conductivity of the zeolite based desiccant materials.
- Development of empirical relationship to predict the effective thermal conductivity of zeolite based desiccant materials at different levels of relative humidity at constant temperature.
- Investigation of the variation in effective thermal conductivity value with relation to adsorption uptake.
- Determination of the change in volumetric heat transfer coefficient due to change in thermal conductivity.

## References

Atuonwu, J.C., Straten, G. van., Deventer, H.C. van., Boxtel, A.J.B. van., 2011a. Model-based energy efficiency optimization of a low temperature adsorption dryer. Chem. Eng. & Technol.34, 1723-1732.

Atuonwu, J.C., Straten, G. van., Deventer, H.C. van., Boxtel, A.J.B. van., 2011b. Improving adsorption dryer energy efficiency by simultaneous optimization and heat integration. Drying Technolo. 29, 1459-1471.

Belessiotis, V., Delyannis, E., 2011. Solar drying. Solar Energy , 85:1665–91.

Benali, M., 2004, Thermal drying of foods: Loss of Nutritive Content and Spoilage Issues, pp. 137-152, in A.S. Mujumdar (Ed.) Dehydration of Products of Biological origin, Enfield, New Hemisphere, USA

Chou, SK., Chua, KJ., 2001. New hybrid drying technologies for heat sensitive foodstuffs. Trends Food Sci Tech. 2001;12(10):359–369. http://dx.doi. org/10.1016/S0924-2244(01)00102-92.

Davey, K.R. (1989) A predictive model for combined temperature and water activity on microbial growth during the growth phase. J. Appl. Bacterial. 67, 483-488.

Doymaz, I., 2005. Sun drying of Figure: an experimental study. J Food Eng. 71, 403-407.

Fournier, M., Guinebault, A., 1995. The shell dryer-modeling and experimentation. Renewable Energy, 6, 459–63.

Fu, B., Labuza, T.P., 1993, Shelf-life Prediction: Theory and Application, Food Control, 4(3), pp. 125-133.

Hacıhafızog, O., Cihan, A. and Kahveci. K., 2008. Mathematical Modeling of Drying of Thin Layer Rough Rice. Food Bioprod. Process. 86, 268-275.

Hutchinson, D., and Otten, L., 1983. Thin Layer Air Drying of Soybeans and White Beans. J. Food Technol. 18, 507-524.

Kumar, D., Kalita, P., 2017. Reducing Postharvest Losses during Storage of Grain Crops to Strengthen Food Security in Developing Countries. Foods. 6, 8. doi:10.3390/foods6010008

Rane, Milind V., Reddy, S. V Kota., and Roshini R. Easow., 2005. "Energy Efficient Liquid Desiccant-Based Dryer." Applied Thermal Engineering 25 (5–6), 769–81. doi:10.1016/j.applthermaleng.2004.07.015

Sachin V.Jangam, Chung Lim Law, Arun S. Mujumdar eds: Drying of foods, vegetables and fruits. (2010)

Saulnier, L., Guillon, F., Chateigner-Boutin, A.-L.: Cell wall deposition and metabolism in wheat grain. J. Cereal Sci. 56, 91–108 (2012). doi:10.1016/J.JCS.2012.02.010

Saulnier, L., Sado, P.-E., Branlard, G., Charmet, G., Guillon, F.: Wheat arabinoxylans: Exploiting variation in amount and composition to develop enhanced varieties. J. Cereal Sci. 46, 261–281 (2007). doi:10.1016/J.JCS.2007.06.014

Sultan, M., El-Sharkawy, I. I., Miyazaki, T., Saha, B. B., Koyama, S., Maruyama, T., Maeda S., and Nakamura, T., 2015. Insights of water vapor sorption onto polymer based sorbents. Adsorption, 21(3), 205-215.

Sultan, M., El-Sharkawy, I. I., Miyazaki, T., Saha, B. B., Koyama, S., Maruyama, T., Maeda S., and Nakamura, T., 2016. Water vapor sorption kinetics of polymer based sorbents: Theory and experiments, Appl. Therm. Eng., 106, 192-202.

Watts, K.C., Bilanski, W.K., Menzies, D.R., 1987. Simulation of adsorption drying of corn, wheat, barley and oats using sodium bentonites. Canad. Agri. Eng. 29(2), 173-178.

Zare, D., Ranjbaran, M., Niakousari, M., and Javidi, M., 2009. Thin Layer Drying and Equilibrium Moisture Content Equations for Canola (Brassica Napus L.). Iran Agric. Res. 30, (1, 2), 11-20.

Zhang, M., Tang, J., Mujumdar, A. S., and Wang, S., 2006. Trends in microwave-related drying of fruits and vegetables. Trends in Food Sci. and Technol.17, 524-534.

# CHAPTER 2

# INTRODUCTION TO DIFFERENT DRYING TECHNIQUES

# Chapter 2

# INTRODUCTION TO THE DIFFERENT DRYING TECHNIQUES

This chapter presents the detail literature review about desiccant drying technologies. A brief review about different drying technologies including convective drying, freeze drying, microwave and vacuum drying is also made. Out of these freeze drying, microwave and vacuum drying technologies regarded as good quality products as they ensure volumetric heating and fast drying while limiting product shrinkage. However, these techniques attributed to high energy costs, overall low efficiencies and difficulty in temperature control of the product. On the other hand desiccant drying provides energy conservation, low temperature drying which helps to reduce thermal degradation of nutrients. In addition hybrid drying system (integration of desiccant and other drying technologies) gives better solution regarding the energy conservation and quality of drying product.

## 2.1 Introduction

It is difficult to process the huge quantity of harvested agricultural products due to perishable in nature and short shelf life. Therefore drying is under practiced from ancient time as preservation technique and still, it is considered as being mostly used preservation technique. It is an energy intensive process that shares the consumption of 15% industrial energy (Kemp, 2005).To make the drying system sustainable and effective, it must be designed to reduce the energy consumption per unit mass and satisfy all the quality requirements.

In recent years, increase in energy demand as well as environmental issue created by existing energy source has promoted to strive for energy preservation.

Generally, the efficiency of dryer ranges from 20% to 60% (Majumdar, 2007). To improve the performance of the drying system, effectiveness of energy utilization is considered as an important factor. In this regard various researches have been done to improve the energy utilization. Mainly there are two types of strategies in practice, one of them is hybrid technology (combination of two or more different technologies) i.e., radio-frequency and microwave, infra-red combined with convective dryers (reviewed in Raghavan, et al., 2005), microwave combined with freeze dryers (Duan et al., 2010) and infra-red combined with freeze dryers (Chakraborty et al., 2011) and others are desiccant based drying technologies, for example, heat pump drying (Ogura and Mujumdar, 2000; Ogura et al., 2003).

## 2.2 Conventional drying techniques

### 2.2.1 Convective drying

Drying refers to the removal of moisture from the solid material. Foods, such as fruits and vegetables, are considered as highly perishable material due to their high moisture content. Some of the agricultural products e.g. cereal grain partially dries in the field when crop approach to its maturity. Grain gives up its moisture to the air but still contain moisture which is in equilibrium with ambient air and harvested at higher moisture content than that of safe storage. Various researches have been done to increase the performance of drying and possible integration of different drying technique to improve the quality of dried product in addition to optimum energy use. Chua and Chou (2003) conducted a review study on low cost drying technologies at farm level. Motivation was attributed to the technologies, readily available to rural areas, easy to construct and operate, better drying kinetic to reduce spoilage and improve processing hygiene. Selected low cost drying technologies include, fluidized bed, spouted bed, infrared, solar, simple convective and desiccant drying. Koyuncu (2006) proposed two different greenhouse type crop dryer designs and investigated its performance through experiments. Model 1 was triangular in shape and model 2 was stair steps type with natural air circulation. Experiments were performed with and without chimney for the drying of pepper. These designs help to increase the temperature 5–9 oC than ambient and more efficient than open sun drying 2-5 times.

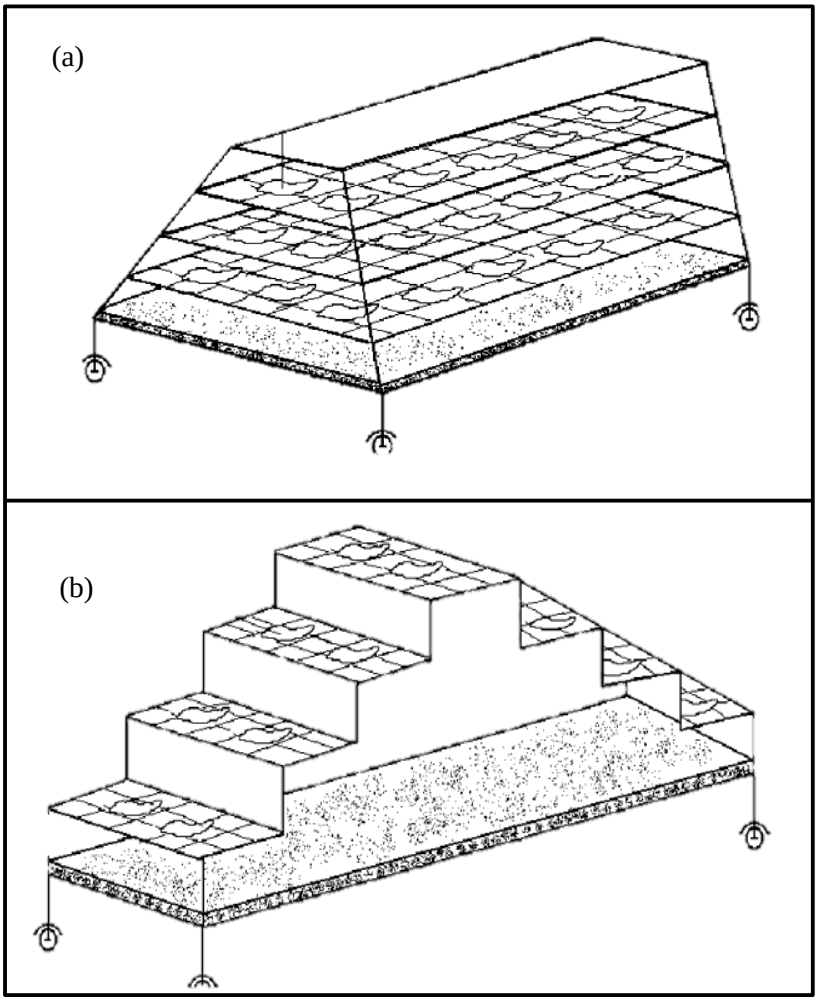


**Figure 2.1** Schematic diagram of greenhouse type dryer: (a)Model 1 (b) Model 2 (Koyuncu 2006).

### 2.2.2 Freeze drying

The drying process in which a frozen food is dehydrated under the vacuum. In freeze drying the moisture contents undergoes directly to a gaseous form from solid form without going to liquid sublimation. This technique makes the dried food to maintain their actual shape and size, and reduces rupturing of cell. Number of foods like meats, vegetables and coffee products are dried and preserved with this process. A product of freeze drying process maintain it nutrient, texture and color and it is often indistinguishable from the original food or products. A freeze dried product can be self-stable up to 25 years or more, if it is put in a cane and, 0.5 year to 3 years if poly bag is used to store the food. This makes freeze drying process a widely used drying process for individual and commercial use. A freeze drying process occurs in three stages;

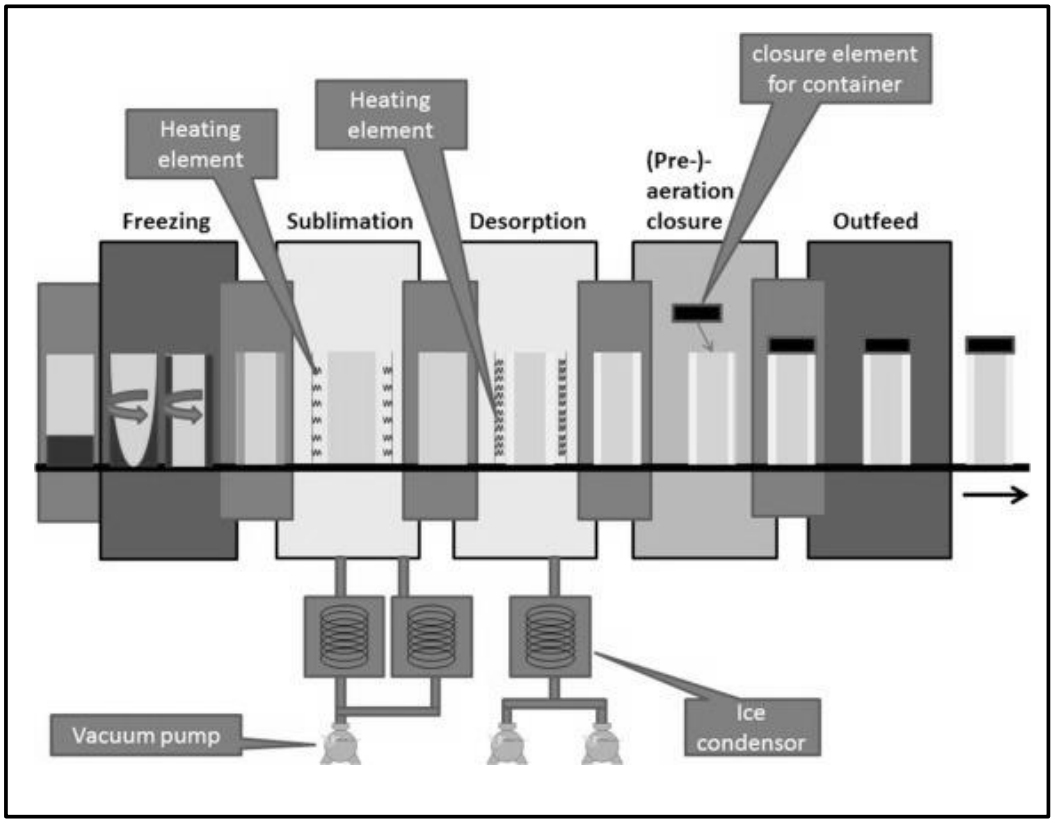


**Figure 2.2** Continuous freeze drying system (Van Bockstal et al. 2018).

i. Pre-freezing: The freeze dried product is frozen below eutectic temperature, ii. Primary drying: Through sublimation, ice is removed from the product and Secondary drying; iii. The excess water contains after primary drying is desorbed by increasing the product temperature higher than ambient temperature. Figure 2.2 represent continuous freeze-drying based on spinning the vials and non-contact energy transfer via infrared (IR) radiation during drying to improves the process efficiency (Van Bockstal et al. 2018).

### 2.2.3 Microwave drying

The physics involved in microwaves drying are purely different from the conventional process of drying. Microwave penetrates into dielectric materials and provides means to generate internal heat. This internally generated heat establishes a vapor pressure difference between the internal product and outer moisture surface also called “moisture pumping”. The moisture pumping forces the moisture to the surface and prevents it from case hardening. In microwaves drying process, the drying rate is very high due to the development of the high vapor pressure differences between interior and surface of the product.

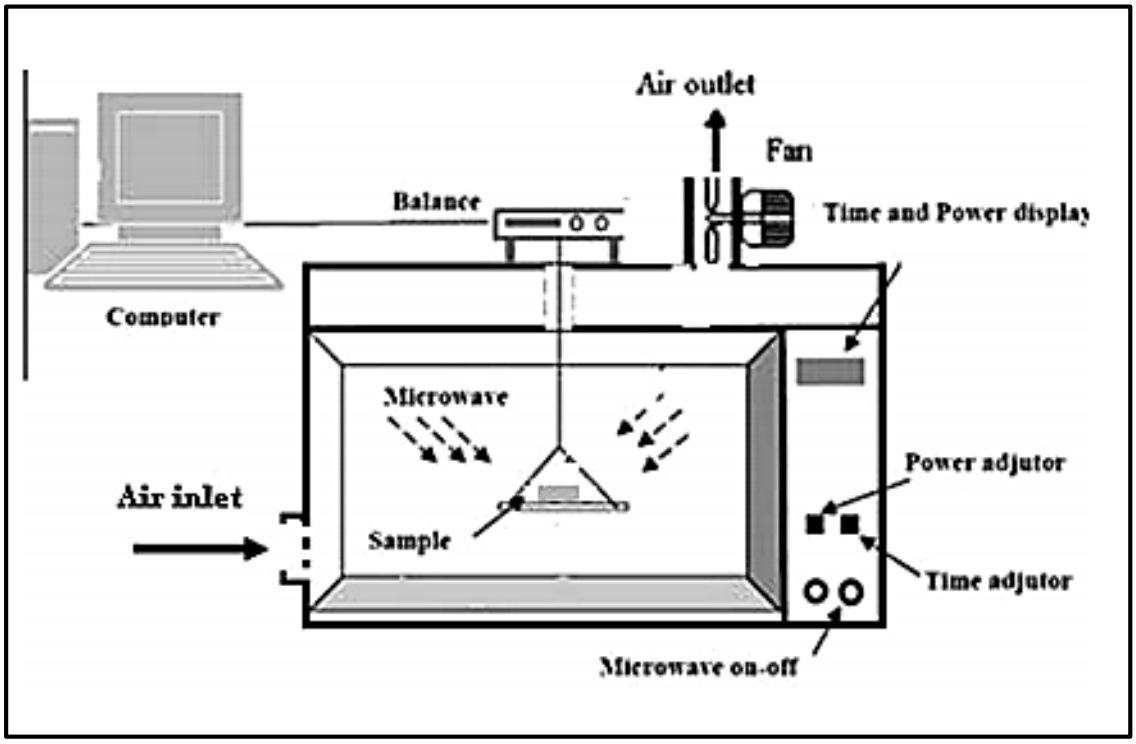


**Figure 2.3** Schematic diagram of microwave-convective oven dryer (Zarein et al., 2015).

Microwave drying technology also used with the combination of some others drying technologies e.g. freeze drying, vacuum drying and convective drying. Figure 2.3 represent the schematic diagram of microwave-convective oven dryer used for the drying of apple (Zarein et al., 2015). It had been used in a lot of industries such as Food, paper, textile etc. However it is difficult to control the temperature of the final product, in addition bad texture of product, limited penetration and uneven heating make it a limited used drying process.

### 2.2.4 Vacuum drying

In convection drying systems, hot airflow used for drying of food, and this caused the degradation of product quality. To prevent the quality degradation during the drying process, vacuum drying had been introduced. In this drying process the water molecules having high energy are diffused on the surface and evaporate in vacuum region. The vacuum helps to reduce the moisture contents on the product surface. This generates a vapor pressure difference between interior and surface of the food, results in fast drying rate. Due to absence of air for dehydration, oxidation process reduces.

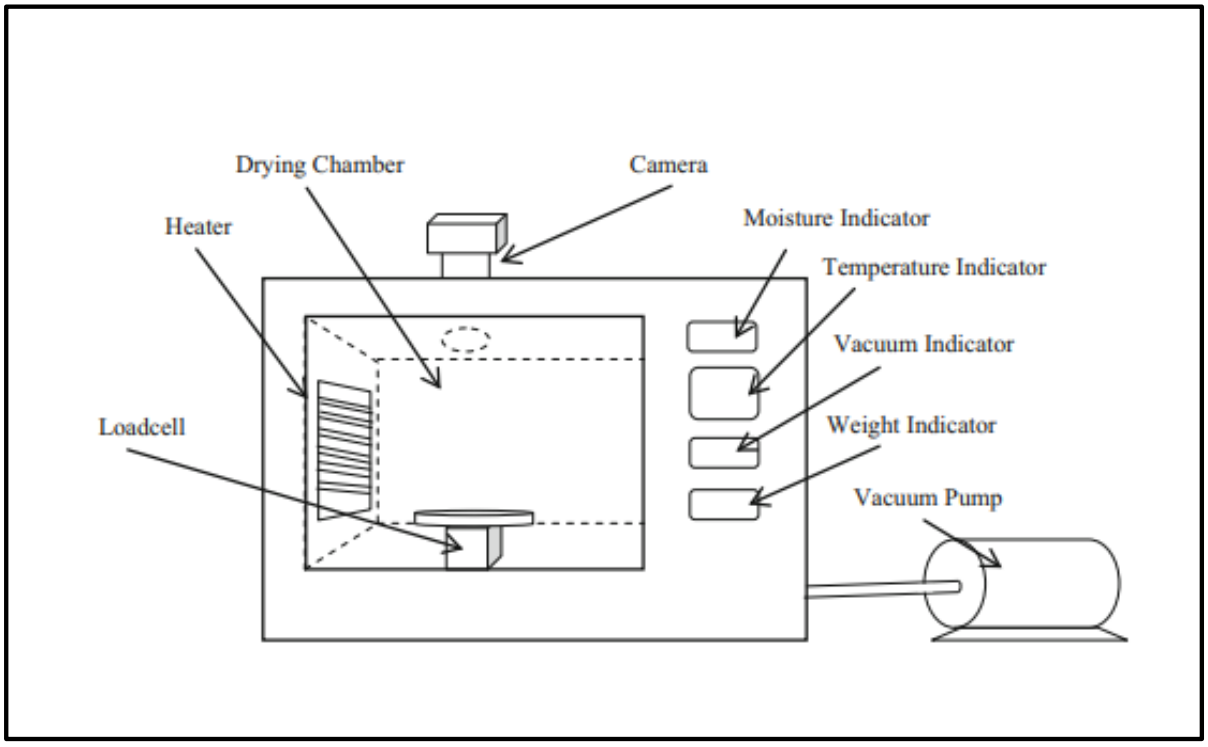


**Figure 2.4** Schematic diagram of vacuum drying (Pourfarzad et al. 2015).

Vacuum drying has high operating costs due to the need to maintain vacuum over long periods of drying though the product flavor, texture and color quality all improved (Gunasekaran, 1999). Figure 2.4 represents a laboratory scale vacuum dryer, designed for the drying of pear slice. The dryer consisted of drying chamber, heating section, temperature control section, vacuum section, weighing section and moisture control section (Pourfarzad et al. 2015).

## 2.3 Desiccant drying

### 2.3.1 Rotor/ wheel type desiccant drying

Nagaya et al. (2006) developed dryer for low temperature and fast drying of vegetables to maintain its color and texture. This system was consisted of desiccant rotor as dehumidifier, heater, linear potentiometer and thermal transducer. The air circulation was controlled by algorithm to maintain the temperature at 49°C. The color of dried vegetables was checked by color channel values, for cabbage, eggplant, carrot, butterbur and spinach. It was also found that spinach retains large value of vitamin C in it and mushrooms can also be

dried in it with a little modification. The results showed that dryer work 12 times faster than sun drying and 6 time faster than conventional desiccant based drying.

Atuonwu et al. (2011) conducted a study to compare the energy efficiency of different drying approaches included conventional, adsorption, adsorption (with heat recovery), condensation and heat pump. Energy efficiency was evaluated by developed model. Results showed that heat pump and adsorption dryers operated at low temperature and degradation of vitamin C reduced. In addition adsorption dryer operated at 50$^{o}$C and conventional dryer at 75$^{o}$C in order to get same efficiency.

De Antonellis et al. (2012) made simulation for the best arrangement of HVAC (heating ventilation air conditioning) desiccant based drying system in order to achieve maximum energy saving. Different configuration of adsorption wheel with the refrigerating machines and co generative engines were suggested to find out the best integration with adsorption wheels for drying. It was found that the reference technology based on cooling coil adoptable only when sensible to latent load ratio was greater than 2. However, 70-80% could be saved as compared to the reference technology if the ratio of sensible to latent load would be within-2 and 2.

Abasi et al. (2016) analyzed the performance of rotary desiccant wheel unit attached with convective type corn dryer. Three temperatures (50 $^{o}$C, 60 $^{o}$C and 70 $^{o}$C) and three flow rates (1 kg/min,1.4 kg/min,1.8 kg/min) were selected for conducting the experiment with and without desiccant wheel unit to determined its effects on drying time and energy consumption. Experimental result showed that in case of drying with desiccant unit, there was increased in drying rate 9.75% and decrease in drying time 7.85%. However, 20.7% increase in total energy consumption employed the necessity to use of solar energy for the regeneration of the desiccant wheel.

Madhiyanon et al. (2007) conducted experiments for the drying of coarsely chopped coconut in a hot air dryer equipped with rotary desiccant wheel. Desiccant material used was silica gel. Drying performance, quality and color of the product was selected as comparing parameters with the hot air drying system. Results showed that RH of the drying air had important effect on the color of product. When drying was performed at drying air velocity 0.23–0.70 m/s and temperature 50-60$^{\circ}$C, the color of product was maintained light. However 30% increase in RH caused marked change in color. Results showed that drying time was

reduced 25 % as compared to normal drying and drying rate was 30-35% more than of conventional system but it is also found that combined system utilized 40-80% more energy than pure hot air system.

De Antonellis et al. (2016) conducted study based on experiments to find the best strategy that could help in reduction of the thermal power consumption in desiccant drying unit. Five different strategies were planned using 3 parameters regeneration temperature ($T_{reg}$), regeneration air velocity ($v_{reg}$) and revolution speed (N). In 1$^{st}$ control: $T_{reg}$ varied without change in $v_{reg}$ and N, in 2$^{nd}$ control: $T_{reg}$ and N varied without change in $v_{reg}$, in 3$^{rd}$ control: $v_{reg}$ varied without change in $T_{reg}$ and N, in 4$^{th}$ control: $v_{reg}$ and N varied without change in $T_{reg}$ and in 5$^{th}$ control: $T_{reg}$, $v_{reg}$ and N all varied. The best control was selected that provide maximum COP at required specific moisture removal capacity. Result showed that optimum control was first to decrease the $v_{reg}$ then reduce the $T_{reg}$ and increased the air velocity at same time whereas simplified control approach was to varied $T_{reg}$ and flow rate that also help in reduction of thermal power consumption but it used 5% more than ideal control.

### 2.3.2 Fixed bed type desiccant drying

Gill et al. (2012) developed a desiccant dryer for the drying of seeds particular paddy, coriander, fenugreek and radish. Dryer consisted of two separate chambers connected with pipes; one chamber used for conditioning of the air whereas others used to hold seed for drying. It work in closed loop and also provided with air flow inversion for uniform deep bed drying. Paddy seed was dried from 13.3 to 2.61% (wb), coriander from 13.4 to 10.08 % (wb), fenugreek from 12.4 to 8.22 % (wb) and radish 10.6 to 6.08 % (wb) in 4hr, 3hr, 4.25hr and 4hr, respectively. This low temperature dryer also cause to increase the average germination rate up to 80 %, 87 %, 86 % and 56 % for paddy, coriander, fenugreek and radish, respectively.

Dina et al. (2015) evaluated the effectiveness of the solar dryer equipped with desiccant thermal storage unit for the drying of cocoa beans. Desiccant selected for this study were $CaCl_2$ and molecular sieve 13x (Na86 [$(AlO_2)$86. $(SiO_2)$106]. 264$H_2O$). A comparison was made on the base of drying time and specific energy consumption.

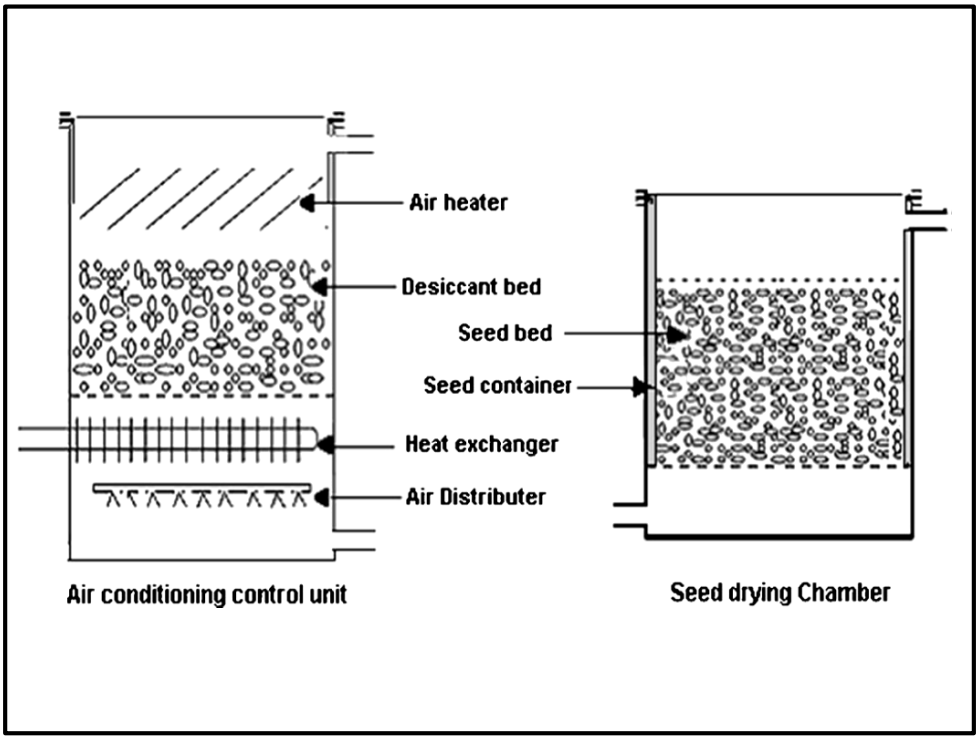


**Figure 2.5** Schematic of air conditioning control unit and seed drying chamber (Gill et al 2012).

In drying chamber the temperature was found 9-12$^{o}$C higher and humidity lower than the ambient, providing suitable drying conditions for cocoa beams. Drying time for solar dryer with absorbent, solar dryer with adsorbent and open sun drying were 30 hr, 40 hr and 55 hr, respectively. In three drying option, specific energy consumption for solar drying with absorbent found minimum i.e. 13.29 MJ/kg moist. However, for solar dryer with adsorbent and open sun drying were 18.94 MJ/kg and 60.4 MJ/kg moist, respectively.

Chramsa-ard et al. (2013) conducted a study to compare the total drying time for chili, with and without dehumidification unit. System used silica gel beds (SGB) with the dimension of 0.55 m × 0.95 m × 0.01 m and solar system for regeneration. In one trial 8 kg of weight (chili) was used and it was found that adsorption varied directly as humidity in air and inversely with the temperature. Drying system with the provision of dehumidification unit had taken 19 hr to bring the initial moisture content 82 % wb to 13 % wb whereas without dehumidification it required 24 hr at the expense of 21.5 kWh more electricity than that of with dehumidification.

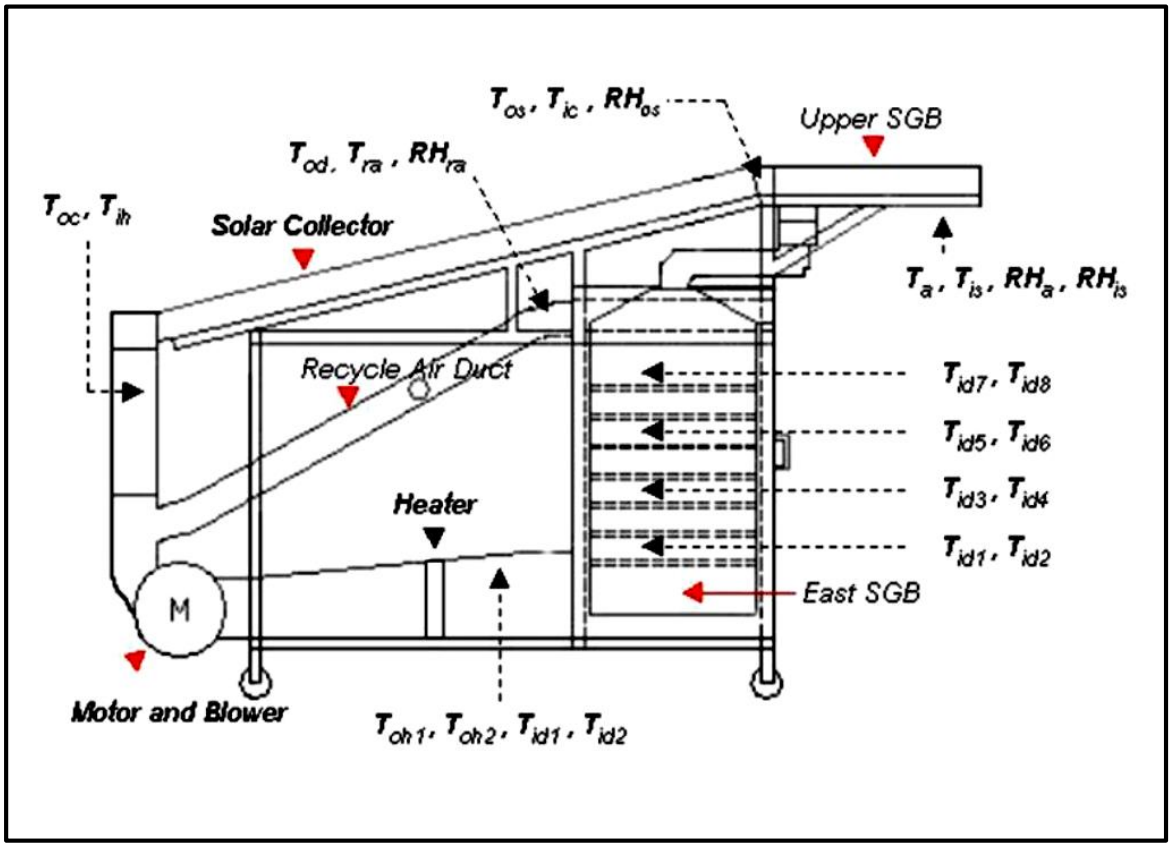


**Figure 2.6** Schematic of the desiccant bed solar dryer system (Chramsa-ard et al., 2013).

Hodali and Bougard (2001) designed an adsorption unit connected with forced convective solar dryer for the drying of apricot. Desiccant material silica gel was used for the development of adsorption unit in order to get good quality and reduction in drying time. Initially, sorption cycle of the desiccant unit determined then the size of other components including solar collector, dryer and adsorption unit were decided. Optimization result showed that collector length would be 10 m, adsorber 1.5 m and dryer 10 m for 15 kg fresh apricots in one layer for 10 cm high and 2 m wide installation.

Thoruwa et al. (2000) conducted experiments to find out the $CaCl_2$ based low cost desiccant material. Three cheap desiccants used were type 1 (bentonite-$CaCl_2$), type 2 (bentonite-$CaCl_2$) and type 3 (kaolinite-$CaCl_2$). Selection of material was based on the high sorption and low cost as well as suitable for the environmental conditions in Kenya. The desiccant material was tested in environmental cabinet, for moisture sorption desiccant material retained into the cabinet for 120 hr at RH 80% and temperature 25°C. While for the regeneration of the desiccant material it retained for 8 hr at RH 20% and temperature 50°C. It

was found that type 1 had maximum absorption of 45% dry weight basis (dwb) whereas type 2 and type 3 had 30% (dwb). It was concluded that these type desiccants best for solar crop drying tropical areas due to low regeneration temperature.

Patil et al. (2015) developed a solar dryer for the drying of agriculture products with regenerative desiccant material. The purpose of designing was to perform the drying in off sunshine hours in order to earlier drying. Experiments were performed using three type of absorber plate (plane, vertical corrugated, horizontal corrugated). Experimental result showed that 68% of the total moisture was removed in day time by using solar energy and 32% was removed by circulating the air through desiccant unit. The drying efficiency of the dryer varies 48 % to 56% and pickup efficiency varied from 52% to 63% respectively.

### 2.3.3 Liquid desiccant drying

Rane et al. (2005) designed and tested a dryer based on liquid desiccant ($CaCl_2$) solution. The purpose of designing was to made it economical and technical more efficient and high energy saving.

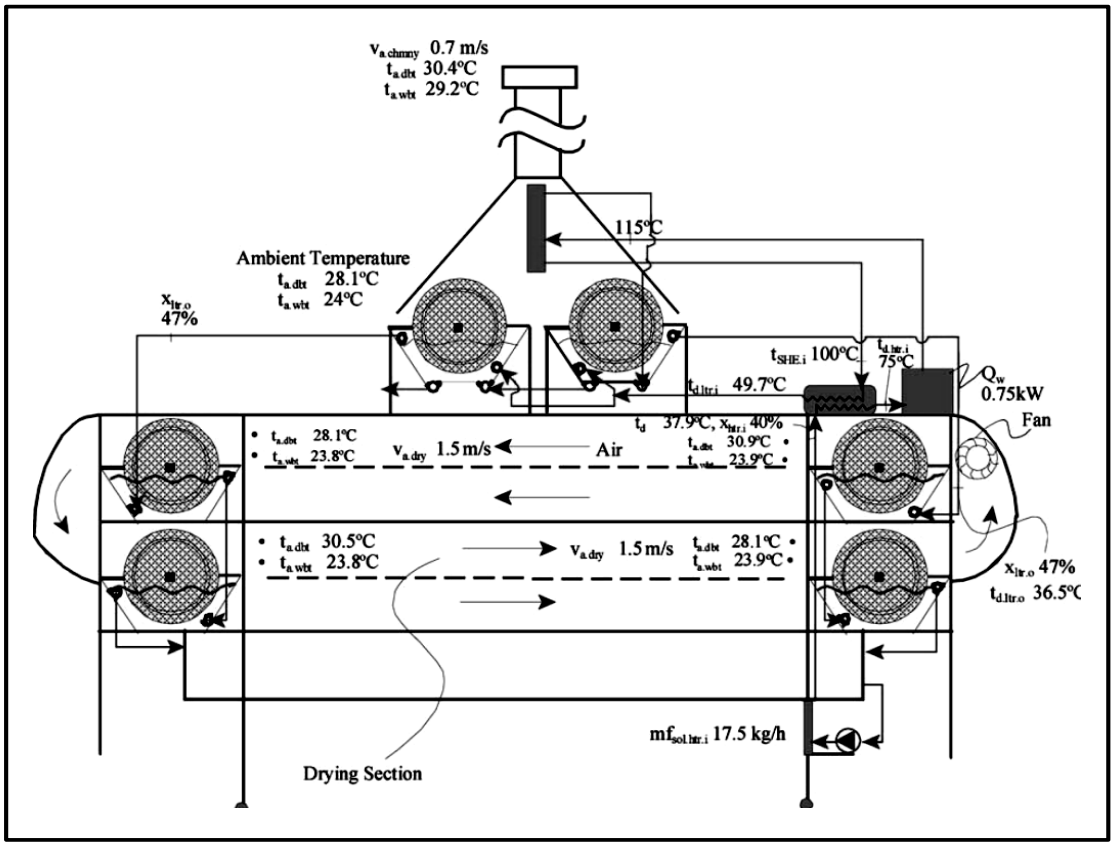


**Figure 2.7** Liquid desiccant based dryer (Rane et al. 2005).

System used two stage regenerators; high temperature generator and low temperature generator. Drying of paper tray was performed this dryer. Experimental results showed that there was 56% energy saving and $CO_2$ emission reduction. It also found that peak specific moisture extraction and average specific moisture extraction rate were 1.86kg/kWh, 1.5kg/kWh respectively whereas average specific moisture extraction rate for hot air based dryer was 0.66kg/kWh of heat.

## 2.4 Hybrid desiccant drying

Kivevele and Huan (2014) discussed the potential use of heat pump drying system integrated with desiccant bed for drying of different agriculture products particularly heat-sensitive. The Comparison of heat pump drying showed high efficiency, accurate temperature control, accurate moisture extraction as compared to others like direct/indirect sun lighting, wood heating, electrical heating, diesel engine heating. Moreover heat pump dryer attached with desiccant unit parallel with the evaporator help to share the latent load. It was also found that heat pump dryer attached with desiccant prove more good for the crops material sensitive to heat as well as energy saving point of view.

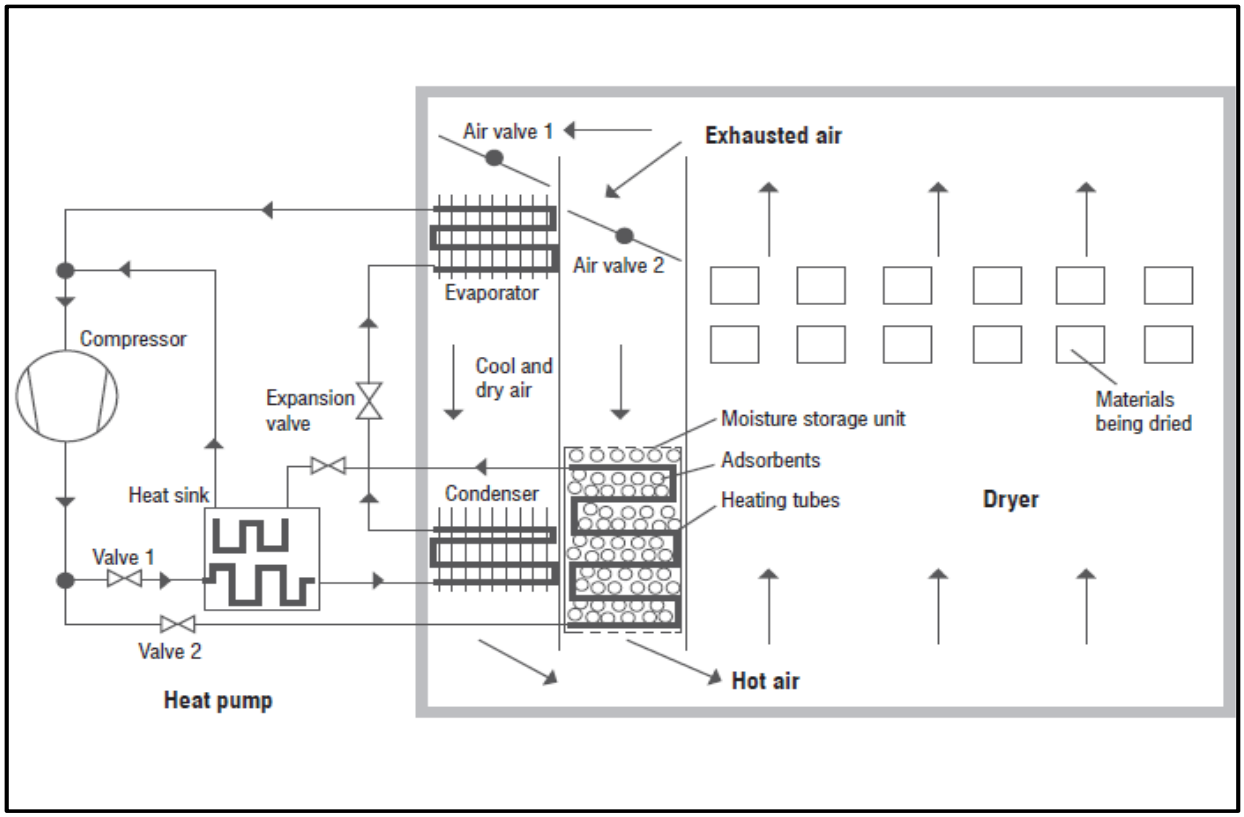


**Figure 2.8** Desiccant assisted heat pump dryer (Kivevele and Huan 2014).

Zhao et al. (2016) designed and analyzed the dryer in which dehumidification was done by using solid desiccant coated heat exchanger. This system was also equipped with heat recovery device (HRD). It was found that as the performance raised to 1.2 which was almost twice than conventional cycle. The electrical coefficient of performance reached about 13.83. when HRD included the thermal efficiency reached to average of 0.88. Results showed that sorptive material coated heat exchanger with HRD could be used in higher humidity and temperature areas.

Sivakumar et al. (2016) developed and analyzed the ammonia-water absorption refrigeration system for heating and cooling to dry the food products. It was found that the system combined COP and cooling are in range of 1.10 to 1.80 and 0.60 to 0.70 respectively, it was also found that when temperature rise from 0°C to 5°C the outlet temperature of condenser was in range of 43°C -55°C. This system had 20% to 35% more efficiency than conventional vapour absorption cooling system. For test case of this dryer sago was dried on 48°C to 53°C which dried in very less time as compared to full day drying in sunshine and the energy use varied from 49.4% to 20.86%.

Ambrosio-Ugri and Taranto (2007) studied the rotating-pulsed fluidized bed drying for the drying of cohesive particulate materials. Ambient air was used for drying after passing it through Silica gel bed to make it dehumidified.

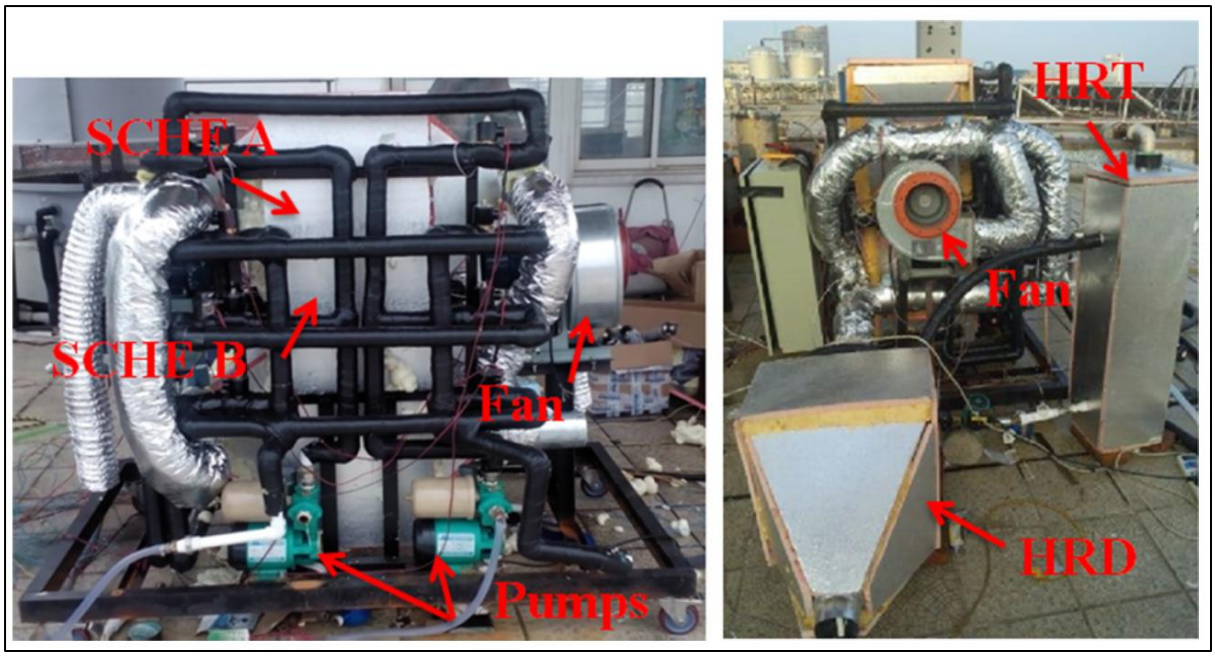


**Figure 2.9** Desiccant system using sorptive material coated heat exchanger and heat recovery device (Zhao et al. 2016).

For experiments 2-hydroxybenzoic acid was used for drying and to made it pulsed fluidized the frequency of disk was 5 Hz for low and 15Hz for high moisture at 85$^{o}$C temperature. Results showed that rotating-pulsed fluidized bed with silica gel proved efficient in drying of cohesive materials and also concluded that if the frequency of disk rotation increased it help to reduction in drying time.

Irtwange and Adebayo (2009) developed a passive type solar dryer on laboratory scale, consist on solar collector with heat storage unit and drying chamber capacity 10 kg. Thermal storage unit consisted on transparent glass sheet as glazing and zinc roofing sheet as absorber. It had been found that developed solar dryer exhibit high drying rate as compared to open sun drying. The mean drying rate of the dryer was 0.7 kg/day per every 10 kg of corn whereas sun-drying rate was 0.3125 kg/day comparatively. It also lead to save of drying time as it required 4 days to dry the cornfrom initial moisture content to 13.1%wb. However for passive solar dryer it required 8-days to dry from initial moisture content to 13.4%wb under sun drying.

Shanmugam and Natarajan (2006) conducted research on experimental investigation of forced convection and desiccant integrated solar dryer. This dryer consisted of drying chamber, solar flat plate collector and desiccant unit which have 60% bentonite, 10% CaCl2, 20% of vermiculite and 10% of cement.


**Figure 2.10** Air cooled vapour absorption system with attached bin dryer (Sivakumar et al. 2016).

Green peas were dried with air flow rates of 0.01, 0.02 and 0.03 kg/m$^2$s and equilibrium moisture content state reached after passing 22, 18 and 14 hours correspondingly. During day time hot air from flat plate collector used to pass through the drying chamber and desiccant bed, for drying of peas and regeneration of desiccant. Whereas in drying during off sunshine hours, air from the plenum used to circulate between the drying chamber and desiccant bed. This system achieved pickup efficiency of 63% and specific moisture extraction rate was in range of 0.55 to 0.82 kg/kW h.

Shanmugam and Natarajan (2007) constructed a solar dryer equipped with desiccant bed and two working mode, sun shine hours and off sun shine hours. Green peas and pineapple slice were used to dry in the dryer of capacity 20 kg.

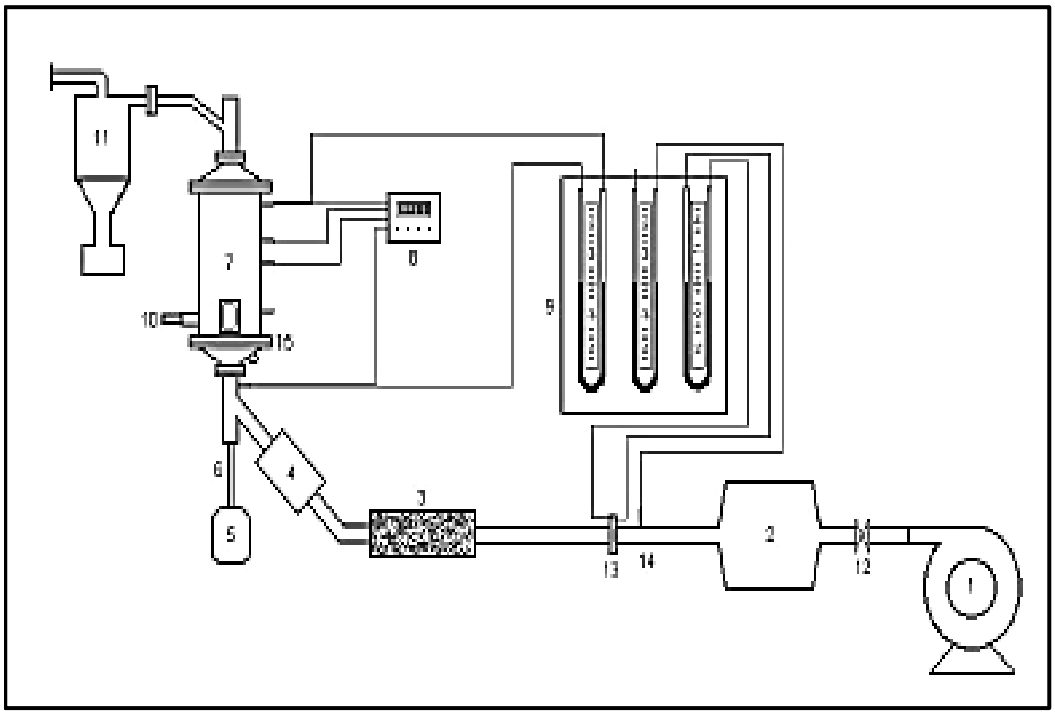


1. Blower
2. air cooler
3. silica gel bed
4. electrical heater
5. electrical motor
6. axis of motor
7. cylinderical bed
8. temperature indicator
9. U tube manometer
10. sampler
11. cyclone
12. globe valve
13. static ptessu
14. perforated plate+ rotative disk

**Figure 2.11** Schematic diagram of fluidized bed (Ambrosio-Ugri and Taranto 2007).

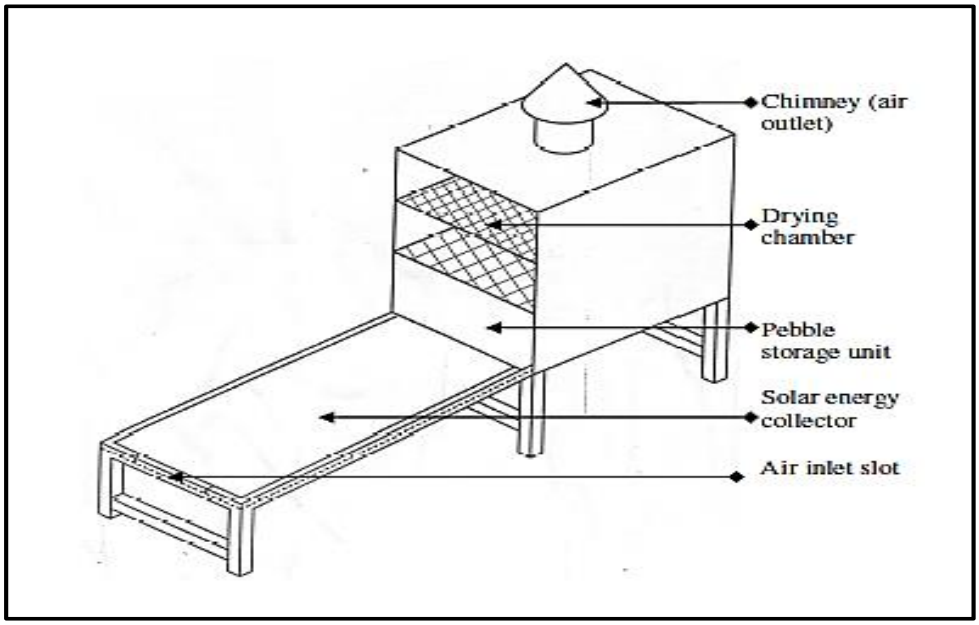


**Figure 2.12** Passive solar grain dryer (Irtwange and Adebayo 2009).

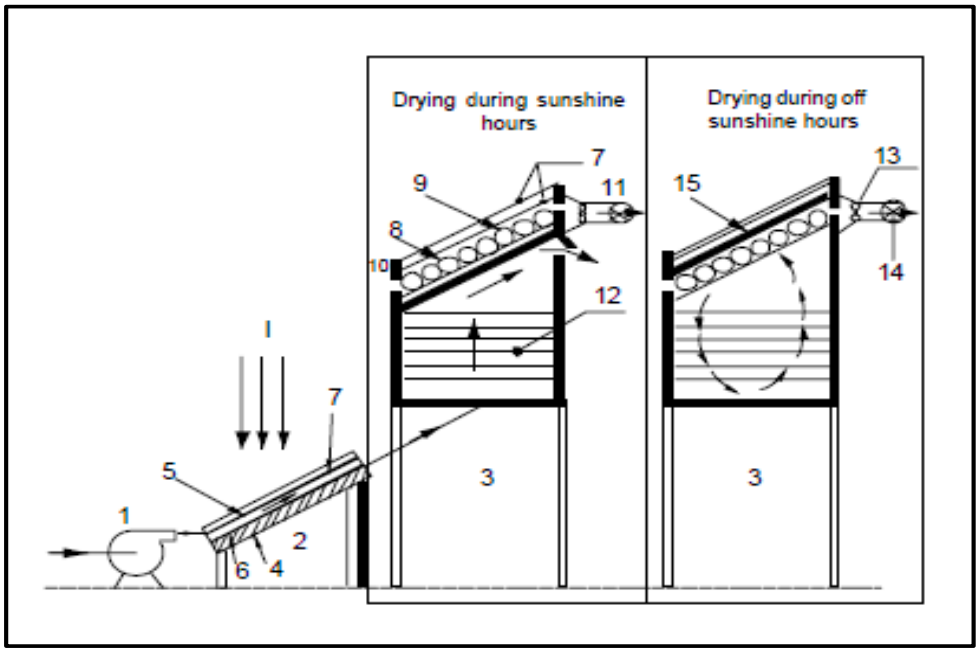


1. Blower
2. flate plate collector
3. drying chamber
4. insolation
5. absorber plate
6. bottom plate
7. transpaternt cover
8. desiccant bed
9. ply wood
10. air inlet
11. duct for air exit
12. drying trays
13. two way fan
14. valve
15. plywood

**Figure 2.13** Schematic view of desiccant integrated solar dryer (Shanmugam and Natarajan 2006).

In day time, food was dried with the help of flat plate solar collector and blower while in the night the air inside dryer was reused through desiccant bed which absorbs moisture from the circulating air. Desiccant bed was regenerated by the solar irradiation in day time in addition, use of reflectors increase the potential of desiccant increase by 20%. It was found that drying efficiency varies between 43 to 55% whereas pickup efficiency between 20 to 60%. It was also found that 60% moisture content was removed by heated air of solar energy and remaining by desiccant.

## 2.5 Aeration and cooling of dried grain

Dai et al. (2002) investigated the applicability of desiccant for the cooling of stored grains. System consists on desiccant wheel and adsorption cooling system powered by solar thermal to control the latent and sensible load, respectively. During day time due to increase in temperature of adsorption bed, desorption of methanol take place due to higher pressure and it starts to collect in the receiver. Whereas at night due to drop in pressure of adsorption bed, adsorbent start to adsorb and thus produce cooling effect.

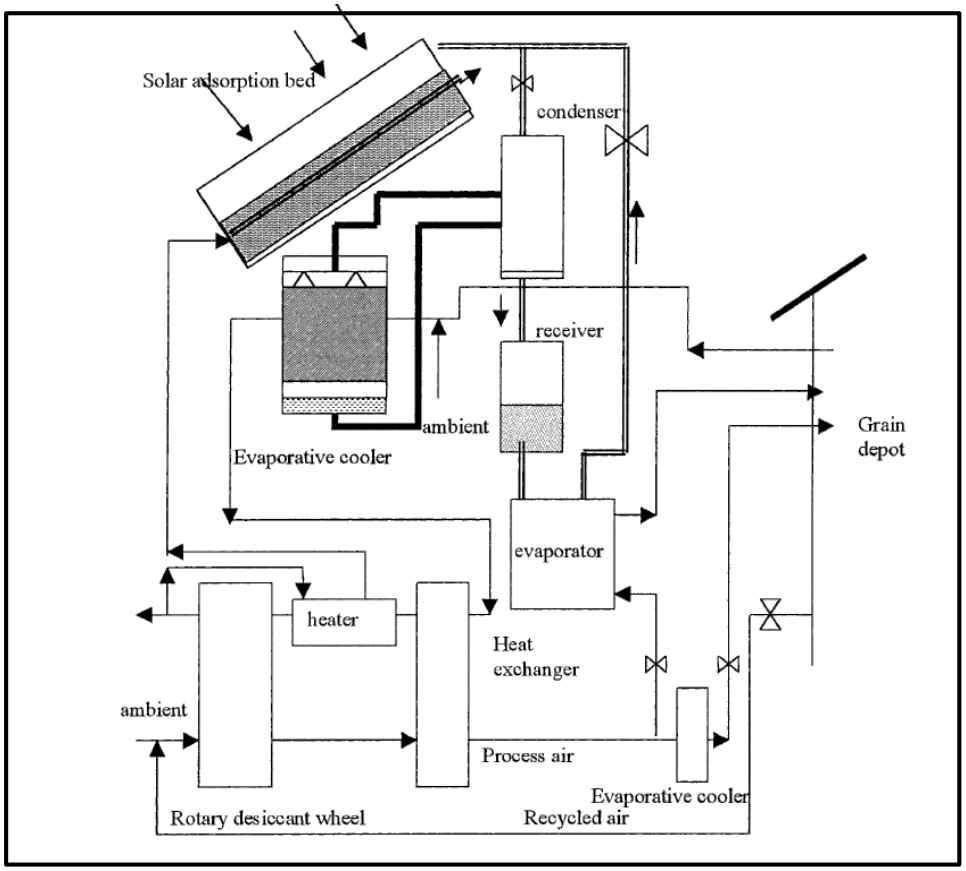


**Figure 2.14** Schematic of the hybrid solar cooling system grains (Dai et al. 2002)**.**

Moisture of the grains is removed by desiccant wheel regenerated by solar heater or burner. This system can be used widely in the regions with abundant solar resources due to such advantages as environmental protection, energy saving and low operation costs

Thoruwa et al. (1998) made a solar dehumidifier for the aeration of stored grains to prevent them from micotoxin contamination by using bentonite $CaCl_2$ as desiccant. Solar dehumidifier had active receiving area of $0.921m^2$ with 32.5g of desiccant packed inside glass. Air flow rate was maintained at 2m3/min using 12V fan operated at night. Desiccant bags happened to $4^oC$ rise in temperature and 40% reduction of RH of circulating air. Moisture removal rate was found 15x10-4 kg per kg of air during dehumidification of air at night time. During day time more than 50% of incident sun energy captured by the system is used for the regeneration of desiccant.

Table 2.1 provides a comparison of the efficiencies and advantages of desiccant dryers, vacuum and hot air dryers. Adsorption drying technology by using desiccant material showed high effenciency in addition to low drying temperature, low operating relative humidity and operating cost. Desiccant drying is therefore an efficient and energy-saving alternative for drying industries.

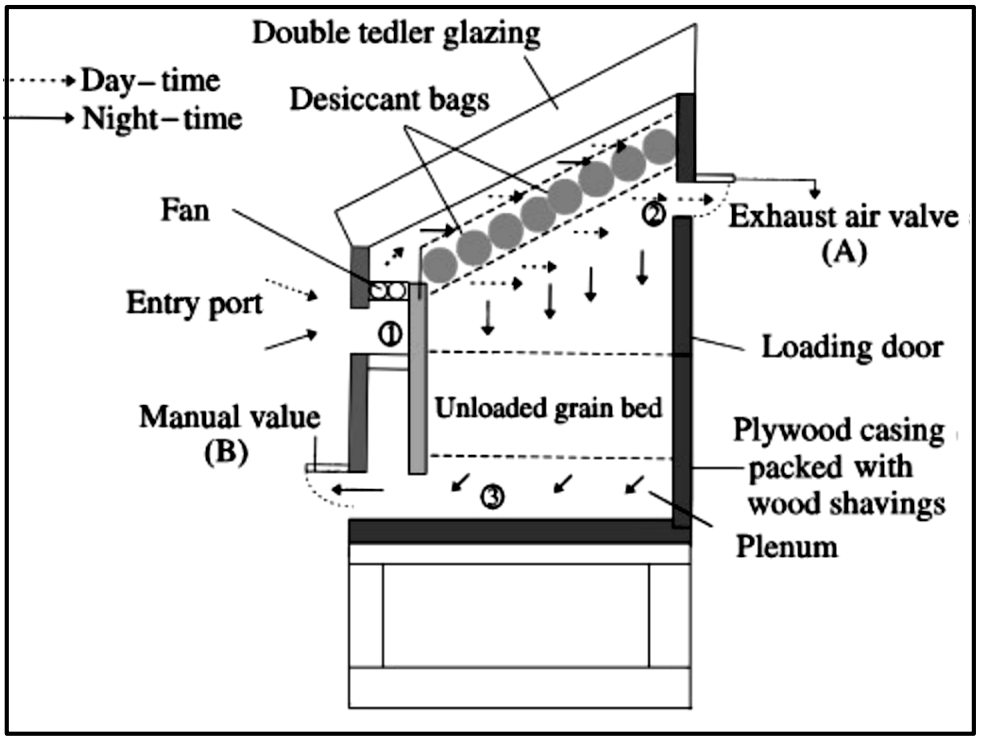


**Figure 2.15** Prototype integrated desiccant/collector dehumidifier mounted on the crop bin (Thoruwa et al. 1998).

**Table 2.1 Comparison of different drying technologies** (Kivevele and Huan 2014; Atuonwu et al., 2010)

| Item | Hot air drying | Vacuum drying | Adsorption drying |
|---|---|---|---|
| Drying efficiency (%) | 35-40 | $\leq 70$ | $\geq 64$ |
| Operating temperature range ($^{o}$C) | 40-90 | 30-60 | 25-50 |
| Operating % relative humidity range | Variable | Low | Low |
| Capital cost | Low | High | Moderate |
| Running cost | High | Very high | Moderate |
| Large scale drying | Suitable | Not suitable | Suitable |

## References

Kemp, I.C., 2005. Reducing dryer energy use by process integration and pinch analysis. Drying Technol., 23(9), 2089-2104.

Mujumdar, A.S., 2007. Principles, classification and selection of dryers. In: Mujumdar, A.S. (ed.), Handbook of Industrial Drying, 3rd ed., Taylor and Francis.

Raghavan, G.S.V., Rennie, F.J., Sunjka, P.S., Orsat, V., Phaphuangwittayakul, W., Terdtoon, P., 2005. Overview of new technologies for drying biological materials with emphasis on energy aspects. Brazillian J. of Chem. Eng., 22(2), 195-201.

Duan X., Zhang M., Mujumdar A.S., Wang R., 2010. Trends in microwave-assisted freeze drying of foods. Drying Technol., 28, 444-453.

Chakraborty, R., Mukhopadhay, P., Bera, M., Suman, S.,2011. Infra-red-assisted freeze drying of tiger prawn: parameter optimization and quality assessment. Drying Technol., 29, 508-519.

Ogura, H., Mujumdar, A.S., 2000. Proposal for a novel chemical heat pump dryer. Drying Technol., 18, 1033-1053.

Abasi, S., Minaei, S., Khoshtaghaza, M.H.: Performance of a recirculating dryer equipped with a desiccant wheel. Dry. Technol. 34, 863–870 (2016). doi:10.1080/07373937.2015.1021421

Ambrosio-Ugri, M.C.B., Taranto, O.P.: Drying in the rotating-pulsed fluidized bed. Brazilian J. Chem. Eng. 24, 95–100 (2007). doi:10.1590/S0104-66322007000100009

De Antonellis, S., Intini, M., Joppolo, C.M., Romano, F.: On the control of desiccant wheels in low temperature drying processes. Int. J. Refrig. (2016). doi:10.1016/j.ijrefrig.2016.06.026

De Antonellis, S., Joppolo, C.M., Molinaroli, L., Pasini, A.: Simulation and energy efficiency analysis of desiccant wheel systems for drying processes. Energy. 37, 336–345 (2012). doi:10.1016/j.energy.2011.11.021

Atuonwu, J.C., Jin, X., van Straten, G., Deventer Antonius, H.C. van, van Boxtel, J.B.: Reducing energy consumption in food drying: Opportunities in desiccant adsorption and other dehumidification strategies. Procedia Food Sci. 1, 1799–1805 (2011). doi:10.1016/j.profoo.2011.09.264

Van Bockstal, P.-J., Corver, J., Mortier, S.T.F.C., De Meyer, L., Nopens, I., Gernaey, K. V., De Beer, T.: Developing a framework to model the primary drying step of a continuous freeze-drying process based on infrared radiation. Eur. J. Pharm. Biopharm. 127, 159–170 (2018). doi:10.1016/J.EJPB.2018.02.025

Zarein, M., Samadi, S.H., Ghobadian, B., 2015. Investigation of microwave dryer effect on energy efficiency during drying of apple slices. J. of Saudi Society of Agri. Sci., 14, 41-47.

Chramsa-ard, W., Jindaruksa, S., Sirisumpunwong, C., Sonsaree, S.: Performance Evaluation of the Desiccant Bed Solar Dryer. Energy Procedia. 34, 189–197 (2013). doi:10.1016/j.egypro.2013.06.747

Chua, K.J., Chou, S.K.: Low-cost drying methods for developing countries. Trends Food Sci. Technol. 14, 519–528 (2003). doi:10.1016/j.tifs.2003.07.003

Dai, Y.J., Wang, R.Z., Xu, Y.X.: Study of a solar powered solid adsorption–desiccant cooling system used for grain storage. Renew. Energy. 25, 417–430 (2002). doi:10.1016/S0960-1481(01)00076-3

Dina, S.F., Ambarita, H., Napitupulu, F.H., Kawai, H.: Study on effectiveness of continuous solar dryer integrated with desiccant thermal storage for drying cocoa beans. Case Stud. Therm. Eng. 5, 32–40 (2015). doi:10.1016/j.csite.2014.11.003

Gill, R.S., Singh, S., Singh, P.P.: Design and development of desiccant seed dryer with airflow inversion and recirculation. J. Food Sci. Technol. 51, 3418–3424 (2012). doi:10.1007/s13197-012-0865-y

Hodali, R., Bougard, J.: Integration of a desiccant unit in crops solar drying installation: Optimization by numerical simulation. Energy Convers. Manag. 42, 1543–1558 (2001). doi:10.1016/S0196-8904(00)00159-X

Irtwange, S. V, Adebayo, S.: Development and performance of a laboratory-scale passive solar grain dryer in a tropical environment. J. Agric. Ext. Rural Dev. 1, 42–49 (2009)

Kivevele, T., Huan, Z.: A review on opportunities for the development of heat pump drying systems in South Africa. 110, 1–11 (2014). doi:10.1590/ sajs.2014/20130236

Koyuncu, T.: An Investigation on the performance Improvement of greenhouse-type agricultural dryers. Renew. Energy. 31, 1055–1071 (2006). doi:10.1016/j.renene.2005.05.014

Madhiyanon, T., Adirekrut, S., Sathitruangsak, P., Soponronnarit, S.: Integration of a rotary desiccant wheel into a hot-air drying system: Drying performance and product quality studies. Chem. Eng. Process. Process Intensif. 46, 282–290 (2007). doi:10.1016/j.cep.2006.06.008

Nagaya, K., Li, Y., Jin, Z., Fukumuro, M., Ando, Y., Akaishi, A.: Low-temperature desiccant-based food drying system with airflow and temperature control. J. Food Eng. 75, 71–77 (2006). doi:10.1016/j.jfoodeng.2005.03.051

Patil, K.S., Mahajan, S.D., Burkul, S.R.: Experimentation of solar dryer with desiccant material for agricultural products. 1–7 (2015)

Pourfarzad, A., Habibi Najafi, M.B., Haddad Khodaparast, M.H., Hassanzadeh Khayyat, M.: Optimization of osmo-vacuum drying of pear (Pyrus communis L.) using response surface methodology. Qual. Assur. Saf. Crop. Foods. 7, 687–696 (2015). doi:10.3920/QAS2014.0447

Gunasekaran, S., 1999. Pulsed microwave-vacuum drying of food materials. Drying Technology, 17(3), 395e412.

Rane, M. V., Reddy, S.V.K., Easow, R.R.: Energy efficient liquid desiccant-based dryer. Appl. Therm. Eng. 25, 769–781 (2005). doi:10.1016/j.applthermaleng.2004.07.015

Shanmugam, V., Natarajan, E.: Experimental investigation of forced convection and desiccant integrated solar dryer. Renew. Energy. 31, 1239–1251 (2006). doi:10.1016/j.renene.2005.05.019

Shanmugam, V., Natarajan, E.: Experimental study of regenerative desiccant integrated solar dryer with and without reflective mirror. Appl. Therm. Eng. 27, 1543–1551 (2007). doi:10.1016/j.applthermaleng.2006.09.018

Sivakumar, R., Elayaperumal, A., Saravanan, R.: Studies on combined cooling and drying of agro products using air cooled internal heat recovered vapour absorption system. Appl. Therm. Eng. 97, 100–108 (2016). doi:10.1016/j.applthermaleng.2015.10.045

Thoruwa, T.F., Johnstone, C., Grant, A.., Smith, J.: Novel, low cost CaCl2 based desiccants for solar crop drying applications. Renew. Energy. 19, 513–520 (2000). doi:10.1016/S0960-1481(99)00072-5

Thoruwa, T.F.N., Grant, A.D., Smith, J.E., Johnstone, C.M.: A Solar-regenerated Desiccant Dehumidifier for the Aeration of Stored Grain in the Humid Tropics. J. Agric. Eng. Res. 71, 257–262 (1998). doi:10.1006/jaer.1998.0321

Zhao, Y., Dai, Y.J., Ge, T.S., Wang, H.H., Wang, R.Z.: A high performance desiccant dehumidification unit using solid desiccant coated heat exchanger with heat recovery. Energy Build. 116, 583–592 (2016). doi:10.1016/j.enbuild.2016.01.021

Kivevele, T., Huan, Z.: A review on opportunities for the development of heat pump drying systems in South Africa. 110, 1–11 (2014). doi:10.1590/ sajs.2014/20130236

Atuonwu, J.C., Straten, G. van., Deventer, H.C. van., Boxtel, A.J.B. van. (2010). Modeling and energy efficiency optimization of a low temperature adsorption based food dryer. In Proceedings of the International Drying Symposium, Magdeburg, Germany, October 3 – 6, 2010, 423-431.

CHAPTER 3

# STEADY-STATE INVESTIGATION OF DESICCANT DRYING SYSTEM FOR AGRICULTURAL APPLICATIONS

# Chapter 3

# STEADY-STATE INVESTIGATION OF DESICCANT DRYING SYSTEM FOR AGRICULTURAL APPLICATIONS

This chapter presents the applicability of desiccant drying system (DDS) for the drying of cereals grain at low temperature and lower humidity. The performance of two drying approaches with two desiccant materials i.e. silica gel and lithium chloride (LiCl) have been analyzed by a desiccant dehumidification model available in literature. Two desiccant drying cases discussed are: Case-I, latent load control effect, Case-II both latent and sensible load control effect. Case-I approach seems more effective towards the drying of delicate and temperature sensitive agricultural product like seeds. However, results showed that Case-II gives more economical and energy saving drying solution for the commercial purpose drying.

## 3.1 Introduction

Drying is a conventional preservation/storage technique which is under practiced from ancient time. Market of dry fruits and vegetables has achieved an earnest abode in the world market (Funebo and Ohlsson, 1998). For example Japan spent 6 billion USD on dry vegetables and seaweed in 1998, which does not include the consumption in restaurants (Japan statistics bureau, 2000). Agricultural products are harvested at higher moisture content than that of safe storage level of moisture in order to avoid the shattering or other losses. Consequently drying is considered an important post-harvest technique for the safe storage of agricultural product. In addition, selling of agricultural products and storage for whole year consumption also require to reduce the moisture level and low temperature storage (Sultan et al., 2018a). There are many drying techniques applied for the removal of moisture from the agricultural products. The basic principle is to create vapor pressure deficit between the product and environment to accelerate the moisture removal. Conventional drying methods

include, drying by airflow, vacuum drying, and freeze-drying but these methods result in low drying rate (Clary et al., 2005; Zhang et al., 2003; Zhang et al., 2005).

High temperature drying causes loss of nutrients and vitamin C, found in agricultural products (Marfil et al., 2008) In addition to higher drying air temperature, higher humidity also affects the color of drying product (Madhiyanon et al., 2007).

Figures 3.1(a)-(b) showed the equilibrium moisture contents (EMC) with relation to temperature and humidity ratio for wheat, barley, rice and corn, respectively. In drying process EMC is the indication of the effect of the water activity which can determine the biological changes in the storage. The significance of humidity control can be seen Figure 3.1, thereby dehumidified air requires low drying temperature in order to achieve 14% EMC. However, in case of higher humidity ratio, higher drying air temperature is required to achieve optimum level of EMC e.g. 14% for wheat. The DDS has ability to dry the agricultural products at low temperature and low humidity ratio. Total drying time reduced by increasing the drying air temperature, flow rate and using less humid air. However, increase in temperature and flow rate is not always favorable because of quality loss and high energy consumption.

Many studies have been reported on desiccant materials for moisture adsorption equilibrium (Dai et al., 2018; Sultan et al., 2015; Gold-worthy and white 2012) and adsorption rate (Hong et al., 2016; Sultan et al., 2016a). On the other hand steady-state investigation of desiccant drying systems for agricultural applications has not been extensively studied in the literature (Madhiyanon et al., 2007; Atuonwu et al., 2011; Atuonwu et al. 2012). From the above prospective, drying charts are developed in this study for four types of grains (i.e. wheat, barley, corn and rice). It will help to select the drying air conditions according to the different drying applications/stages. Two cases of desiccant drying are considered and optimized accordingly for the purpose of seed and commercial drying at the expense of minimum energy. DDS can also play a role to reduce the drying time by providing fast adsorption rate. Present study discusses energy consumption for two different desiccant drying approaches. It is worth mentioning that the drying rate is not considered for the simplicity of analysis.

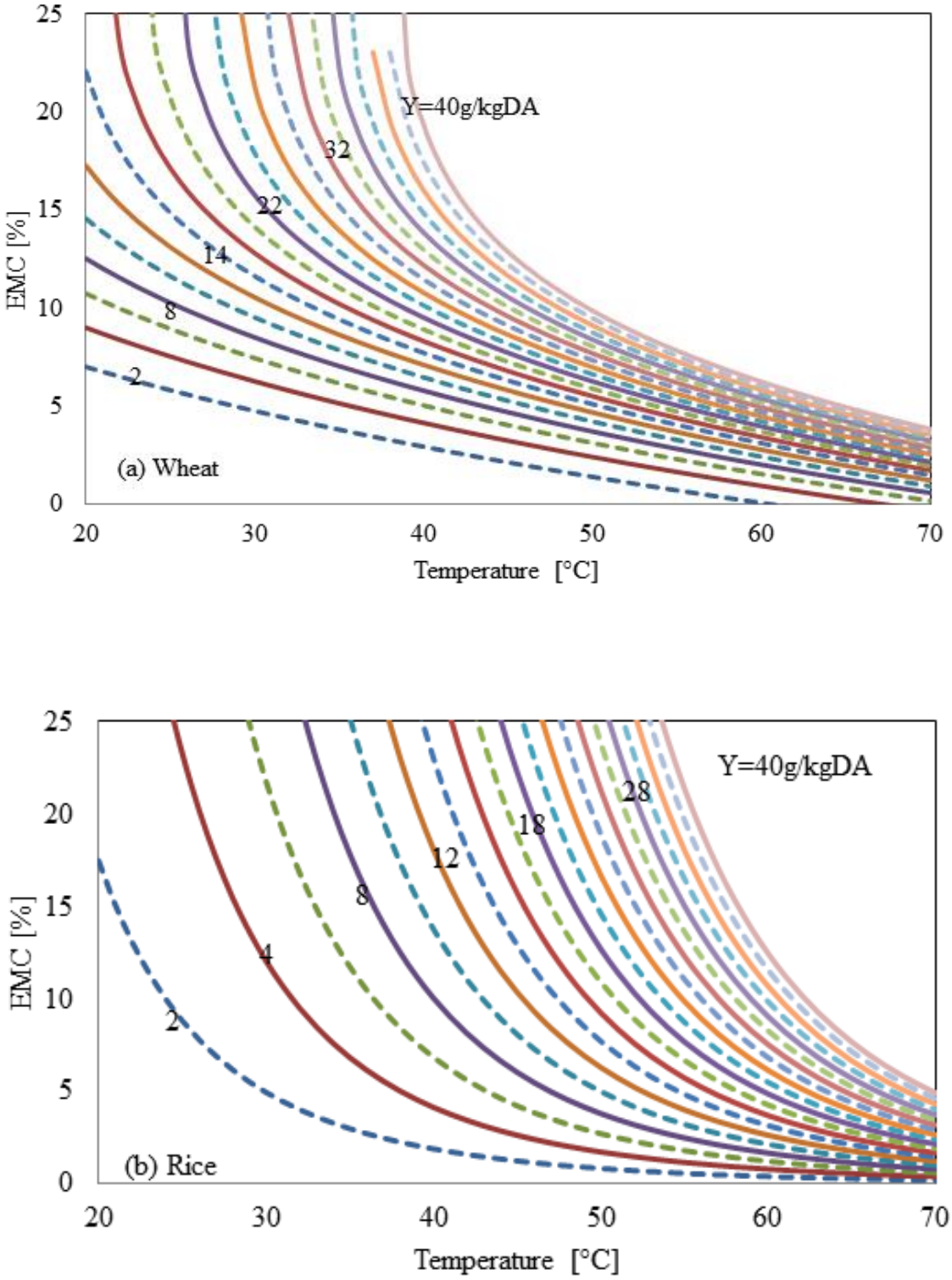


**Figure 3.1 (a)** Effect of temperature and humidity ratio on EMC for wheat and rice.

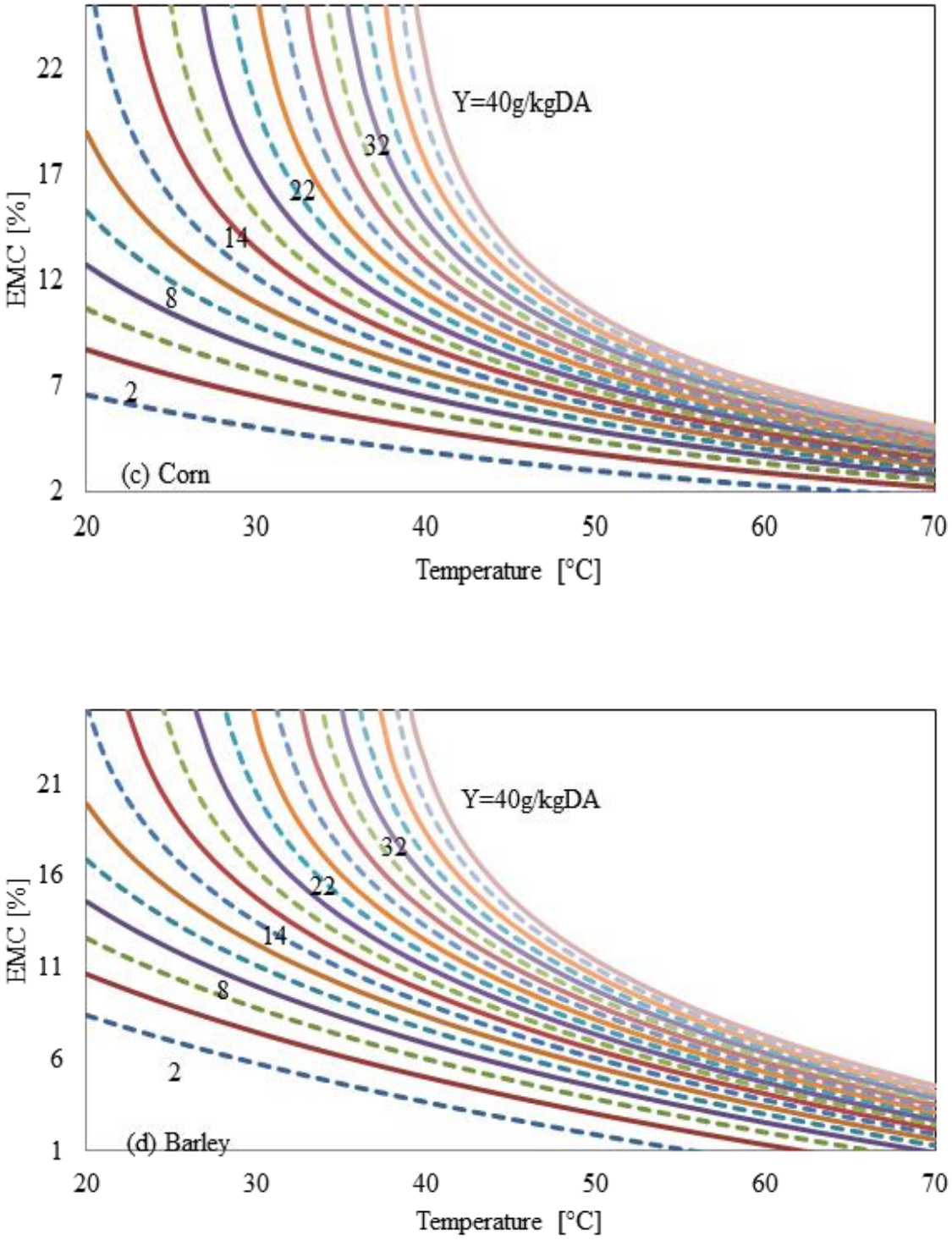


**Figure 3.1 (b)** Effect of temperature and humidity ratios on EMC for barley and corn.

## 3.2 Development of drying charts

Equilibrium moisture contents (EMC) is the function of temperature and relative humidity of drying air. The knowledge of EMC is important for the development of control strategies for the safe storage of agricultural products. Different types of grains require different amount of moisture level for storage. For the storage of one year, the dry-bulb MC of wheat, barley, corn and rice should be reduced up to the level of 13%, 13%, 14% and 15%, respectively (Bruce, 2018; AAFC, 1987; Rice knowledge bank, 2018). Figures 3.2 (a)-(b), present various possible combination of temperature and humidity of drying air by which safe storage moisture level can be achieved. However, maximum allowable drying temperature and humidity are the factors which further limit these possible drying air combinations. As the maximum recommended drying air temperature for the purpose of seed are 60ºC, 45ºC, 45ºC and 42ºC for wheat, corn, barley and rice, respectively (AAEC, 1987). Whereas for commercial usage maximum recommended drying air temperature are 65ºC , 55ºC, 60ºC (AAEC, 1987) and 50ºC (Rice knowledge bank, 2018) for wheat, corn barley and rice, respectively.

Quality of supply air can be ensured by maintaining the temperature, humidity and flow rate which helps to remove the respiratory heat, $CO_2$ and $O_2$ level in the storage. DDS is capable of maintaining these parameters to ensure the quality of drying. In Figures 3.2(a)-(b), it has been shown that many possible combinations can be formed by following the required EMC line. However possible combination includes high temperature with high humidity and low temperature with low humidity. It has been shown that if the latent load of the supply air is controlled, same EMC is achieved at lower temperature. Low temperature as well as low humidity is considering favorable drying conditions for conservation of nutrients (Kosuke et al., 2006). In this way, DDS helps to achieve these conditions by lowering the humidity of drying air (Mahmood et al., 2015).

## 3.3 Proposed desiccant drying system

Figure 3.3 represents the schematic diagrams of the proposed solid desiccant based drying system. It mainly consists of: (i) a desiccant wheel used to dehumidify the air; (ii) heater for process air heating (bio-mass/gas or electric); (iii) drying bin/structure; (iv) heater for regeneration of desiccant wheel (electric driven or preferably bio-mass/gas driven).

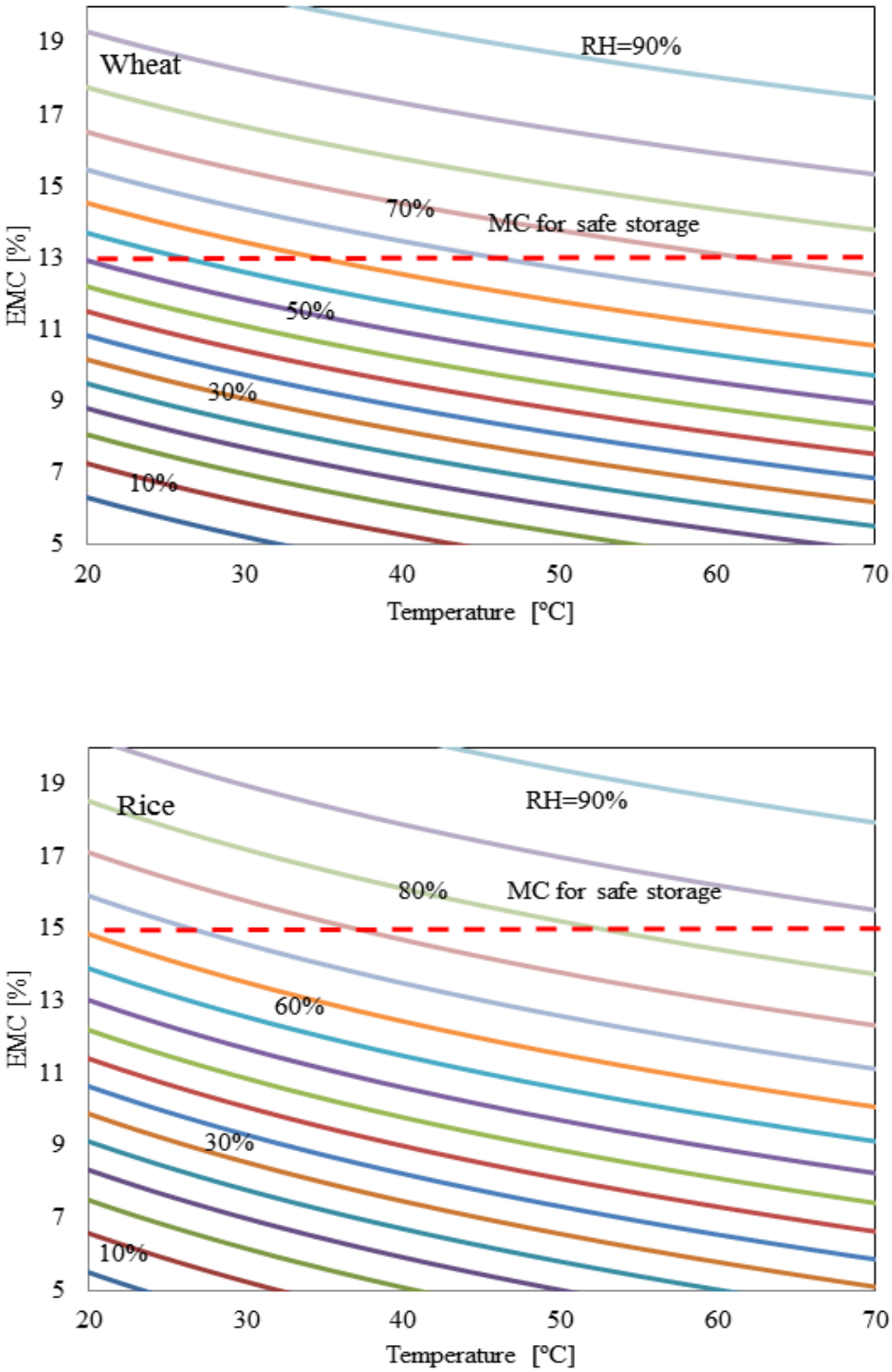


**Figure 3.2 (a)** Drawing chart for wheat and rice.

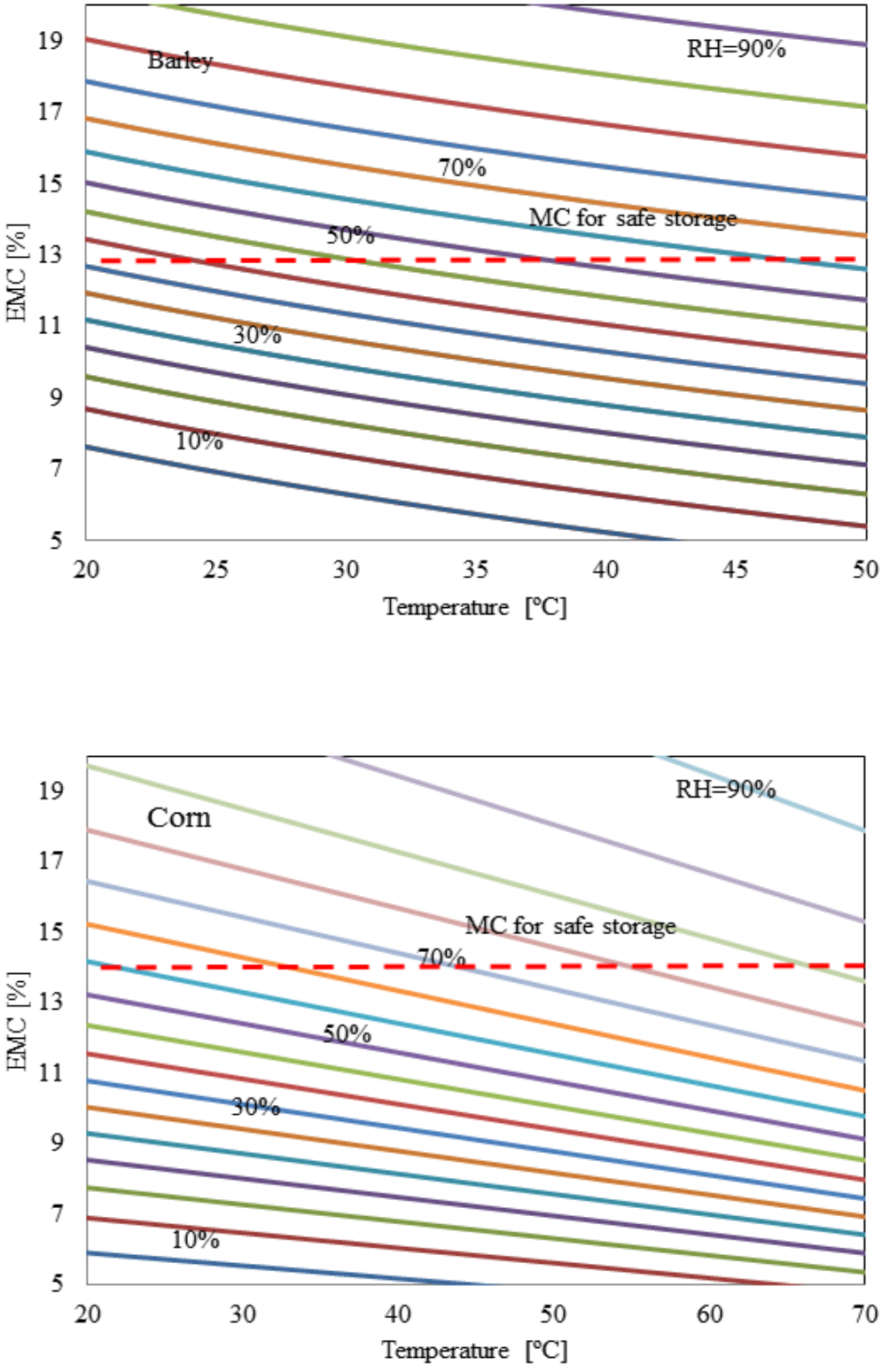


**Figure 3.2 (b)** Drawing chart for Barley and Corn.

When air passes through these components it undergoes alteration of psychrometric air conditions. Dehumidification of the air, heating of the dehumidified air, evaporation of product moisture and heating of regeneration air are represented by point 1 to 7 in Figure. 3.3.

Point 1 represents the ambient air condition at the inlet of desiccant wheel. Point 2 represents the dehumidified air condition at the outlet of desiccant wheel. Point 3 represents the heating of drying air at required temperature. Processed air is supplied to the inlet of the drying structure, while passing through the drying structure, its humidity increases as moisture is absorbed by the air due to vapor pressure deficit (Sultan et al., 2016b) and leaves the DDS at point 4. Ambient air is heated from point 5 to 6 at required regeneration temperature and pass through the desiccant wheel.

Solar or thermal waste water heat could be used for the regeneration of desiccant wheel (Miyazaki et al., 2011). Air simultaneously passes through the adsorption and regeneration sides of desiccant wheel during drying process.

## 3.4. Materials and methods

### 3.4.1 Materials

In present study two desiccant materials used are silica gel and LiCl. Desiccant material silica gel is reported as most commonly used desiccant material used in desiccant air conditioning due to its strong affinity towards moisture (Pramuang and Exell, 2007) and can absorb 40% of its own weight (Beccali et al., 2003)

Desiccant material LiCl is a hygroscopic salt and also one of the important desiccant materials used for the dehumidification. LiCl has strong affinity towards moisture and can absorb water vapor as a solid desiccant. It continues to attract moisture even turn in to liquid solution (Beccali et al., 2002).

### 3.4.2 Research methodology

In present study two desiccant drying cases discussed are:

Case-I: Latent load control effect (Regeneration air temperature $T_6$ changes 50ºC, 55ºC, 60ºC, 65ºC, 70ºC, 75ºC and 80ºC to get different levels of humidity ratio)

Case-II: Latent and sensible load control effect (Drying air temperature $T_3$ is changes 50ºC,

52ºC, 54ºC, 56ºC, 58ºC and 60ºC for humidity ratio $Y_2$ 0.010 and 0.008 kg/kg DA).

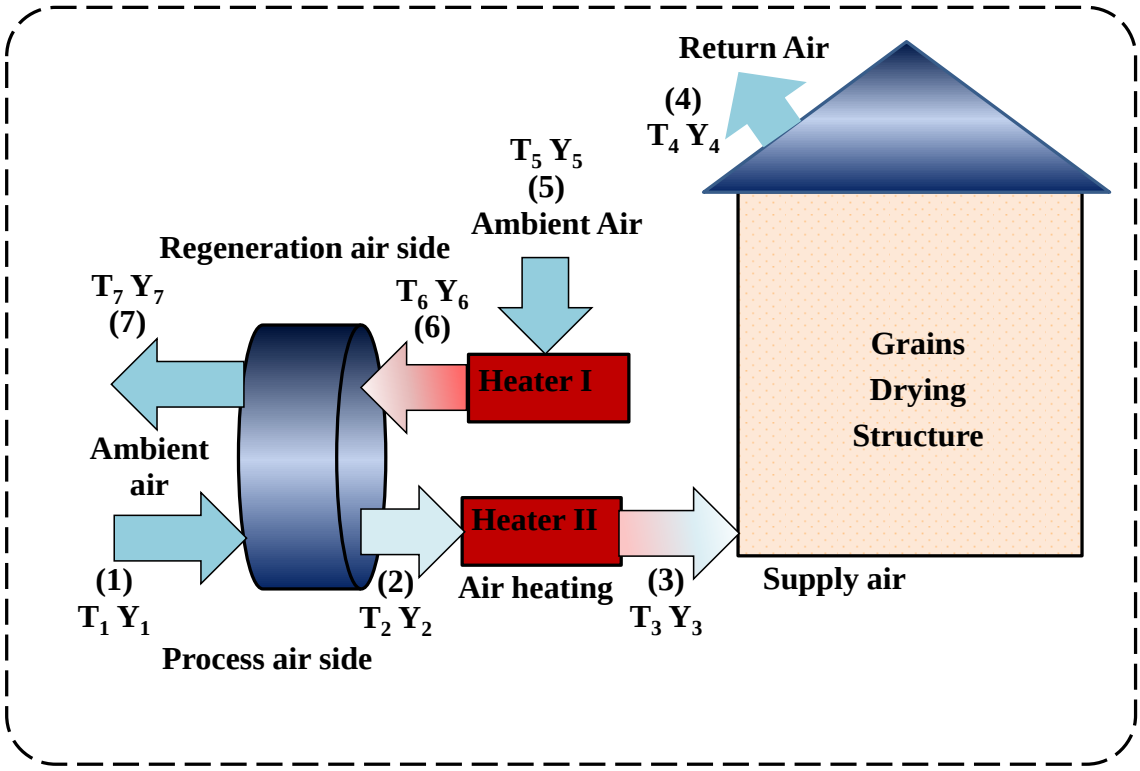


**Figure 3.3** Schematic diagram of desiccant drying system.

For Case-I various levels of humidity ratio of process air are obtained at regeneration air temperature 50ºC, 55ºC, 60ºC, 65ºC, 70ºC, 75ºC and 80ºC. Figure 3.4(a) is the psychrometric representation of Case-I where point 1 is the ambient air conditions $T_1$ 25ºC and $Y_1$ 0.014 kg/kg DA. Point 2 represents various levels of dehumidification achieved at different regeneration temperature. For desiccant material silica gel, temperature of process air is 40ºC, 43ºC, 45ºC, 47ºC, 49ºC, 51ºC and 52ºC and humidity ratio is 0.0097, 0.0089, 0.0083, 0.0077, 0.0072, 0.0068 and 0.0064 kg/kg DA at regeneration temperature 50ºC, 55ºC, 60ºC, 65ºC, 70ºC, 75ºC and 80ºC, respectively. However for desiccant material LiCl temperature of process air is 41ºC, 44ºC, 46ºC, 48ºC, 50ºC, 52ºC and 54ºC and humidity ratio is 0.0104, 0.0093, 0.0087, 0.0082, 0.0077, 0.0073 and 0.007 kg/kg DA at regeneration temperature 50ºC, 55ºC, 60ºC, 65ºC, 70ºC, 75ºC and 80ºC, respectively.

Point 2 and 3 are same for Case-I as process air without heating supplied to the outlet of drying structure. Point 4 represents the exhaust air from the drying structure and it is assumed that temperature of the air at point 4 is equal to the wet bulb. Point 5 is the start of regeneration stream, $T_5$ 25ºC $Y_5$ 0.014 kg/kgDA. Point 6 represents the heating of ambient air

at 50ºC, 55ºC, 60ºC, 65ºC, 70ºC, 75ºC and 80ºC for regeneration of desiccant wheel.

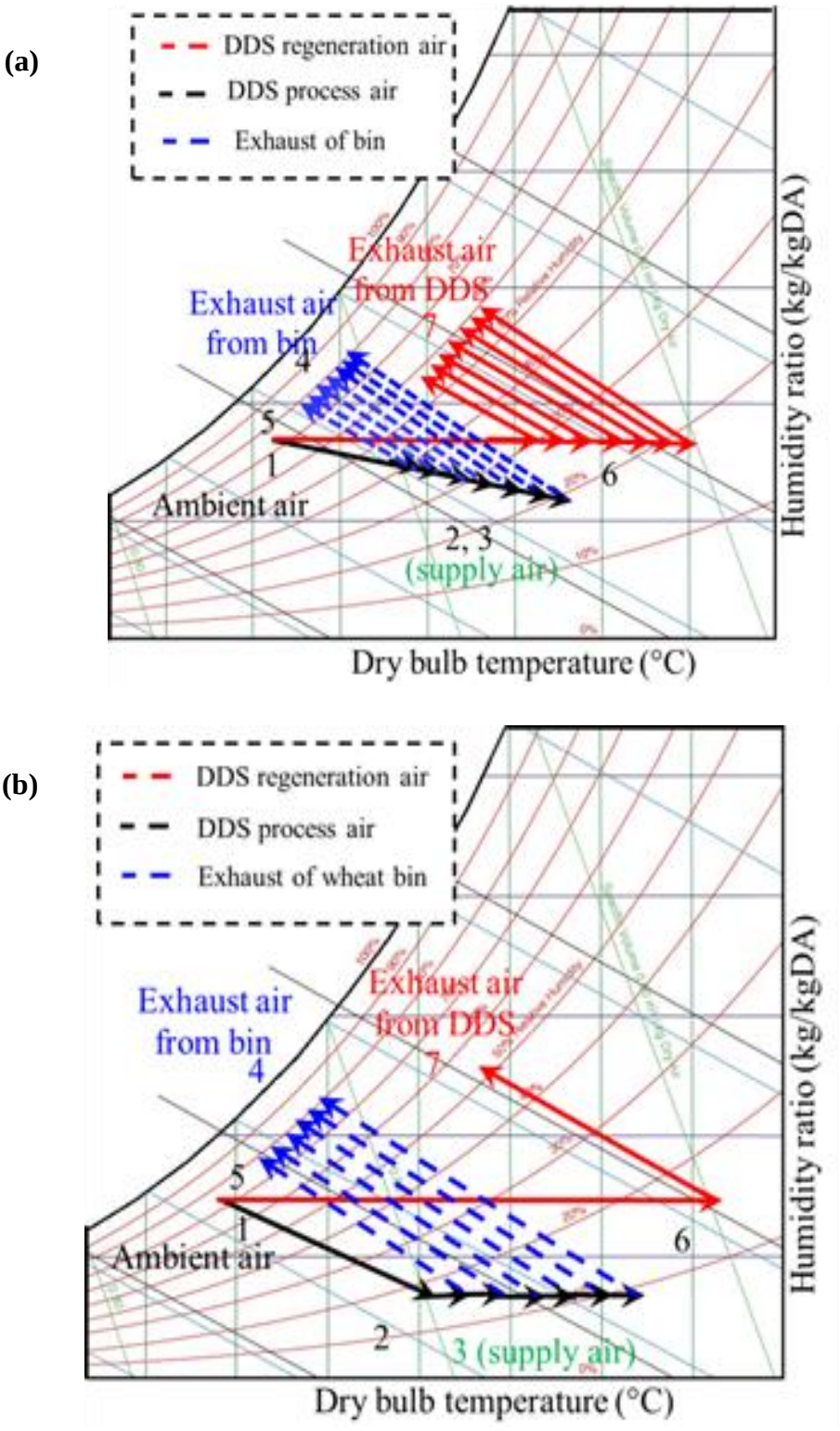


**Figure 3.4 (a)** Psychrometric representation of case-I (i.e. latent load control), **(b)**.Psychrometric representation of Case-II (i.e. latent and sensible load control)

Point 7 represents the air conditions at the outlet of regeneration side of desiccant.

For Case-II, process air at humidity ratio $Y_2$ (0.010 and 0.008) kg/kgDA are heated at various levels of drying air temperature $T_3$ 50ºC, 52ºC, 54ºC, 56ºC, 58ºC and 60ºC. Figure 3.4(b) is the psychrometric representation of the Case-II where point 1 is the ambient air conditions $T_1$ 25ºC and $Y_1$ 0.014 kg/kgDA. Point 2 is the process air conditions after passing through the desiccant and temperature of the air is 39ºC for desiccant material silica gel and 42ºC for desiccant material LiCl at humidity ratio 0.010 kg/kgDA. However at humidity ratio 0.008 kg/kgDA temperature of process air is 46ºC for desiccant material silica gel and 50 ºC for desiccant material LiCl. Point 3 represents sensible heating of the process air at temperature 50ºC, 52ºC, 54ºC, 56ºC, 58ºC and 60ºC and permits it to flow through the drying structure. Point 4 is the air conditions at the outlet of drying structure and temperature is assumed to be equal to wet bulb. Point 5 to 6 represents the heating of ambient air for the purpose of regeneration of desiccant and regeneration temperature is 48ºC for desiccant material silica gel and 51ºC for desiccant material LiCl at humidity ratio 0.010 kg/kgDA. However at humidity ratio 0.008 kg/kgDA temperature of regeneration air is 63ºC for desiccant material silica gel and 68ºC for desiccant material LiCl. Point 7 is the air conditions at the outlet of regeneration side of desiccant.

Air conditions for point 1 to 7 are determined as follow:

- Point 1 ambient air condition T1 25ºC and Y1 0.014 kg/kgDA.
- At point 2 ambient air is dehumidified $Y_1$ to $Y_2$ and temperature increases from $T_1$ to $T_2$ due to heat of adsorption released by desiccant material. For determining the air conditions at point 2 Beccali et al model is used. In Case-I different levels of humidity ratio are determined for all regeneration temperatures. Whereas in Case-II sensible load effect is determined for all drying air temperature at drying air humidity ratio 0.010 and 0.008 kg/kg DA.
- Point 3 represents the sensible heating of the air by using biomass/electric air heater. In Case-I process air is not heated. However for Case-II process air is heated at different temperature levels 50ºC, 52ºC, 54ºC, 56ºC, 58ºC and 60ºC. Point 3 air conditions are also used to estimate the EMC which determined the quantity of moisture removed from the grains through its one pass.
- Point 4 represents the air conditions at the outlet of the drying structure. Air carries moisture from the grains and its temperature decreases and humidity increases.

- Point 5 is ambient air conditions and start of regeneration stream where $T_5 = T_1$, $Y_5 = Y_1$
- Point 6 represents the heating of air for the purpose of regeneration of desiccant.$T_6$ is determined by solving Eq. (3.1) or (3.2) (depending on the type of desiccant material used) with Eq. (3.4) simultaneously.
- Point 7 represents the outlet air condition of the regeneration side of the desiccant wheel.

The equations 1-4 describe the (Beccali et al., 2003) model. For the calculation of enthalpy corresponding to the type of desiccant wheel Eq. (3.1) and (3.2) are used for desiccant material silica gel and LiCl respectively.

$$h_2 = (0.1312h_6 + 0.8688h_1) \tag{3.1}$$

$$h_2 = (0.1861h_6 + 0.8139h_1) \tag{3.2}$$

Where $h_1$, $h_2$, *and* $h_6$ are the enthalpy of air conditions at inlet of adsorption side, outlet of adsorption side and inlet of regeneration side of desiccant wheel (kJ $kg^{-1}$), respectively. Enthalpy as a function of absolute humidity and temperature at particular point is calculated by Eq. (3.3):

$$h = \frac{(2501 + 1.805T)}{1000} + 1.006T \tag{3.3}$$

Relative humidity at point 2 is determined by using the relative humidity at point 1 and 6 (Beccali et al., 2002):

$$RH_2 = (0.9428RH_6 + 0.0572RH_1) \tag{3.4}$$

At particular point, RH is determined as a function of absolute humidity and temperature by following empirical relation (Beccali et al., 2002).

$$RH = (18.6715Y + 1.7976)e^{-0.053T} \tag{3.5}$$

EMC is a function of drying air temperature and relative humidity. Its values are

determined by using Eq. (3.6) and (3.7) for wheat, rice, barley and Corn. Modified-Chung-Pfost equation is used for wheat, barley and rice.

$$EMC = \frac{1}{-C_3}\ln\left(\frac{T_3 + C_2}{-C_1}\ln RH_3\right) \tag{3.6}$$

Eq. (3.6) uses three empirical coefficients i.e. $C_1$, $C_2$, and $C_3$, which are taken from the literature and suppose to best fitted against the moisture isotherm equations for selected cereals (wheat, barley and rice). In this study, the numerical values of the optimized parameters of $C_1$, $C_2$, and $C_3$ for desorption isotherms of wheat are 545.25, 64.047 and 0.17316, respectively (Sun and Woods, 1994) and for barley are 338.032, 16.581 and 0.182 respectively (Gely and Pagano, 2012) and for rice are 227.091, 16.912 and 0.179 (Sun, 1998). However Modified Oswin equation is used for the determination of EMC of corn, empirical coefficient $C_1$, $C_2$, and $C_3$ associated with the equation are 13.9005, -0.076819 and 2.96243 respectively (Aguerre et al., 2003).

$$EMC = \frac{C_1 + C_2 T_3}{\left(\frac{1}{RH_3} - 1\right)^{\frac{1}{C_3}}} \tag{3.7}$$

Energy required for the regeneration of desiccant and heating of drying air is calculated by using Eq. (3.7) (Motevali et al., 2014).

$$Q_{total} = F_a C_p (T_3 - T_2) + F_a C_p (T_6 - T_5) \tag{3.8}$$

where $F_a$ is the air mass flow rate (kg $s^{-1}$)during regeneration and heating; $C_p$ is the specific heat capacity of air (kJ $kg^{-1}K^{-1}$);$T_2$, $T_3$, $T_5$ and $T_6$ are the desiccant wheel outlet air temperature, drying air temperature, ambient air temperature and regeneration temperature (ºC), respectively.

Performance index, Φ (kg $kW^{-1}$) is introduced in order to evaluate the desiccant drying approaches. The Φ can be defined as amount of moisture removed per unit drying energy.

$$\Phi = \frac{DM(EMC_{initial} - EMC_{drying\ cond.})}{Q_{total}} \tag{3.9}$$

where *EMC*, *DM* and $Q_{total}$ are the equilibrium moisture content (-) at ambient condition,

equilibrium moisture content (-) at particular drying air condition, dry matter (kg) and total thermal energy for heating and regeneration of the air (kJ $s^{-1}$), respectively.

## 3.5 Results and discussion

To determine the effect of latent load control, ambient air is dehumidified at various levels of humidity ratio by changing the regeneration air temperature from 50ºC to 80ºC. Figures 3.5(a)-(b) represent the process air conditions at different levels of regeneration air temperature for desiccant materials; silica gel and LiCl. In addition Figures 3.5(a)-(b) also represent the EMC curves at different levels of RH and temperature for four types grains. EMC at particular drying condition determined the drying potential of the air. This is due to the fact that drying depends on the vapor pressure gradient (Sultan et al., 2016) and DDS helps by removing the moisture from drying air by adsorption. The main tenacity of drawing the process air conditions on EMC curves are to compare the EMC values developed by particular regeneration temperature. It has been found that by increasing the regeneration temperature, EMC value decreases for both desiccant materials.

Total thermal energy required for the regeneration of desiccant is calculated for Case-I. Figure 3.6 represents the total thermal energy required at different regeneration temperature 50ºC, 55ºC, 60ºC, 65ºC, 70ºC, 75ºC and 80ºC. It has been found that as the regeneration temperature increases from 50 ºC to 80ºC for both desiccant materials, Q also increases from 12.66-27.85kJ $s^{-1}$.

Increase in thermal energy input is due to the fact that increase in regeneration temperature, provides more dehumidified process air (Sultan et al., 2018b). Desiccant material silica gel produces more dehumidified air under same regeneration temperature as compared to LiCl. However temperature of processed air is lower for silica gel which shows that for the drying of temperature sensitive grains. On other hand desiccant material LiCl, process air conditions develop low EMC at same regeneration temperature which showed that LiCl is more economical to use regarding the thermal energy consumption.

Figure 3.7 represents the performance index for 1000 kg of grains at different levels of regeneration temperature. Higher value of Φ at low regeneration temperature represented that drying air can carry more moisture in one pass at the consumption of less energy as represented by Eq. (3.9). It has been shown that value of Φ decreases as the regeneration temperature increases.

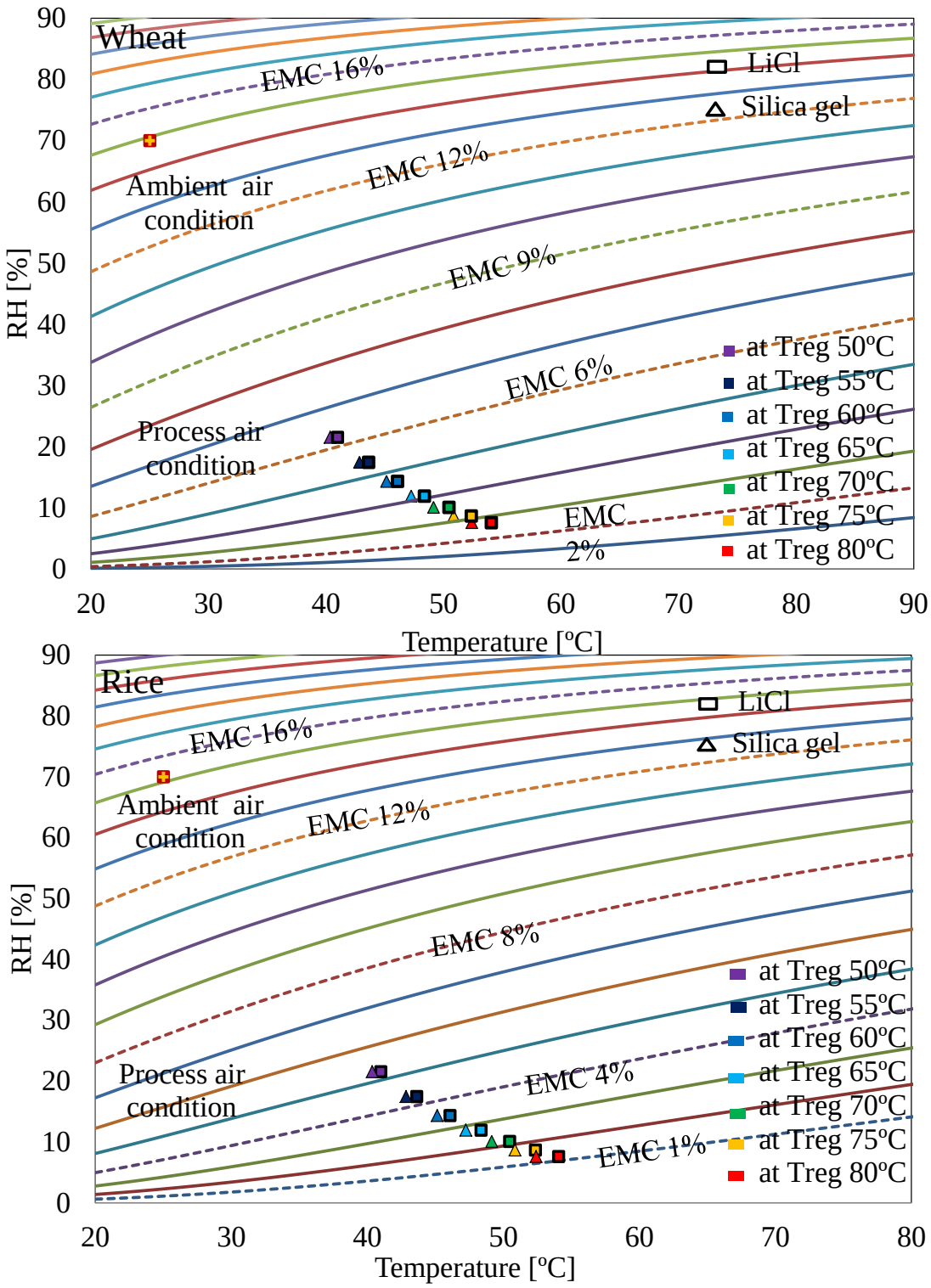


**Figure 3.5 (a)** Pictorial representation of process air conditions at different levels of regeneration temperature on EMC chart for Case-I for wheat and rice.

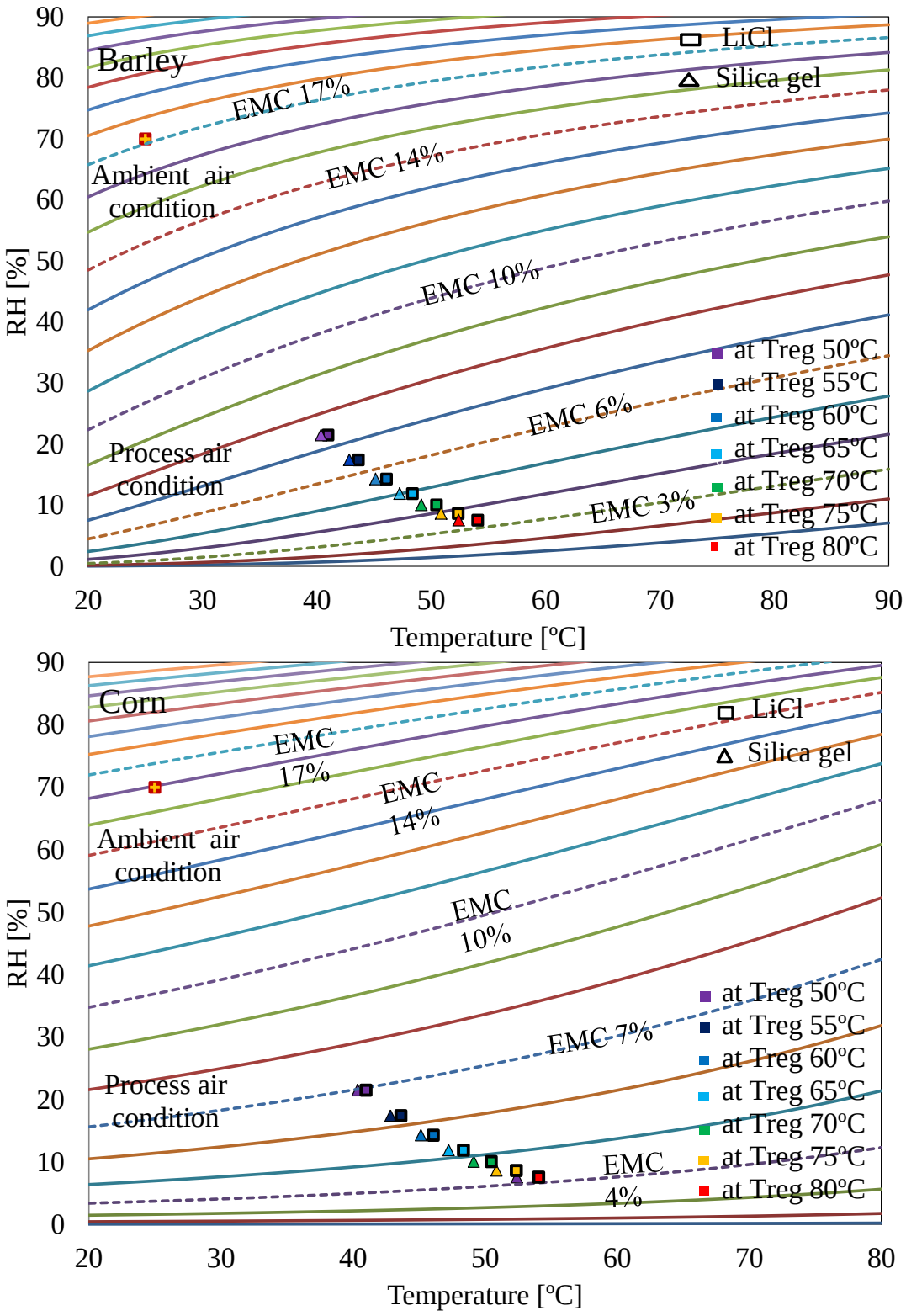


**Figure 3.5 (b)** Pictorial representations of process air conditions at different levels of regeneration temperature on EMC chart for Case-I for barley and corn.

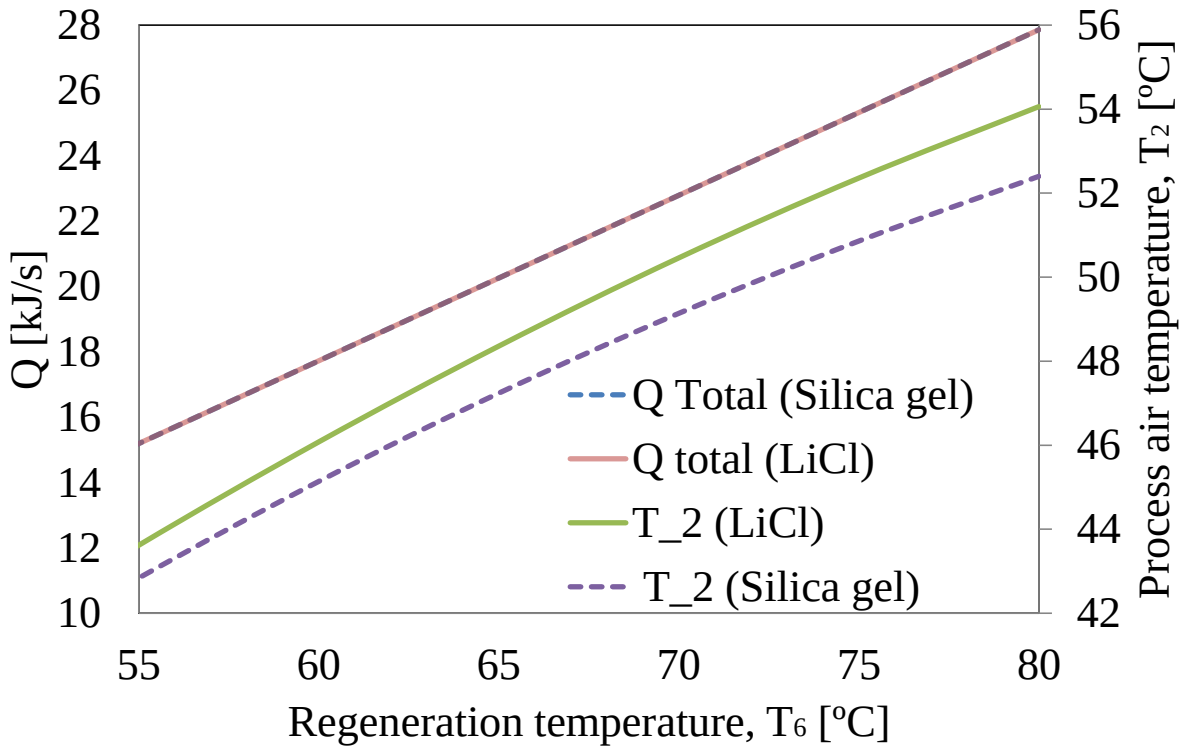


**Figure 3.6** Total thermal energy and process air temperature required for Case-I at regeneration temperature ranging from 50ºC-80ºC.

As increase in regeneration temperature accompanied by the increase in total input energy but on the other hand there is no significant change in the process air temperature and humidity ratio as also shown by Figures 3.5(a)-(b).

Case-I optimum drying air conditions founded are at minimum regeneration temperature 50ºC for all types of grains. It also showed that there is no significant difference between the value of Φ of desiccant material silica gel and LiCl. However Φ varies at different regeneration temperatures from 6.4 to 3.90 kg $kW^{-1}$for wheat grains, 6.74 to 4.30 kg $kW^{-1}$for barley, 5.58 to 3.31 kg $kW^{-1}$for corn and 6.25 to 4.00 for rice in case of LiCl. However, desiccant material silica gel it varies from 6.35 to 3.87 kg $kW^{-1}$for wheat, 6.70 to 4.26 kg $kW^{-1}$for barley, 5.36 to 3.29 for corn and 6.21 to 3.95 kg $kW^{-1}$for rice.

Case-II is determined by dehumidifying the air at humidity ratio 0.010 kg/kg DA and 0.008 kg/kg DA and then heating of the dehumidified air at various temperatures 50ºC, 52ºC, 54ºC, 56ºC, 58ºC and 60ºC.

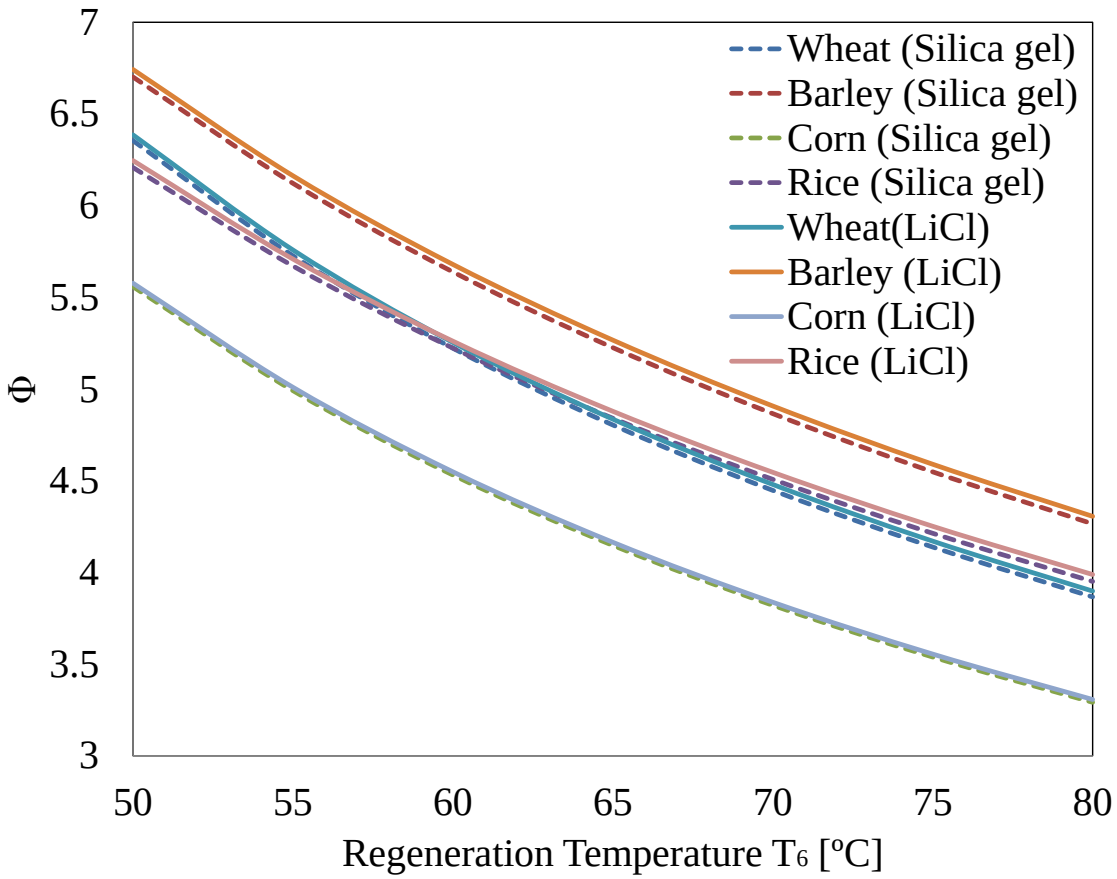


**Figure 3.7** Effect of regeneration temperature on performance index for Case-I.

Figure 3.8(a)-(b) represents the process air conditions of Case-II. EMC curves are determined for four types of grains and process air conditions are plotted on it for Case–II. It has been shown that for both desiccant materials at particular humidity ratio, processed air have same value of EMC as heating temperature is same. However lower value of EMC is obtained by increasing the drying air temperature. Total thermal energy required to hold the latent and sensible load control effect is also determined for Case-II.

Figure 3.9 presents the total thermal energy required for regeneration and heating of the process air at humidity ratio of 0.010 and 0.008 kg/kg DA at different levels of temperature 50ºC, 52ºC, 54ºC, 56ºC, 58ºC and 60ºC. It has been found that for desiccant material silica gel and LiCl, Q increases by increasing the drying air temperature from 13.65-17.7 kJ $s^{-1}$ for silica gel and 13.86-17.92 kJ $s^{-1}$for LiCl at humidity ratio 0.010kg/kg DA. Whereas for humidity ratio 0.008kg/kg DA, it varies from 16.72-20.77 kJ $s^{-1}$ for desiccant material silica gel and 17.50-21.55 kJ $s^{-1}$ for desiccant material LiCl. The reason of higher thermal energy at 0.008kg/kg DA is that it requires high regeneration temperature.

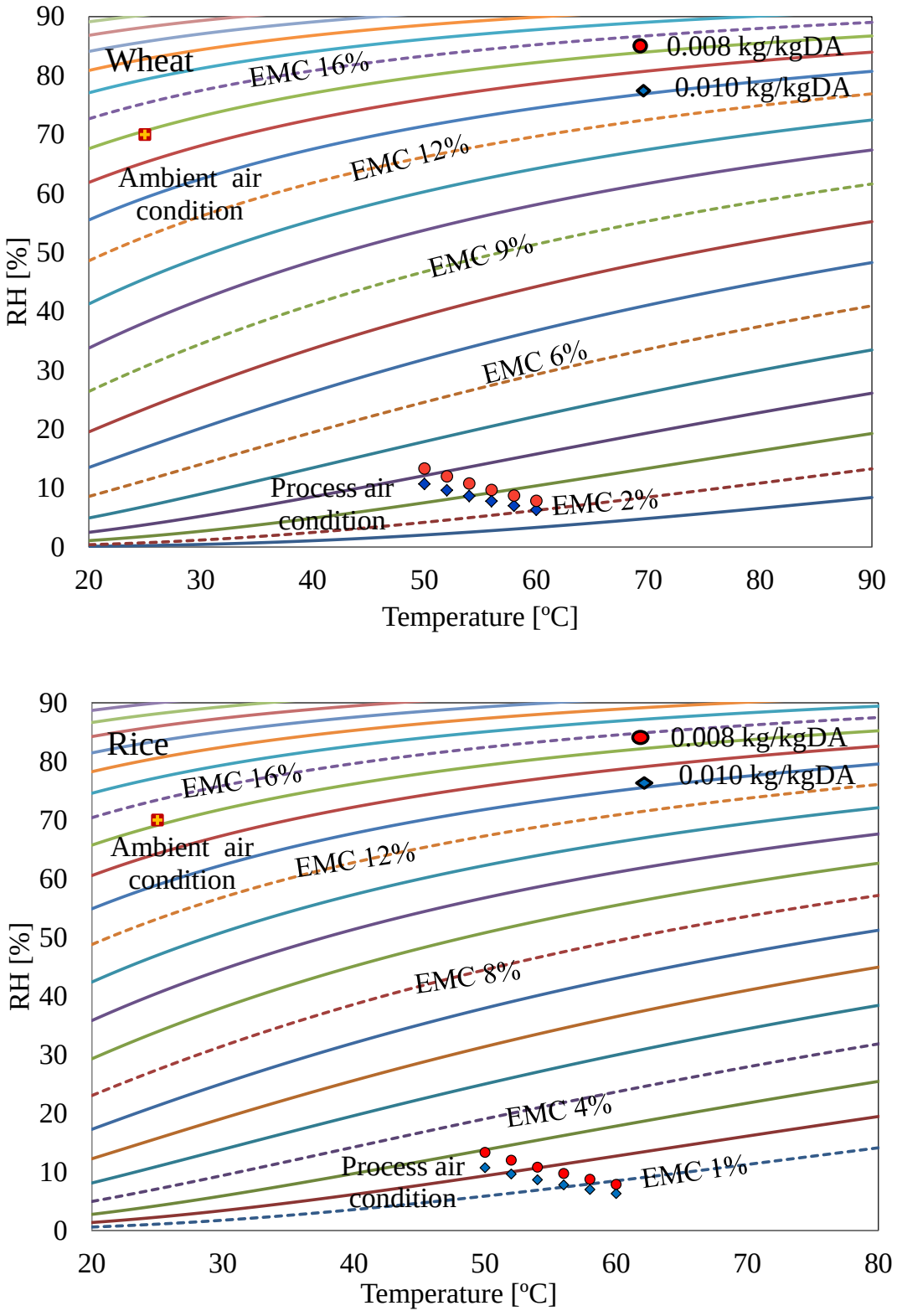


**Figure 3.8 (a)** Pictorial representation of process air conditions at different levels of air heating on EMC chart for Case-II for wheat and rice.

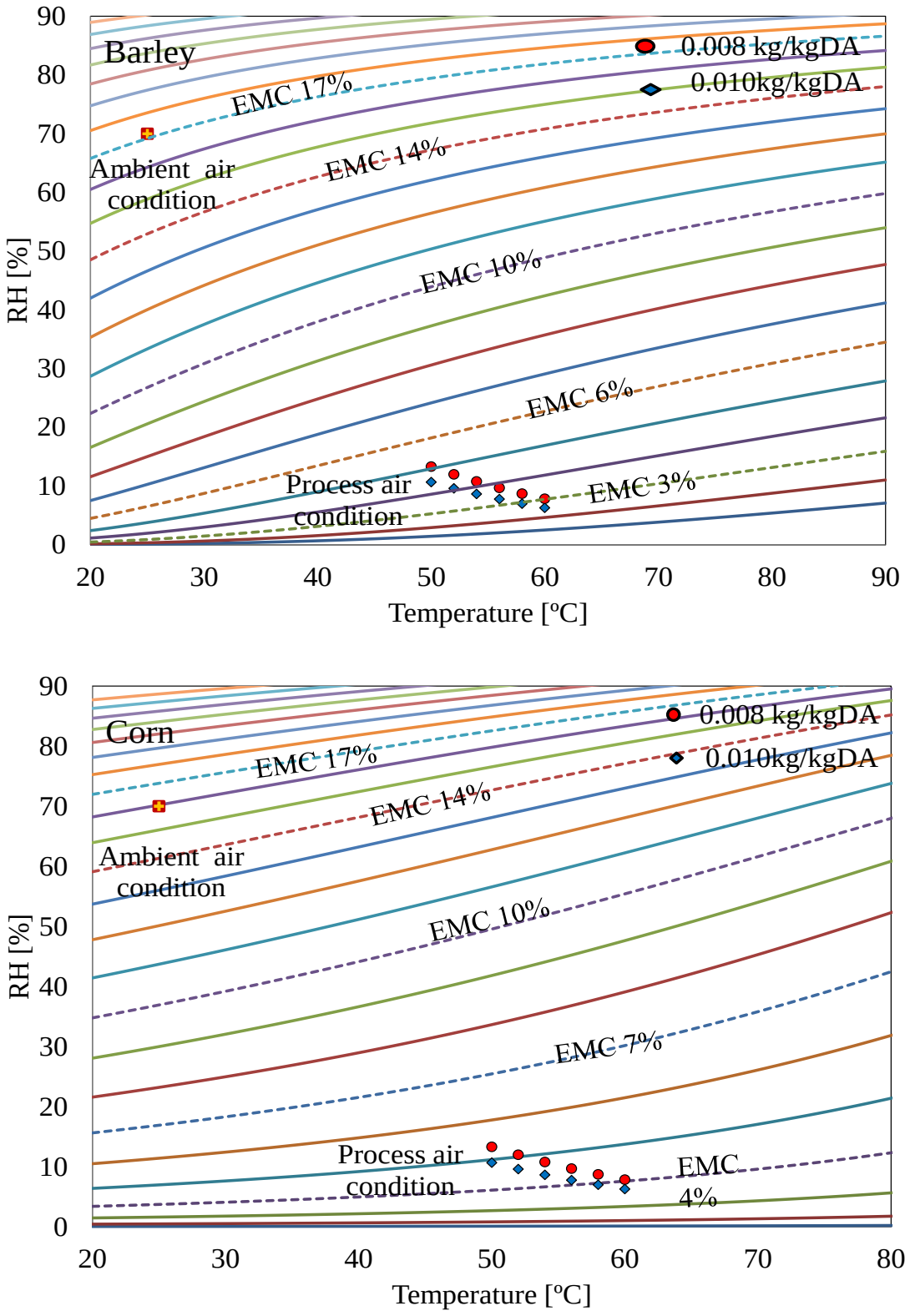


**Figure 3.8 (b)** Pictorial representation of process air conditions at different levels of air heating on EMC chart for Case-II for barley and corn.

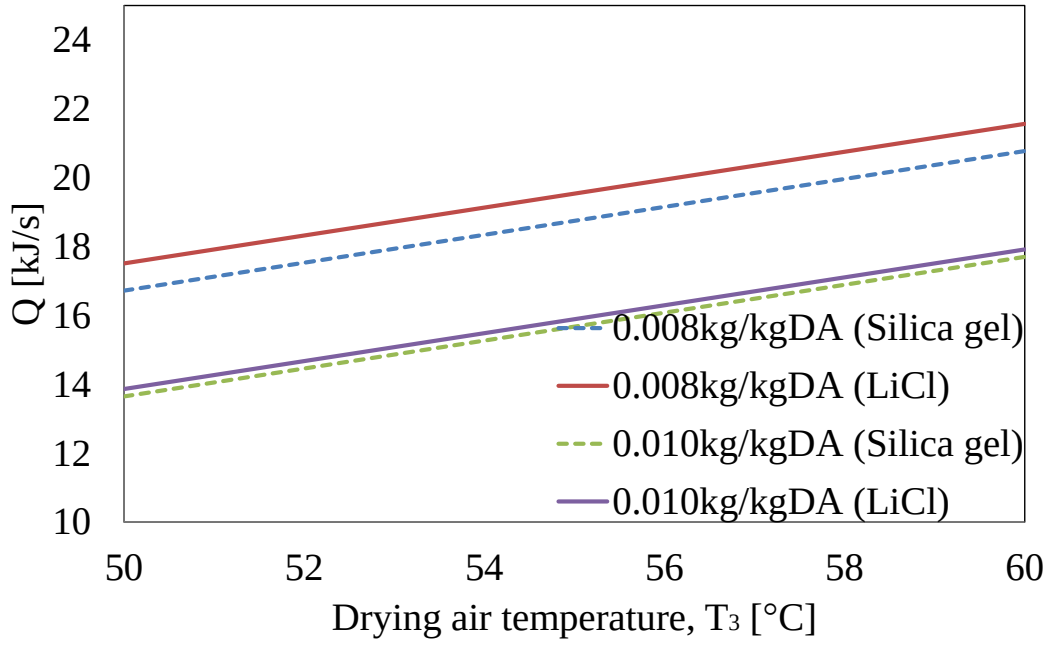


**Figure 3.9** Total thermal energy at different process air temperature for Case-II

Likewise silica gel produce more dehumidified air at as compared to LiCl that's why energy required for regeneration is less for particular humidity ratio of process air. Which showed that silica gel is more economical to use for Case-II.

In case of sensible load control, less energy is required for the regeneration of silica gel as compared to LiCl that's why for Silica gel total energy consumption is low. Regeneration energy required for silica gel is 9.3 kJ $s^{-1}$ and LiCl is 10.5 kJ $s^{-1}$ at humidity ratio 0.010 kg/kg DA.

Figures 3.10 represent the performance index for 1000 kg of grains for Case-II. It has been found that by increasing the temperature of process air, Φ decreases same like Case-I. However in Case-II, its value are more as compared to Case-I. Maximum value found for desiccant material silica gel, at humidity ratio 0.010 kg/kg DA are 6.65 kg $kW^{-1}$for wheat, 7.72 kg $kW^{-1}$for barley, 6.09 kg $kW^{-1}$for corn and 7.14 kg $kW^{-1}$for rice. However at humidity ratio 0.008 kg/kg DA its values are 5.71 kg $kW^{-1}$, 6.60 kg $kW^{-1}$, 5.17 kg $kW^{-1}$and 6.11 kg $kW^{-1}$for wheat, barley, corn and rice, respectively.

In Case-II, higher value of Φ at humidity ratio 0.010kg/kg DA, prove that it is more feasible approach as compared to drying at 0.008kg/kgDA. However it also showed that Case-II drying at 50ºC and humidity ratio 0.010kg/kgDA at regeneration temperature 63ºC have the highest potential to carry the moisture at the expense of less energy.

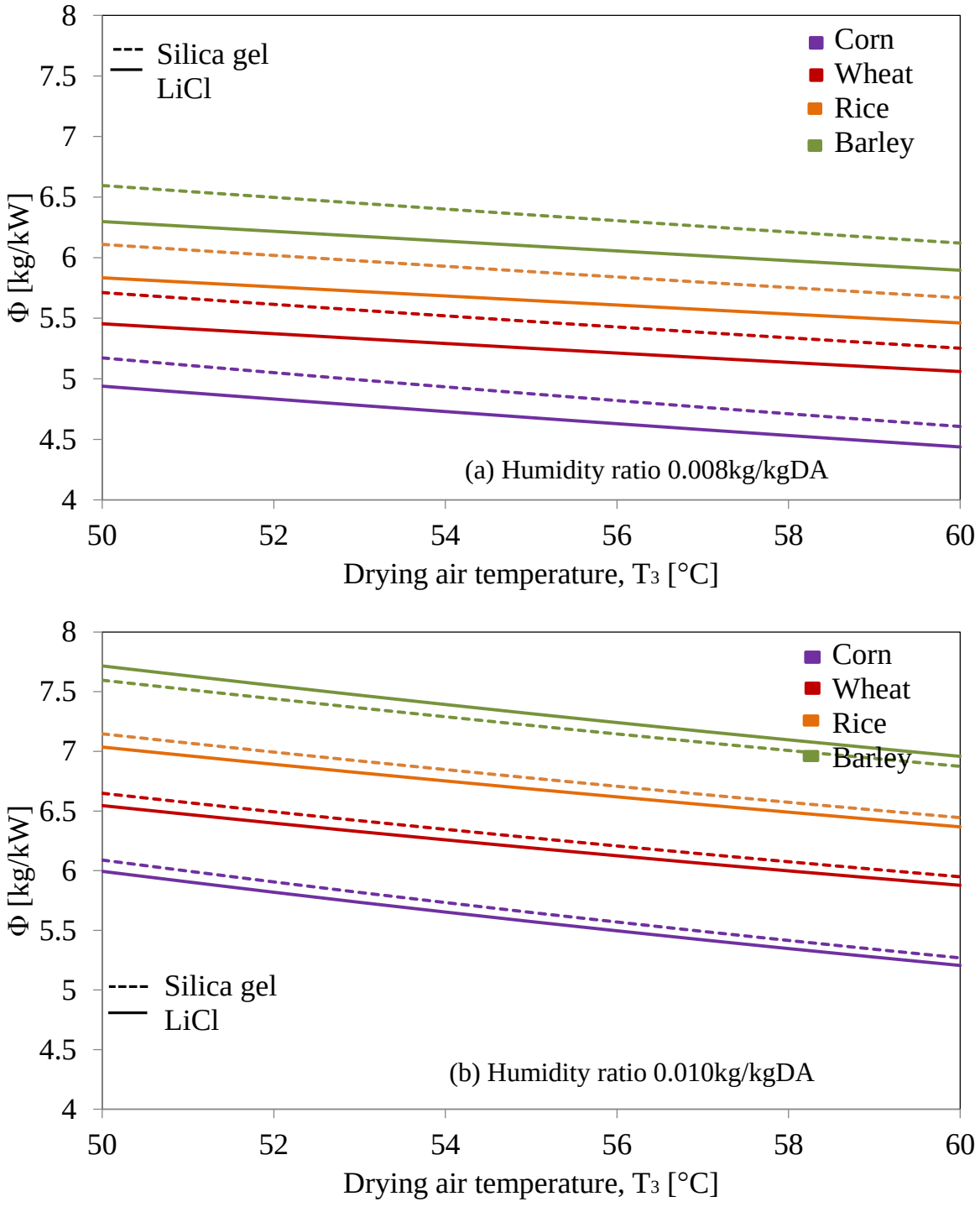


**Figure 3.10** Effect of drying air temperature on performance index for Case-II for humidity ratio: (a) 0.008kg/kg DA (b) 0.010kg/kg DA.

Whereas these conditions only suitable for commercial drying as drying air temperature is higher than the seed drying limit. It is concluded that Case-I at minimum possible regeneration temperature 50ºC consequently drying air temperature 41ºC is optimum condition for seed drying whereas for Case-II, drying at humidity ratio 0.010kg/kg DA at drying air temperature 50ºC is not in the range of seed drying. However these conditions are found quite reasonable for commercial purpose drying as the expense of minimum energy.

## 3.6 Conclusions

This study investigated steady state solid desiccant drying technique for the drying of four types of grains wheat, barley, corn and rice. Two desiccant drying approaches discussed are; latent load control and both latent & sensible load control effect. Beccali et al. model, Modified Chung-Pfost and Modified Oswin EMC equations are used to evaluate the both cases. Case-I deals with the drying of cereals grain without heating at various levels of humidity ratio of processed air. Whereas Case-II deals with the dehumidification of the ambient air at certain level and then heating the process air up to safe temperature limit. Case I results showed that by increasing the regeneration temperature moisture carrying capacity of the air increases however at the expense of more energy. Case I drying air conditions found effective for seed drying as drying air temperature not exceed the recommended seed drying temperature limit. Whereas, optimum drying conditions devising maximum potential to carry the moisture at the expense of minimum energy is at regeneration temperature 50ºC. Case-II results showed that it is more suitable for commercial drying as drying air temperature is higher as compared to Case-I. Whereas, optimum drying conditions for Case-II are drying air temperature 50ºC and humidity ratio 0.010kg/kg DA.

## 3.7 Nomenclature

| | |
|---|---|
| Cp | Specific heat capacity [kJ kg $K^{-1}$] |
| DDS | Desiccant drying system |
| DM | Dry matter [kg] |
| EMC | Equilibrium moisture content [%] |
| $F_a$ | Mass flow rate [kg $s^{-1}$] |

| | |
|---|---|
| h | Enthalpy [kJ $kg^{-1}$] |
| MC | Moisture content [%] |
| Q | Energy [kJ $s^{-1}$] |
| T | Dry bulb temperature [ºC] |
| Y | Humidity ratio [kg/kgDA] |
| Φ | Performance index[kg $kW^{-1}$] |

## References

AAFC, Heated air grain dryer, (O. H. Friesen, ed.), Publication 1700/E. AAFC, Ottawa, 1987.

Aguerre, R. J., Suarez C., and Viollaz, P. E., 1983. Moisture desorption isotherms of rough rice. Int. J. Food Sci. Technol., 18, 345-351.Motevali, A., Minaei, S., Banakar, A., Ghobadian, B., Khoshtaghaza, M. H., 2014. Comparison of energy parameters in various dryers Energy Convers. Manag., 87, 711-725.

Atuonwu, J.C., Jin, X., van Straten, G., Deventer Antonius, H.C. van, van Boxtel, J.B.: Reducing energy consumption in food drying: Opportunities in desiccant adsorption and other dehumidification strategies. Procedia Food Sci. 1, 1799–1805 (2011). doi:10.1016/j.profoo.2011.09.264

Atuonwu, J.C., van Straten, G., van Deventer, H.C., van Boxtel, A.J.B.: On the controllability and energy sensitivity of heat-integrated desiccant adsorption dryers. Chem. Eng. Sci. 80, 134–147 (2012). doi:10.1016/j.ces.2012.06.006

Beccali M, Butera F, Guanella R, Adhikari RS. 2002. Performance evaluation of rotary desiccant wheels, Proceedings of (WREC)-VI, Cologne, Germany, July 2002.

Beccali, M., Butera, F., Guanella, R., Adhikari, RS., 2003. Simplified models for the performance evaluation of desiccant wheel dehumidification. Int. J. of Energy Res., 27, 17–29.

Clary, C. D., Wang, S. J., & Petrucci, V. E., 2005. Fixed and incremental levels of microwave power application on drying grapes under vacuum. J. Food Sci., 70(5), 344-349.

Dai, Y.-J., Tang, Y.-Q., Fang, W.-Z., Zhang, H., Tao, W.-Q.: A theoretical model for the effective thermal conductivity of silica aerogel composites. Appl. Therm. Eng. 128, 1634–1645 (2018). doi:10.1016/J.APPLTHERMALENG.2017.09.010

Funebo, T., and Ohlsson, T., 1998. Microwave-Assisted Air Dehydration of Apple and Mushroom. J. Food Eng. 38 (3), 353–67. doi:10.1016/S0260-8774(98)00131-9.Japan

Gely M. C., and Pagano, A. M., 2012. Moisture desorption isotherms and isosteric heat of sorption characteristics of malting barley (Hordeum distichum, L.) Lat. Am. Appl. Res., 42, 237-243.

Goldsworthy, M., White, S.D.: Limiting performance mechanisms in desiccant wheel dehumidification. Appl. Therm. Eng. 44, 21–28 (2012). doi:10.1016/j.applthermaleng.2012.03.046

Hong, S.W., Ahn, S.H., Chung, J.D., Bae, K.J., Cha, D.A., Kwon, O.K.: Characteristics of FAM-Z01 compared to silica gels in the performance of an adsorption bed. Appl. Therm. Eng. 104, 24–33 (2016). doi:10.1016/j.applthermaleng.2016.05.058

Kosuke, N., Ying, Li., Zhehong, Jin., Masahiro, F., Yoshinori A., and Atsutoshi, A., 2006. Low-temperature desiccant-based food drying system with airflow and temperature control. J. Food Eng., 75, 71-77.

Madhiyanon, T., Adirekrut, S., Sathitruangsak, P., Soponronnarit, S., 2007. Integration of a rotary desiccant wheel into a hot-air drying system: Drying performance and product quality studies. Chem. Eng. and Processing 46, 282-290.

Mahmood M. H, Sultan M, Miyazaki T, Koyama, S., 2016. Desiccant air-conditioning system for storage of fruits and vegetables: Pakistan preview. EverGreen, 3: 12–17.

Marfil, P. H M., Santos, E. M., and Telis, V. R N., 2008. Ascorbic Acid Degradation Kinetics in Tomatoes at Different Drying Conditions. LWT - Food Sci. and Technol. 41 (9), 1642–47. doi:10.1016/j.lwt.2007.11.003.

Miyazaki T, Nikai I and Akisawa A (2011) Simulation analysis of an open-cycle adsorption air conditioning system-Numeral modeling of a fixed bed dehumidification unit and the Maisotsenko cycle cooling unit. Int. J. of Energy for a Clean Environment. 12, 341–354.

Motevali, A., Minaei, S., Banakar, A., Ghobadian, B., Khoshtaghaza, M. H., 2014. Comparison of energy parameters in various dryers Energy Convers. Manag., 87, 711-725.

Pramuang, S. and Exell, R.H.B., 2007. The regeneration of silica gel desiccant by air from a solar heater with a compound parabolic concentrator. Renew. Energy, 32(1), 173-182.

Rice knowledge Bank, http://www.knowledgebank.irri.org/step-by-step-production/postharvest/storage/moisture-content-for-safe-storage (accessed 16 Feb 2018).

Statistics bureau, Japan statistical year book. Government of Japan: management and coordination agency (2000).

Sultan M, Miyazaki T, Saha BB, Koyama, S., 2016b. Steady-state investigation of water vapor adsorption for thermally driven adsorption based greenhouse air-conditioning system. Renew. Energy, 86, 785–795.

Sultan, M., El-Sharkawy, I. I., Miyazaki, T., Saha, B. B., Koyama, S., Maruyama, T., Maeda S., and Nakamura, T., 2015. Insights of water vapor sorption onto polymer based sorbents. Adsorption, 21(3), 205-215.

Sultan, M., El-Sharkawy, I. I., Miyazaki, T., Saha, B. B., Koyama, S., Maruyama, T., Maeda S., and Nakamura, T., 2016a. Water vapor sorption kinetics of polymer based sorbents: Theory and experiments, Appl. Therm. Eng., 106, 192-202.

Sultan, M., Miyazaki, T., Koyama, S., and Khan, Z. M., 2018b. Performance evaluation of hydrophilic organic polymer sorbents for desiccant air-conditioning applications Adsorp. Sci. & Technol., 36(1-2), 311-326.

Sultan, M., Miyazaki, T., Mahmood, M. H., and Khan, Z. M., 2018a. Solar assisted evaporative cooling based passive air-conditioning system for agricultural and livestock applications Nomenclatures. J. Eng. Sci. and Technol. 13 (133), 693–703. http://jestec.taylors.edu.my/Vol 13 issue 3 March 2018/13_3_10.pdf.

Sun, D. W., 1998. Selection of EMC/ERH Isotherm Equations for Drying and Storage of Grain and Oilseed, J Stored Prod Res. (in Proceedings of CIGR XIIIth International Congress on Agricultural Engineering), 6, 331-336.

Sun, D. W., and J. L. Woods. 1994. The selection of sorption isotherm equations for wheat based on the fitting of available data. J. Stored Products Res., 30(1), 27 - 43.

Zhang, M., Li, C. L., & Ding, X. L., 2003. Optimization for preserva- tion of selenium in sweet pepper under low-vacuum dehydration. Drying Tech., 21(3), 569-579.

Zhang, M., Li, C. L., & Ding, X. L., 2005. Effects of heating conditions on the thermal denaturation of white mushroom suitable for dehydration. Drying Techn., 23(5), 1119- 1125.

CHAPTER 4

# INVESTIGATION OF ADSORPTION KINETICS OF DESICCANT DRYING AND COMPARISON WITH CONVENTIONAL DRYING

# Chapter 4

# INVESTIGATION OF ADSORPTION KINETICS OF DESICCANT DRYING AND COMPARISON WITH CONVENTIONAL DRYING

This chapter presents the drying kinetic of freshly harvested wheat grains in order to reduce the moisture to an optimum level. Fast and low-temperature drying systems are required by today's drying industries in order provide economical and safe drying. Therefore, comparison of desiccant drying has been made with the conventional method in terms of drying kinetics, allowable time for safe storage, the total time for drying cycle, and overall energy consumption. It has been found that the proposed desiccant drying system provides high drying rate and allows higher time for the safe storage. As the desiccants possess water adsorbing ability by means of vapor pressure deficit, therefore, the desiccant system successfully provided low-temperature drying which ensures the quality of wheat grains. Overall energy consumption is estimated for both drying system and it is found that the desiccant system requires less energy at all drying temperatures. In addition, the overall performance index of the desiccant system is higher at all temperatures. The study is useful for developing a low-cost and sustainable drying technology for various agricultural products.

## 4.1 Introduction

Moisture adsorbing/absorbing materials have been used for the drying of agricultural products including wheat grains from ancient time. Desiccants are hygroscopic materials and possess moisture adsorbing ability due to vapor pressure difference (Sultan et al. 2015a). Therefore, it has been used for dehumidification and air-conditioning processes for various agricultural applications e.g. greenhouses (Sultan et al., 2016a) and agricultural product storage (Mahmood et al., 2016). Certainly, desiccants possess the drying potential that can be

used for various agricultural products, and consequently many studies have been reported in the literature (Erdogan et al., 2017; Kant et al., 2016; Dina et al., 2015; Watts et al. 1987). In desiccant based drying system (DDS), the desiccant unit handles the latent load of drying air whereas heater is used for sensible heating of drying air in order to access the minimum vapor pressure. The ability of DDS to deal the sensible and latent component of vapor pressure distinctly (Sultan et al., 2015a) makes it versatile for drying of various agricultural products.

The drying conditions always influence the quality of agricultural produce i.e. color, surface texture, cooking behavior etc. Figure 4.1 presents the influence high drying temperature on the quality of wheat grains which clearly shows the damage in wheat quality. In addition, pictorial view of insect attack (Kozlowski, 1972) is also superimposed on the same figure which could be expected when non-favor able temperature/humidity conditions are employed to the grains. Post-harvested agricultural products including wheat grains possess high moisture level at the time of harvest and therefore cannot be stored for a long time unless proper storage/treatment has been employed (Mahmood et al., 2016). In this regard, wheat grains need to dry up to a level of 14% moisture content (dry basis) in order to avoid mold growth as well as the insect's attack (Whitesides 1995). It has been found in the literature that the DDS can address the environmental and economic issues of drying of wheat grains.

According to Chramsa-ard et al., (2013), a drying system requires 19 hours to bring the moisture content from 82% to 13% (wet basis) with the aid of air dehumidification whereas it takes 24 hours without dehumidification, thereby, 21.5 k W h energy can be saved. Similarly, in another study by (Dina et al. 2015), the desiccant drying consumes only 13.29 MJ/kg energy as compared to 60.4 MJ/kg in case of cocoa beans. In case of DDS, it is very important to select the optimum working range of system components in order to obtain maximum energy saving (De Antonellis et al., 2016). The drying time decreases with the decrease in air humidity and increase in air temperature, and collectively based on the net vapor pressure difference between grains and the encountered air. Therefore, the DDS can also play a role to reduce the drying time by providing fast adsorption rate process. In this regard, many studies on desiccant materials have been reported for total moisture adsorption equilibrium (Sultan et al., 2015b; Xia et al., 2008) and moisture adsorption rate (Sultan et al., 2016b; Sun and Chakraborty 2015).

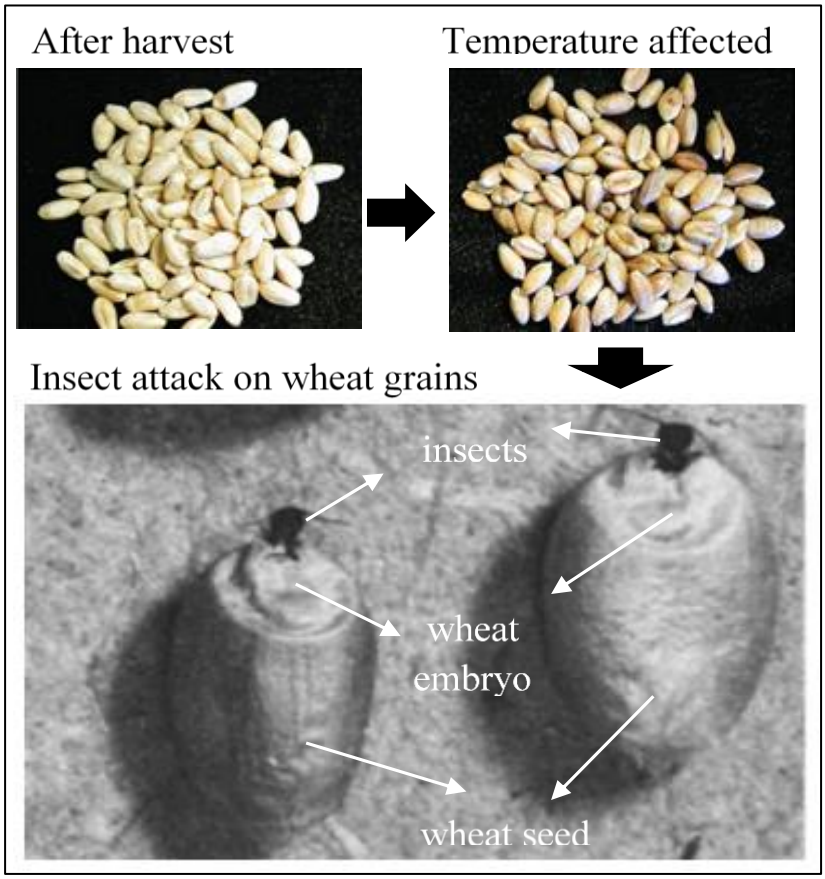


**Figure 4.1** Influence on ambient air conditions on the quality of wheat grains: effect of drying temperate (top right) and pictorial view of insect attack (bottom) (Kozlowski, 1972).

Similarly, different parameters of desiccant based drying system are optimized for energy minimization, e.g. drying air temperature and drying rate (Abasi et al., 2016); desiccant rotor speed for optimum dehumidification and enthalpy recovery(Zhang and Niu 2002); maximum energy saving (De Antonellis et al., 2012); desiccant rotor speed, and temperature and velocity of regeneration air (Zhang and Niu 2002). Consequently, the study is objected towards the performance evaluation of DDS in compared with conventional drying system (CDS). Consequently, drying speed and corresponding energy requirements have been estimated and compared for both systems.

## 4.2 Desiccant drying system

In this study, we proposed a solid desiccant based drying system (DDS) for the drying of wheat grains. Drying of agricultural products is crucial not only to avoid fungus/mold attacks but also to increase the shelf life of agricultural products (Mahmood et al., 2016).

It helps to minimize demand and supply gap which ultimately brings economic stability of the agricultural products. Consequently, this can improve food shortage and malnutrition issues worldwide. Figure 4.2(a)-(b) represent the schematic and psychrometric diagrams of the proposed solid desiccant based drying system (DDS). It mainly consists of: (i) a desiccant wheel used to dehumidify the air; (ii) heater for process air heating (bio-mass/gas or electric); (iii) drying bin/structure; (iv) heater for regeneration of desiccant wheel (electric driven or preferably bio-mass/gas driven).

The numbers 1 to 7 showed in Figure 4.2 are the sequence and states of conditions of air during the drying process. It starts from the suction of ambient air by a desiccant wheel from state 1 to 2. At state 2, the specific humidity decreases from $Y_1$ to $Y_2$ due to adsorption of the moisture from the air by the desiccant wheel. Furthermore, air temperature increases from $T_1$ to $T_2$ due to the heat of adsorption released by desiccant material (Sultan et al., 2017).

At state 3, air from the desiccant wheel further heated up to a certain temperature represented by $T_3$ in order to establish a certain vapor pressure deficit between the wheat grains and the encountered air. Thus, dehumidified and heated air move forward from state 3 to 4 while drying the wheat grains due to the vapor pressure deficit (Sultan et al., 2016a). The air takes moisture from the grains while passing through it and therefore specific humidity increases (from $Y_3$ to $Y_4$) and temperature decrease (from $T_3$ to $T_4$). The net conditions depend on the drying air condition equilibrium with wheat grains. In Figure 4.2, state 5 to 6 shows the heating of air from $T_5$ to $T_6$ for the regeneration of the desiccant wheel. At state 6, heated air streams are passed through the desiccant which takes the adsorbed water as thereby the specific humidity increases from $Y_6$ to $Y_7$.

During the drying process, ambient air is continuously passed through the adsorption and regeneration sides of the desiccant wheel. The detailed procedure for system analysis and operating conditions are discussed in the coming heading.

## 4.3 Research methodology

In this study, we used 10 tons of wheat gains initially containing typical 26% of moisture contents (dry basis), for the calculations of conventional (CDS) and desiccant (DDS) drying systems.

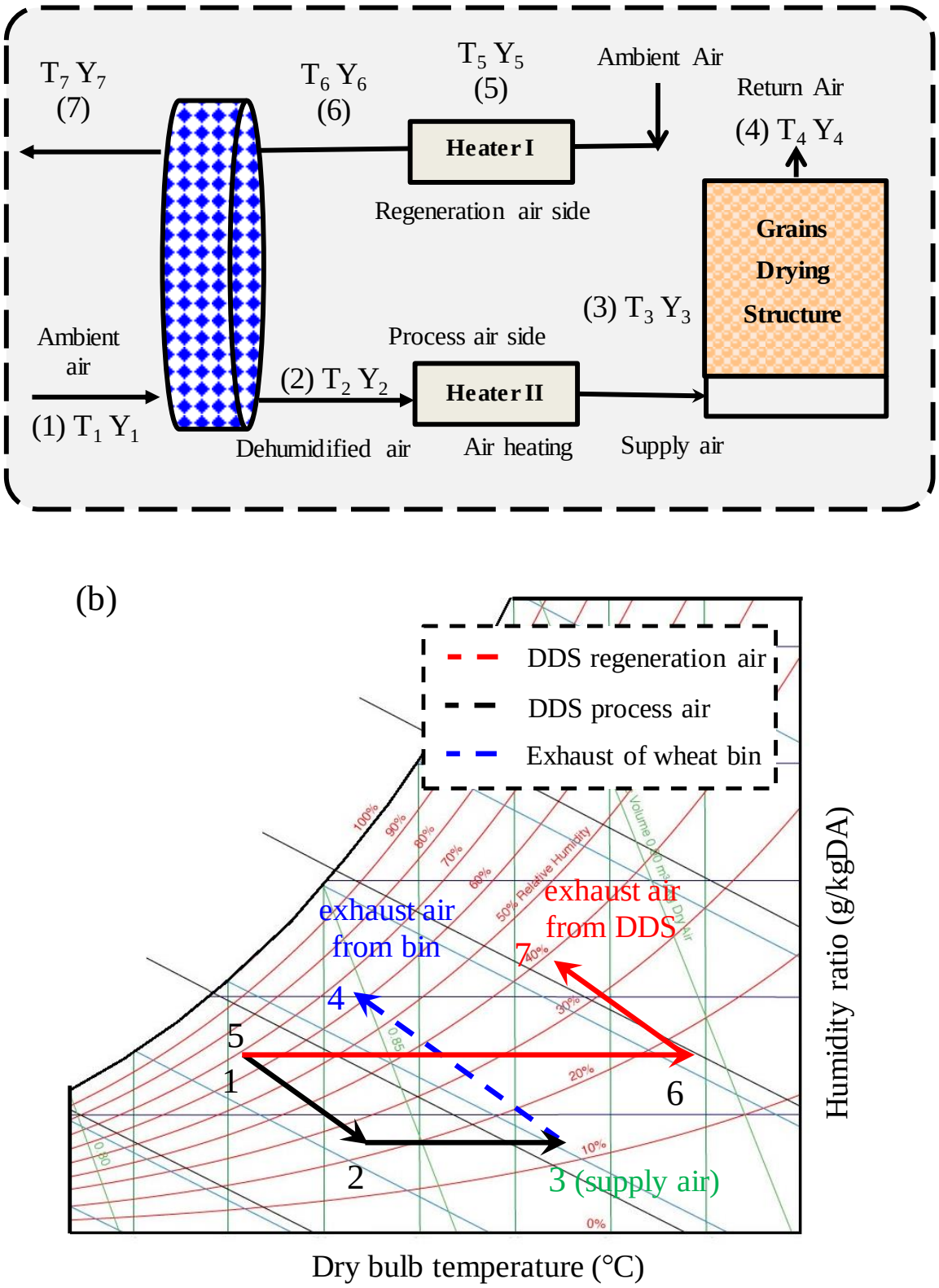


**Figure 4.2** Proposed solid desiccant drying system (DDS) for drying of wheat grains: (a) schematic diagram and (b) psychrometric cycle of the system.

The dryer size is determined by the drying area required per kg of wheat grains. Total volume required for wheat grains is calculated by means of Eq. (4.1).

$$V = \frac{W_t}{\rho_b} \tag{4.1}$$

where $W_t$ is total weight of moist wheat grains (kg); and $\rho_b$ is the wheat bulk density (kg/m$^3$). Therefore, volume of the drying bin of the wheat grain is 12.98 m$^3$. The dryer area and height used for the drying calculation are 7.42 m$^2$ and 1.75 m, respectively. As very high drying temperature can affect the quality of wheat grains, therefore, drying temperature is limit to 60 ºC according to the guidelines of FAO (2011).

The modified Chung-Pfost equation (Oberoi et al., 2017) is well-known in the literature which can be used for the measurements of equilibrium relative humidity (ERH) of the air streams in the drying chamber. Therefore, it has been used in this study for the measurement of ERH of the air in the wheat drying chamber. The modified Chung-Pfost equation has been defined in the form as given by Eq. (4.2) (Oberoi et al., 2017). It can be noticed that the Eq. (4.1) uses three empirical coefficients i.e. $C_1$, $C_2$, and $C_3$, which are supposed to optimize for the best fit against the moisture isotherm equations for the particular grains. In this study, the optimized parameters are obtained for the wheat grains from a reference study by (Sun and Woods 1994). Consequently, the numerical values of the optimized parameters of $C_1$, $C_2$, and $C_3$ for desorption isotherms of wheat are 545.25, 64.047 and 0.17316, respectively (Sun and Woods 1994).

$$\ln ERH = \frac{-C_1}{T_3 + C_2} \exp(-C_3 M) \tag{4.2}$$

where M (-) represents the moisture content (dry basis) of the wheat grains in this study. The dry basis moisture content is the ratio of wheat moisture contents (kg) and dry grains of wheat (kg). In order to reduce the moisture content of the wheat grains for safe annual storage to the optimum limit of the moisture content (i.e. 14%) (Whitesides 1995), the drying time can been calculated by means of drying rate simply by using the well-known drying rate equation as given by Eq. (4.3).

$$t = W_d \frac{\sum_{i=1}^{t} (M_i - M_{i+1})}{\left(\frac{dw}{dt}\right)} \tag{4.3}$$

where $t$ is drying time (s); M (-) is moisture content (dry basis); $W_d$ is drying matter of wheat grains (kg); and $w$ is weight of moisture (kg). The term $\left(\frac{dw}{dt}\right)$ is drying rate (kg/s) which is calculation by means of following relationship:

$$\left(\frac{dw}{dt}\right) = k_a A(Y_o - Y_i) \tag{4.4}$$

where $k_a$ and $A$ are the mass transfer coefficient (kg/s-m$^2$) and area of drying structure/bin (m$^2$), respectively. $Y_i$ and $Y_o$ are absolute humidity of air (g/kgDA) at inlet and outlet end of dryer, respectively. As the mass transport is not a constant rate process, therefore, drying is considered as combination of constant and falling rate drying rate. It is assumed that the moisture is removed from the grain surface by the dry airflow for the first drying period. Later, water ceased to behave as it is on free surface and transported from the grain inside to the surface, thereafter, drying rate decreases which is known as falling drying rate. Consequently, thin layer drying model in the form of time and temperature, is used to predict the moisture content of grains during drying process as defined by Eq. (4.5) (Mohapatra and Rao 2005).

$$\frac{M_t - M_e}{M_o - M_e} = (\tau_1 T_3 + \tau_2)\exp(\tau_3 t) \ + (\tau_4 T_3 + \tau_5)\exp(\tau_6 t) \tag{4.5}$$

where constants are $\tau_1 = 0.03197$, $\tau_2 = -1.009$; $\tau_3 = -0.034$; $\tau_4 = -0.032$; $\tau_5 = 1.9918$; $\tau_6 = -0.009$. The parameters $T$, $t$, $M_t$, $M_o$ and $M_e$ are drying air temperature (ºC), drying time (min), moisture content (dry basis) at time $t$, initial moisture content (dry basis) at $t$ = 0, and equilibrium moisture content at $t$ = ∞, respectively. Equilibrium moisture contents ($M_e$) is calculated by using Modified-Chung-Pfost equation as defined by (4.2) in the following form(Sun 1998):

$$M_e = \frac{1}{-C_3}\ln\left(\frac{T_3 + C_2}{-C_1}\ln RH_3\right) \tag{4.6}$$

As thin layer drying model equation cannot precisely evaluate the drying time of 10 tons wheat grains, therefore, for the sake of simplicity and counterbalance, it is only used to calculate the successive change in moisture content used in Eq. (4.3) i.e. $M_i - M_{i+1}$. However, mass transfer coefficient is determined by assuming packed bed air flow and governing equations as defined by Eq. (4.7) to (4.10) (Whitaker 1972):

$$k_a = \frac{h}{c_p} = \frac{Nu\ k}{c_p\ D_P}\left(\frac{1-\varepsilon}{\varepsilon}\right) \quad (4.7)$$

$$N_u = (0.5\ R_e^{\frac{1}{2}} + 0.2\ R_e^{\frac{2}{3}})P_r^{\frac{1}{3}} \quad (4.8)$$

$$Re = \frac{\rho v D_p}{\mu(1-\varepsilon)} \quad (4.9)$$

$$Pr = \frac{c_p \mu}{k} \quad (4.10)$$

where $k_a$ and $h$ the mass transfer coefficient (kg/s-m$^2$) and heat transfer coefficient (J/(m$^2$s ºC), respectively. $k$ is thermal conductivity (W/m-K). $N_u$, $R_e$ and $P_r$ are Nusselt number (-), Reynolds number (-) and Prandtl number (-), respectively. The void fraction (ε) is estimated by means of bulk ($\rho_b$) and true ($\rho_t$) densities (kg/m$^3$) of wheat grains, respectively (Bhise et al., 2014) i.e. $\varepsilon = 1 - (\rho_b/\rho_t)$. The resulted value of $\varepsilon$ is equal to 0.4375. The particle diameter ($D_P$) is estimated by means of $D_p = 6V_p/A_p$. The value of particle volume, $V_p$ (m$^3$) and particle surface area, $A_p$ (m$^2$) obtained from the reference (Gastón et al., 2002), consequently, the resulted $D_p$= 0.00347 m. The amount of moisture ($W_w$) to be removed from the grains is calculated by using the following relationship:

$$W_w = W_t \frac{(M_i - M_f)}{(100 - M_f)} \quad (4.11)$$

where $W_w$ and $W_t$ are weight of moisture and total weight of moist grains, respectively. $M_i$ and $M_f$ are initial and final moisture contents (wet basis), respectively. The moisture contents can be changed to wet basis ($M_{wb}$) from dry basis ($M_{db}$) and vice versa by the following relationship.

$$M_{wb} = \frac{M_{db}}{100 + M_{db}} \quad (4.12)$$

Wheat grains in the top most layers of the drying bin contains high-level moisture as compared to the bottom layers, therefore, these are supposed to more susceptible to quality deterioration due to molds, fungus etc. Therefore, the allowable storage time is set by means of temperature and moisture content of the grains in the top most layers of drying structure. Allowable storage time model of wheat drying is used to determine the number of days

allowed for drying of grains (Fraser 1980). The allowable storage time ($t_{allow}$) equation of drying systems can be written in the following form as given by:

$$\log(t_{allow}) = \tau_7 + \tau_8 M_t + \tau_9 T_4 \quad (4.13)$$

where $t_{allow}$, $M_t$ and $T_4$ are allowable storage time (days), moisture content wet basic (%), and air temperature (ºC), respectively. The constant are $\tau_7 = 4.129$; $\tau_8 = -0.0997$; and $\tau_9 = -0.0576$. On the other hand, time required to dry the grains depends on air flow rate, therefore, drying calculations are optimized within allowable storage time. Consequently, air flow rates are selected accordingly for the purpose of optimization.

Total energy consumption for desiccant drying system (DDS) is calculated by the sum of thermal and mechanical energies. In case of DDS, thermal energy is used for air heating ($E_{th\ 2\text{-}3}$) and desiccant regeneration ($E_{th\ 5\text{-}6}$). However, thermal energy is used for heating of air solely ($E_{th\ 2\text{-}3}$) in case of conventional drying system (CDS). Input thermal energy associated with a desiccant drying system for heating and regeneration is calculated as follow (Motevali et al., 2014):

$$E_{th\ 2-3} = F_a C_p t (T_3 - T_2) \quad (4.14)$$

$$E_{th\ 5-6} = F_{a,r} C_{p,r} t (T_6 - T_5) \quad (4.15)$$

where $t$ is the time (s); $F_{a,r}$ and $F_a$ are the air mass flow rate (kg/s)during regeneration and heating, respectively. $C_{p,r}$ and $C_p$ are the specific heat capacity of air (kJ/kg-K) during regeneration and heating, respectively. The parameter $T_6$, $T_5$, $T_3$ and $T_2$ are the regeneration temperature, ambient air temperature, dryer inlet air temperature and desiccant wheel outlet air temperature (ºC) respectively. It is noteworthy, that the specific heat capacity and density of moist air are calculated from literature (Tsilingiris 2008). In addition, mechanical energy consumed by the system is sum of the mechanical energy used for the handling and associated processes (Motevali et al., 2014).

$$E_{mec} = E_{mec,1-2} + E_{mec,3-4} + E_{mec,6-7} \quad (4.16)$$

$$E_{mec} = (\Delta P A_{reg} V_{reg} t)_{1-2} + (\Delta P A_{ads} V_{ads} t)_{3-4} + (\Delta P A_{in} V_{in} t)_{6-7} \quad (4.17)$$

where $\Delta P$ is pressure drop (kPa); $t$ is drying time (sec); $A_{bin}$ is drying bin area ($m^2$); $A_{ads}$ and $A_{reg}$ are areas ($m^2$) of the desiccant wheel at adsorption and regeneration sides, respectively. $V_{in}$ is air velocity (m/s) at drying bin inlet whereas $V_{ads}$, $V_{reg}$ are the air velocities (m/s) of the desiccant wheel at adsorption and regeneration sides, respectively. For the conversion of electrical energy to mechanical energy 46% device conversion efficiency factor is used (Summers 1971). The pressure drop across the processes and regeneration side of the wheel is assumed 0.325 kPa whereas for grain drying structure it is calculated from the reference (Molenda et al., 2005):

$$\frac{\Delta P}{\Delta L} = 2\left(\frac{123.9}{R_e} + 1.657\right)\left(\frac{1-\varepsilon}{\varepsilon}\right)\left(\frac{\rho {V_{in}}^2}{D_p}\right) \tag{4.18}$$

where $\frac{\Delta P}{\Delta L}$ pressure drop per unit length of drying bin (m) in the direction of air flow. Specific energy consumption (SEC) is calculated which is the energy utilization for removing one kg of moisture for drying of wheat grains as given by (Torki-Harchegani et al., 2016):

$$SEC = \frac{E_{th}+E_{mec}}{W_w} \tag{4.19}$$

where $SEC$, $W_w$, $E_{th}$, $E_{mec}$ and are the specific energy consumption (kJ/kg), the weight of water to be removed (kg), total thermal (kJ) and mechanical (kJ) energy consumptions, respectively. The coefficient of performance (COP) index is defined by the total energy consumed for removing water quantity ($W_w$) divided by the total input energy to the dryer, as given by:

$$COP \text{ index} = \frac{E_w}{E_{th}+E_{mec}} = \frac{W_w\, h_{fg}}{E_{th}+E_{mec}} \tag{4.20}$$

$E_w$ is the energy consumed to remove $m_w$ (kg) of moisture and it is calculated from latent heat of vaporization of water vapors, $h_{fg}$ i.e. $E_w = W_w\, h_{fg}$ (Motevali et al., 2014). Latent heat of vaporization of water vapors (kJ/kg) is calculated at any temperature by a correlation given by Aghbashlo et al. (2012) i.e. $h_{fg} = 2.503 \times 10^6 - 2.386 \times 10^3 (T_{abs} - 273.16)$.

The simplified scheme and arrangement of the methodology used for the analysis of conventional and desiccant drying systems are given in Figure 4.3. The points presented in Figure 4.3 are corresponding to the state points used in Figure 4.2. The conditions of air

associated with the desiccant wheel are estimated from a reference study (Kang and Lee 2017).

In the reference study, a desiccant wheel of 580 mm diameter is used. The desiccant wheel is made up of polymer based desiccant material with frontal area ratio (process: regeneration) of 1:0.7. Consequently, the states 1 to 7 shown in Figure 4.2 can be further explained as follows:

- State 1: Typical ambient air condition i.e. $T_1$ = 32 ºC and $Y_1$ = 13.37 g/kgDA.
- State 2: Dehumidification of air takes place, and outlet conditions of the desiccant wheel are estimated from the reference study available in literature via reference Kang and Lee 2017.
- State 3: Sensible heating of the air by using air heater (electric or preferably bio-gas/mass) for the desired $T_3$.
- State 4: Humidity of air is increased as it carries moisture from the wheat grains. This process is supposed to follow the isenthalpic process.
- State 5: It is same as state 1 conditions i.e. ambient air conditions.
- State 6: Sensible heating of the air at $T_6$ to regenerate desiccant wheel.
- State 7: Exhaust air conditions of the regeneration air from the desiccant wheel. It corresponds to the process 1 to 2.

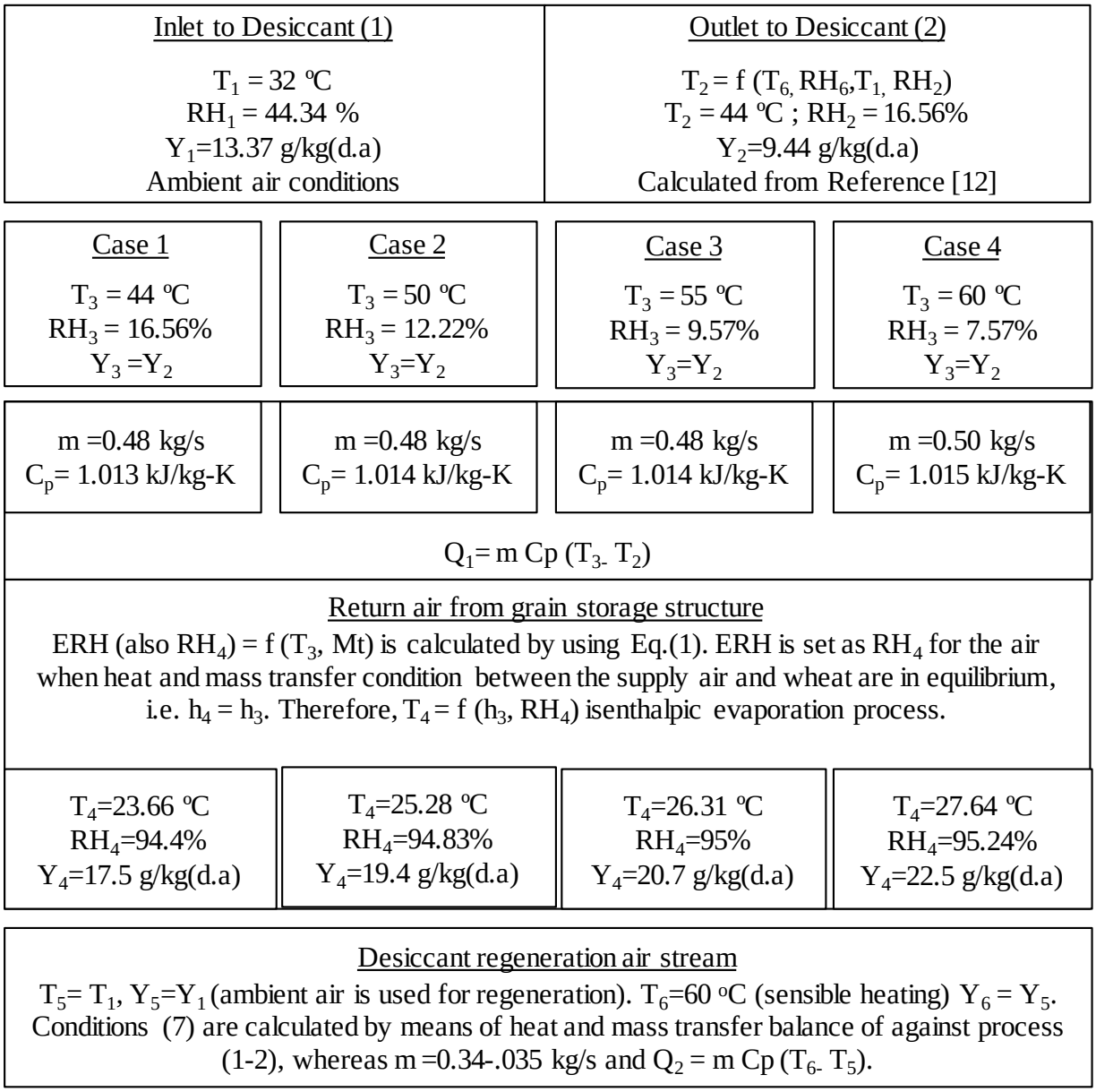


**Figure 4.3** Simplified scheme and arrangement of the methodology used for the analysis of drying systems.

## 4.4 Results and discussion

The equilibrium moisture content (EMC) is determined for desiccant (DDS) and conventional (CDS) drying systems by using Eq. (6). Figure 4.4 presents the drying of wheat grains from initial moisture content 26% (dry basis) to equilibrium moisture content at different drying air temperatures varying from 50ºC to 60ºC. The drying curves show that drying rate is constant at the start of drying process whereas it decreases as the moisture

content approaches to the equilibrium moisture content. Drying rate decreases as the moisture gradient between the inside and outside of the grains decrease near the equilibrium conditions. In comparison with CDS, the DDS possesses high drying rate and takes relatively less time to approach a particular EMC value in order to provide a certain level of wheat grains drying. This behavior is consistent at all drying air temperatures. As EMC is a function of temperature and relative humidity, therefore, DDS drying air conditions are associated with the small value of EMC hence more driving potential for moisture ratio as expressed by Eq. (5). However, drying air conditions of CDS require high EMC consequently delay in moisture content removal.

The effect of drying air temperature on drying cycle is presented in Figure 4.5(a)-(d) for both drying methods at 44 ºC, 50 ºC, 55 ºC and 60 ºC, respectively at same air velocity 0.09 m/s, in order to dry wheat grains up to a standard level of moisture content i.e. 14% dry basis. It has been found that desiccant drying requires less drying time at all drying temperatures as compared to conventional drying method. This is due to the fact that dehumidified air provides more driving force for evaporation at same drying air temperature. The observation agrees well with the reported results in literature for drying of agricultural products as shown in Table 4.1.

Table 4.1 Some study reported on effect of RH of air on drying rate

| Product | Drying conditions | Results |
|---|---|---|
| Rice | RH = 40-70 %<br>T = 40 -80 ºC<br>v = 0.5, 0.8 and 1.1 m/s | Drying time reduced by less humid drying air (Tohidi et al. 2017) |
| Chopped coconut pieces | With dehumidification<br>RH= 10.7, 17.8, 24.6<br>T = 60.3, 50.3, 51.3 ºC<br>v = 0.7, 0.7, 0.23 m/s<br>without dehumidification<br>RH = 14.5, 19.6, 29<br>T = 60.4, 50.3, 50.4 ºC<br>v = 0.7, 0.7, 0.23 m/s | Dehumidification of air at 10.7, 17.8 and 24.6 % required 4, 5 and 8 hours, respectively. Whereas without dehumidification it required 5.33, 6.67 and 10.33 hours at RH 14.5, 19.6 and29 % respectively (Madhiyanon et al. 2007) |
| Apple | RH = 40, 55, 70<br>T =35, 45, 55 ºC<br>V = 0.2, 0.4, 0.6 m/s | For temperature 35 ºC and air velocity 0.2 m/s, decreasing in RH from 70% to 40% decreased the drying time 51.67% whereas decrease in RH from 70% to 55%, decreased the total drying time 40% (Kaya et al. 2007) |

It is also indicated that increase in drying air temperature accompanied by a decrease in drying time. This is due to the fact that increase in air temperature speeds up the heat transfer between drying air and wheat grains due to the vapor pressure difference. In addition, high temperature may not favorable in order to keep the optimum quality of wheat grains as reported in the introduction section. As the maximum recommended drying temperature is 60ºC for wheat and 44ºC for seeds (De Antonellis et al., 2016). However, beyond this limit, it may affect the quality of grains in term of color, vitamins, and nutrients. Grains drying at industrial level requires safe storage limit of moisture contents, otherwise, spoiling of grains may be the development of molds and fungus. Therefore, the allowable safe storage time is calculated by using Eq. (13).

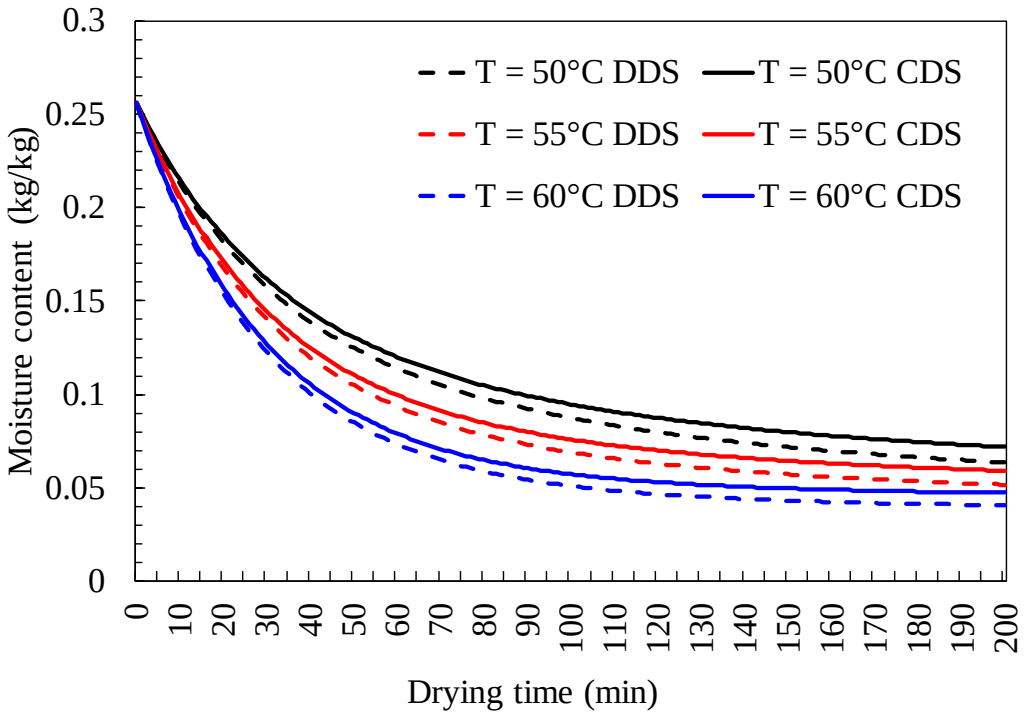


**Figure 4.4** Effect of drying temperature on the drying time for wheat grains by means of drying curves.

Table 4.2 represents the allowable safe storage time for both drying methods at different supply air conditions. The allowable time for safe storage is based on initial moisture content and equilibrium temperature ($T_4$). Therefore, DDS method gives high allowable time as compared to the conventional system because it possesses low $T_4$. Drying of grains within the allowable time period is shown in Table 4.2. The air velocity selected was the minimum air velocity for DDS and CDS at particular drying temperature that

complete the drying cycle within the allowable drying time. By increasing the supply air temperature for the same drying system, drying air velocity is adjusted to compensate the drying time within the allowable time. It can be seen that relatively higher drying air velocity is used for high-temperature supply air because allowable time decreases with high temperature. Higher air velocity is considered in case of conventional drying it has less potential to carry out moisture and takes more time for the drying of the same quantity of grains. Minimum drying air velocity is optimized for all cases to complete the drying cycle about 2 hr before the allowable time.

**Table 4.2** Optimum storage and drying time for conventional and desiccant drying systems at different drying air temperature.

| Drying air Temperature (ºC) | DDS | | | | CDS | | | |
|---|---|---|---|---|---|---|---|---|
| | Air velocity (m/s) | $T_4$ (ºC) | [1]Drying cycle time (hr) | [2]Optimum storage (hr) | Air velocity (m/s) | $T_4$ (ºC) | [1]Drying cycle time (hr) | [2]Optimum storage (hr) |
| 44 | 0.074 | 23.66 | 126.21 | 128.62 | 0.169 | 26.08 | 91.99 | 93.35 |
| 50 | 0.076 | 25.28 | 101.25 | 103.80 | 0.155 | 27.49 | 75.85 | 77.43 |
| 55 | 0.076 | 26.31 | 88.46 | 90.60 | 0.153 | 28.6 | 64.66 | 66.83 |
| 60 | 0.082 | 27.64 | 73.19 | 75.91 | 0.149 | 29.65 | 56.69 | 58.10 |

[1]Time calculated for wheat grains drying from 26% to 14% moisture content. It depends on relative humidity and temperature of drying air, whereas drying air velocity is adjusted in order to complete the drying cycle with in the limit of optimum storage time.

[2]Optimum storage is the time permitted for drying of wheat grains at particular drying conditions, which depends on moisture content (before drying) and temperature of wheat grains in the top layers of drying structure.

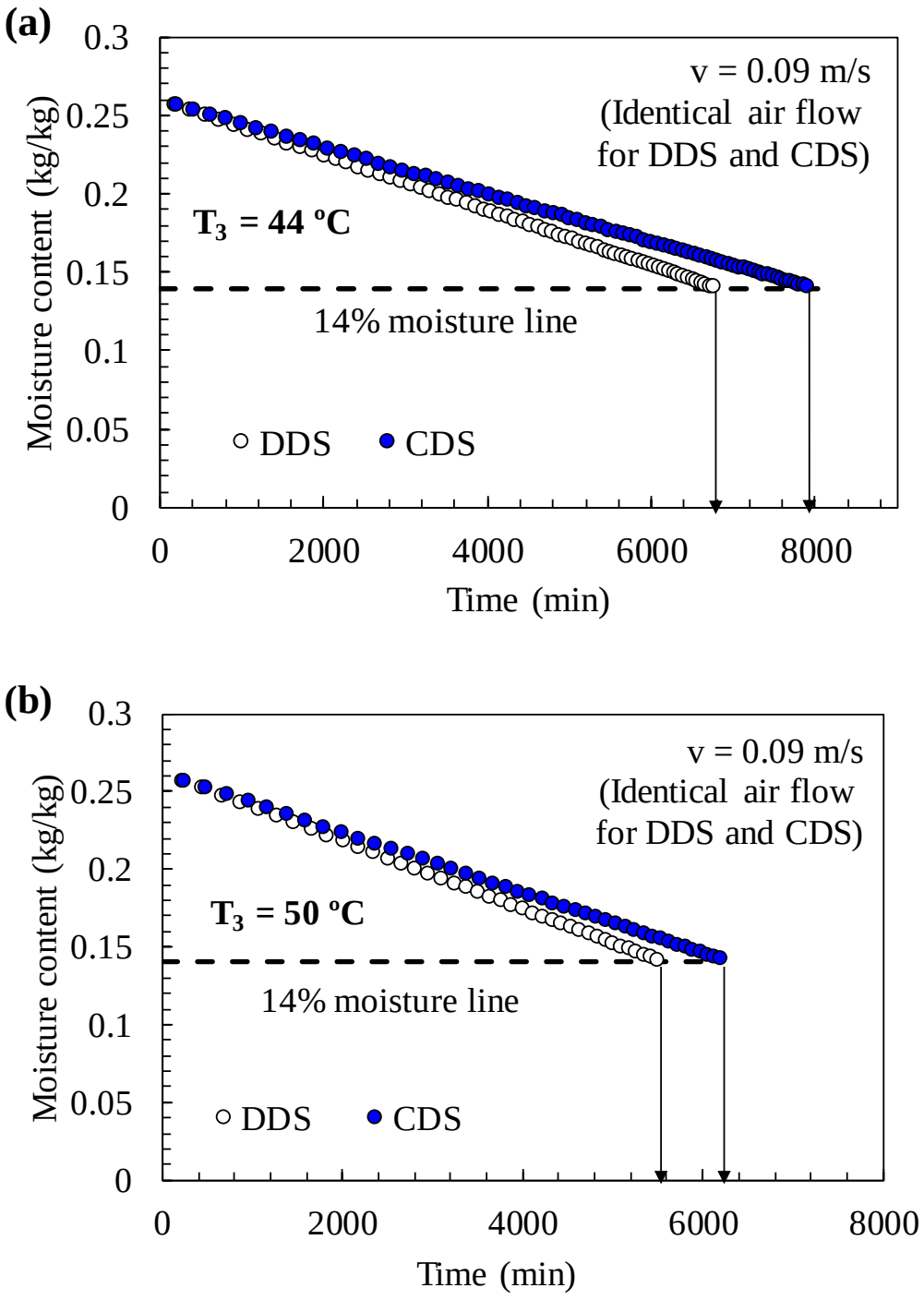


**Figure 4.5 (a)** Comparison of drying time between conventional (CDS) and desiccant (DDS) drying system in order to dry of wheat grains from 26% to 14% moisture contents at drying air temperature of: (a) 44 ºC, (b) 50 ºC, (c) 55 ºC and (d) 60 ºC.

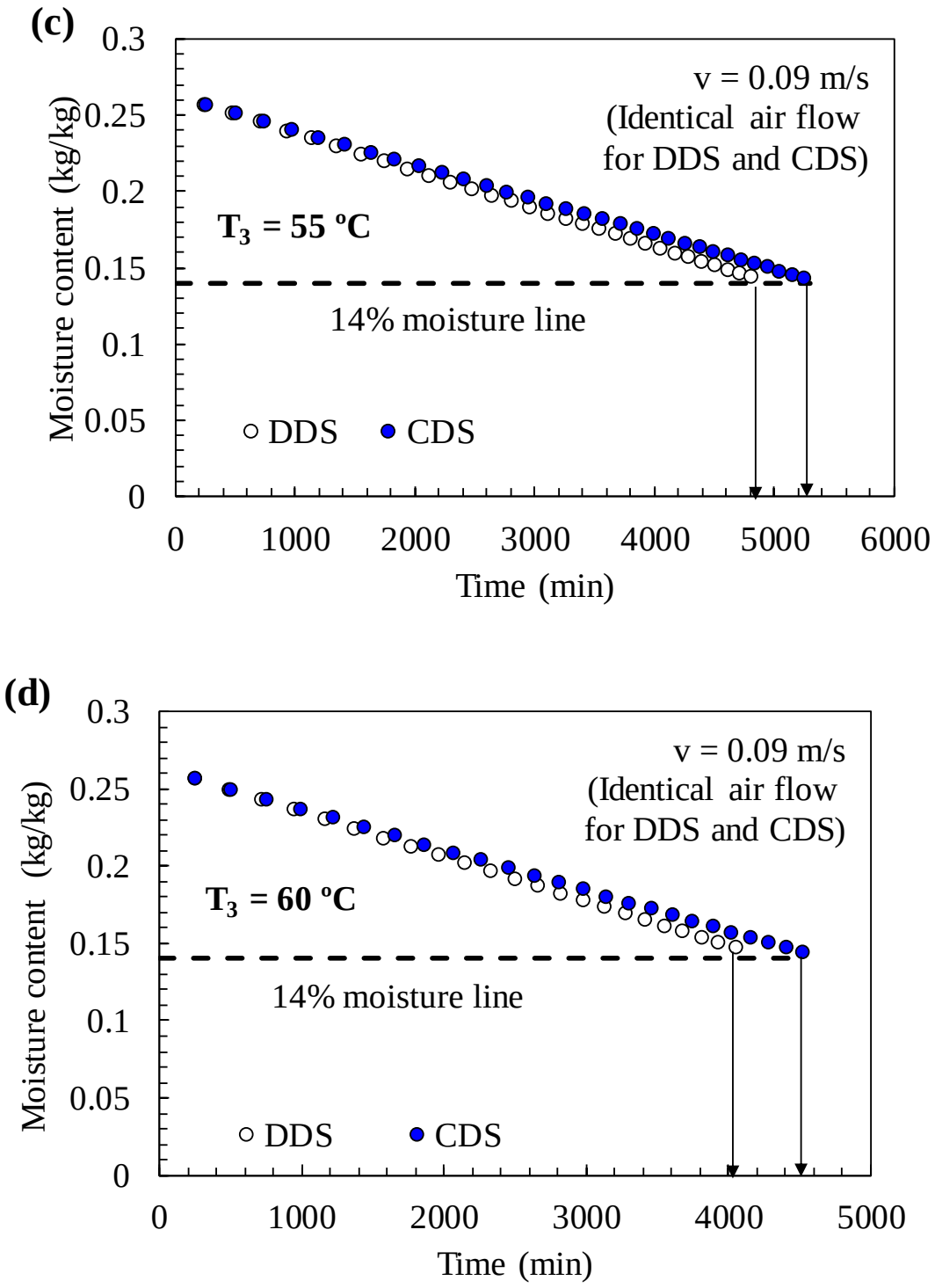


**Figure 4 5 (b)** Comparison of drying time between conventional (CDS) and desiccant (DDS) drying system in order to dry of wheat grains from 26% to 14% moisture contents at drying air temperature of: (a) 44 ºC, (b) 50 ºC, (c) 55 ºC and (d) 60 ºC.

Thermal and mechanical energy consumption per kilogram of dried grain is calculated for the moisture removal from 26% to 14% dry basis, as presented in Figure 4.6. Total energy is increasing with the increase in drying temperature for both systems. It is ranging from 0.46

MJ to 0.50 MJ/kg of grain for DDS, whereas, it is ranging from 0.46 MJ to 0.56 MJ/kg of grain in case of CDS. On the other hand, thermal energy consumed are (0.44, 0.46, 0.48 and 0.484) MJ/kg of grain for DDS and (0.46, 0.50, 0.53 and 0.55) MJ/kg of grain for CDS, at drying air temperature of (44, 50, 55 and 60) ºC, respectively. Conventional drying system consumed more thermal energy as compared to desiccant drying for all drying air temperature. Drying of grains at relatively higher ambient air humidity is the fact, which brings higher equilibrium moisture content for CDS method.

It ultimately decreases moisture removal rate due to high vapor pressure. Therefore, high drying air velocity is required to complete drying cycle within allowable storage time which results in more energy consumption. Specific energy consumption (SEC) required to remove the unit mass of moisture from the wheat grains at different drying conditions in estimated for desiccant and conventional drying systems as shown in Figure 4.7. It has been increasing with the increase in drying temperature and ranging from 4.86 MJ/kg to 5.25 MJ/kg in case of DDS and 4.88 MJ/kg to 5.84MJ/kg in case of CDS. The desiccant based drying method requires less energy consumption as compared to CDS at drying temperatures, and the results presented in Figure 4.7 are similar to the one obtained by Bazyma et al., (2006).

Consequently, coefficient of performance (COP) index is estimated by means of Eq. (20) and results are presented in Figure 4.8 for both drying methods.

The COP index decreases with the increase in drying temperature for both methods. However, it is ranging from 0.4498 to 0.4939 for desiccant drying, and 0.4044 to 0.4914 for conventional drying. Therefore, it has been concluded that the desiccant based drying system provides low-cost and energy-efficient drying at fast drying rate while employing low drying temperature which ensures the quality of the wheat grains.

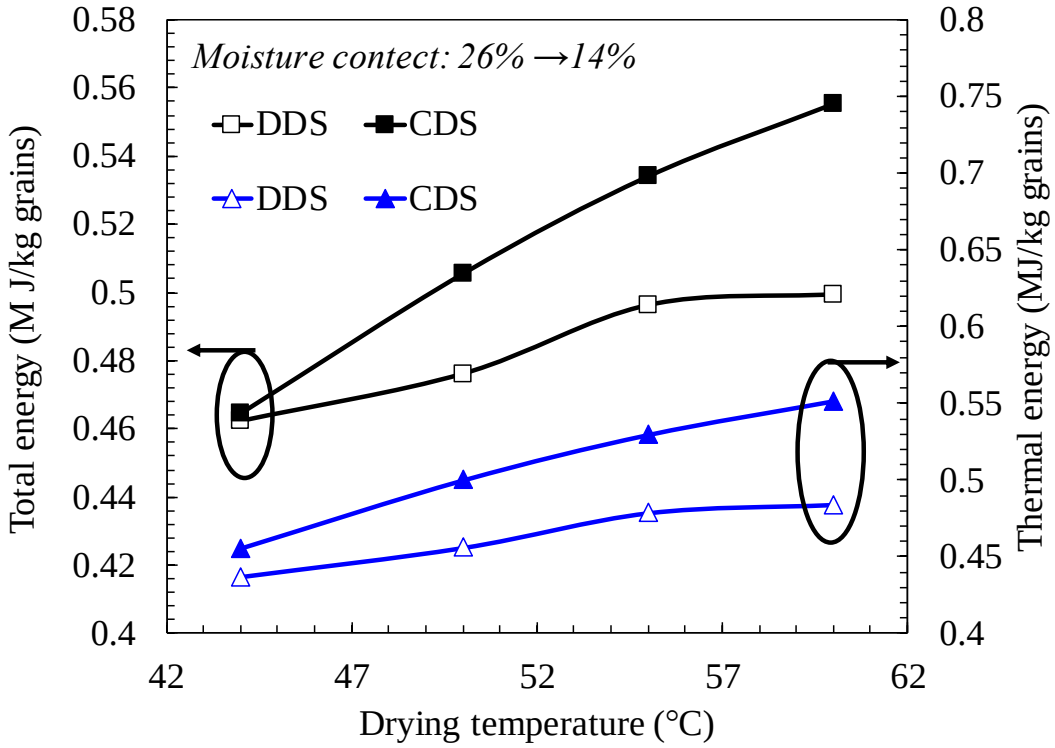


**Figure 4.6** Thermal and total energy consumption by DDS and CDS systems at different drying temperatures in order to dry the wheat grains from 26% to 14% moisture content.

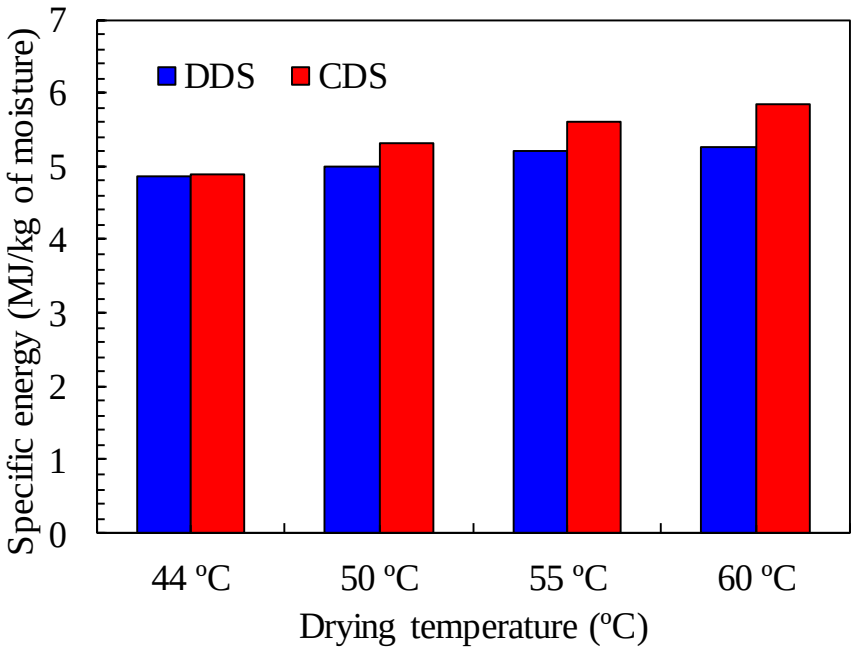


**Figure 4.7** Comparison of specific energy per kilograms of moisture required by desiccant and conventional drying methods.

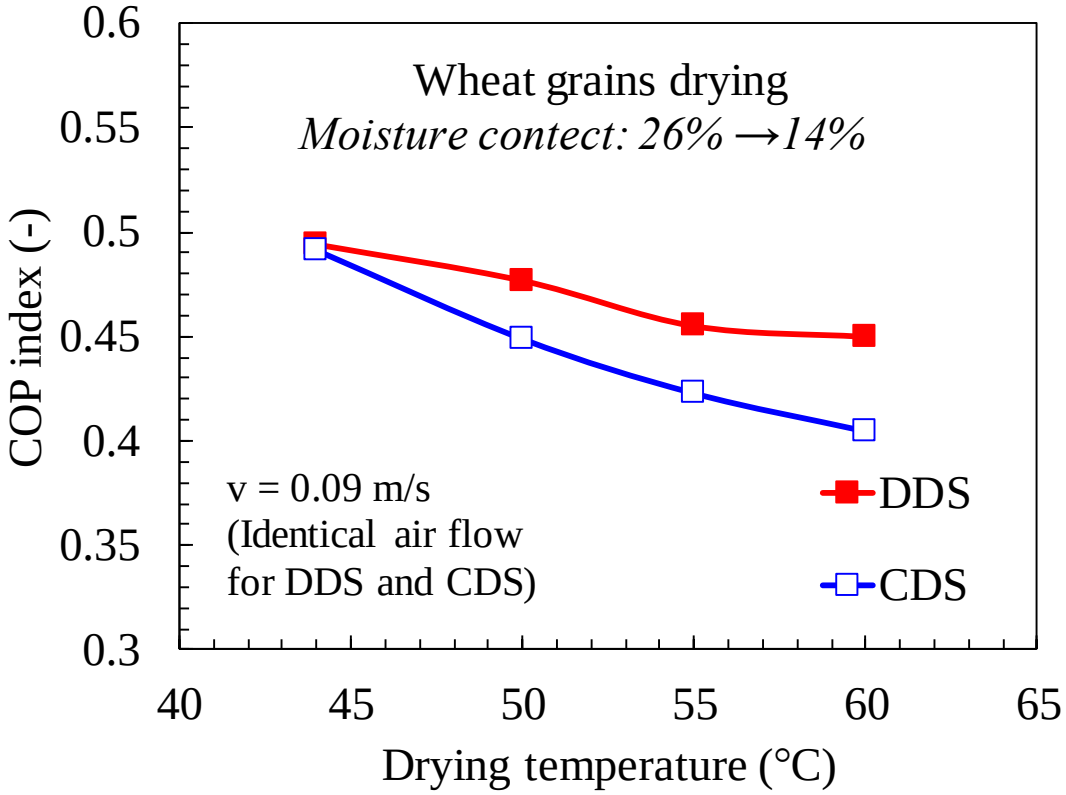


**Figure 4.8** Overall performance comparison between conventional and desiccant drying system for different operating drying temperatures.

## 4.5 Conclusions

The study investigates the solid desiccant based drying system for wheat drying application. Thermodynamic expressions are presented in detail with the aid of available literature for the performance evaluation of desiccant drying systems. Results are compared with the conventional drying techniques in order to see the applicability of desiccant drying system. Quick and low temperature drying is the main objective of today's drying industries that can be used for various applications including the wheat grains. In this regard, the desiccant can play a role due to their water sorption ability by means of vapor pressure deficit. The results of this study showed that the desiccant based drying process helps to provide low-temperature drying by which the quality of wheat grains can be assured. The study reports that the desiccant drying systems possess relatively higher drying rate as compared to conventional drying method. It could be useful not only for domestic drying applications but also for industrial applications. Upon comparison with conventional drying

methods, it has been found that the proposed drying system is not only useful for providing quick and low-temperature drying but also helps in overall energy saving. The performance index of desiccant drying system is found higher than the conventional system at drying temperatures. It has been concluded that the desiccant based drying systems can provide low-cost and energy-efficient drying for wheat grains; therefore, the study helps to design sustainable and economical drying systems for developing countries.

## 4.6 Nomenclature

| | |
|---|---|
| A | Area ($m^2$) |
| $A_p$ | Particle area ($m^2$) |
| CDS | Conventional drying system (-) |
| $C_p$ | Specific heat capacity (kJ $kg^{-1}K^{-1}$) |
| $C_1$,$C_2$,$C_3$ | Coefficient of equation (-) |
| DDS | Desiccant drying system (-) |
| $D_p$ | Particle diameter(m) |
| E | Energy (kJ) |
| h | Heat transfer coefficient (J $m^{-2}$ $s^{-1}$ $K^{-1}$) |
| $h_{fg}$ | Latent heat of vaporization (kJ $kg^{-1}$) |
| ka | Mass transfer coefficient (kg $m^{-2}$ $s^{-1}$) |
| k | Thermal conductivity (W $m^{-1}$ $K^{-1}$) |
| $M_e$ | Equilibrium moisture content (kg $kg^{-1}$) |
| M | Moisture content (kg $kg^{-1}$) |
| $m_w$ | weight of water (kg) |
| Nu | Nusselt number (-) |
| P | Pressure (Pa) |
| Pr | Prandlt number (-) |
| Re | Reynolds number (-) |
| RH | Relative humidity (%) |
| SEC | Specific energy consumption (kJ $kg^{-1}$) |
| T | Dry bulb temperature (ºC) |
| t | Time(min) |

| | |
|---|---|
| V | Volume of drying bin ($m^3$) |
| v | Air velocity ($m\ s^{-1}$) |
| W | Dry matter (kg) |
| $w_i$ | Grain weight (kg) |
| Y | Humidity ratio ($g\ kg^{-1}$ DA) |
| ε | Void fraction (-) |
| ρ | Density of air ($kg\ m^{-3}$) |
| μ | Viscosity ($N\ s\ m^{-2}$) |
| ***Subscripts*** | |
| (1)-(6) | Stated of air conditions expressed in Fig. 1 |
| i | Initial condition |
| f | Final condition |
| wb | Wet basis |
| db | Dry basis |
| s | Saturation |
| th | Thermal |
| mec | Mechanical |
| ma | Moist air |

## References

Abasi S, Minaei S, and Khoshtaghaza M. 2016. Performance of a recirculating dryer equipped with a desiccant wheel. Drying Technology 34(8): 863-870. doi:10.1080/07373937.2015.1021421.

Aghbashlo, Mortaza, Hossien Mobli, Shahin Rafiee, and Ashkan Madadlou. 2012. Energy and Exergy Analyses of the Spray Drying Process of Fish Oil Microencapsulation. Biosystems Engineering 111 (2). IAgrE: 229–41. doi:10.1016/j.biosystemseng.2011.12.001.

Antonellis Stefano De, Manuel Intini, Cesare Maria Joppolo, and Francesco Romano 2016. On the Control of Desiccant Wheels in Low Temperature Drying Processes.

International Journal of Refrigeration 70. Elsevier Ltd: 171–82. doi:10.1016/j.ijrefrig.2016.06.026.

Antonellis Stefano De, Cesare Maria Joppolo, Luca Molinaroli, and Alberto Pasini 2012. Simulation and Energy Efficiency Analysis of Desiccant Wheel Systems for Drying Processes. Energy 37 (1). Elsevier Ltd: 336–45. doi:10.1016/j.energy.2011.11.021.

Bazyma, Leonid A, Vladimir P Guskov, Andrew V Basteev, Alexander M Lyashenko, Valeriy Lyakhno, and Vladimir A Kutovoy (2006). The Investigation of Low Temperature Vacuum Drying Processes of Agricultural Materials. Journal of Food Engineering 74 (3): 410–15. doi:10.1016/j.jfoodeng.2005.03.030.

Bhise S R, A Kaur, and M R Manikantan (2014). Mositure Dependent Physical Properties of Wheat Grain (PBW 621). International Journal of Engineering Practical Research 3 (2): 3–8. doi:10.14355/ijepr.2014.0302.03.

Chramsa-ard, Wisut, Sirinuch Jindaruksa, Chatchai Sirisumpunwong, and Sorawit Sonsaree (2013). Performance Evaluation of the Desiccant Bed Solar Dryer. Energy Procedia 34. Elsevier B.V.: 189–97. doi:10.1016/j.egypro.2013.06.747.

Dina, Sari Farah, Himsar Ambarita, Farel H Napitupulu, and Hideki Kawai (2015). Study on Effectiveness of Continuous Solar Dryer Integrated with Desiccant Thermal Storage for Drying Cocoa Beans. Case Studies in Thermal Engineering 5. Elsevier: 32–40. doi:10.1016/j.csite.2014.11.003.

Erbay, Zafer, and Arif Hepbasli (2013). Advanced Exergy Analysis of a Heat Pump Drying System Used in Food Drying. Drying Technology 31 (7): 802–10. doi:10.1080/07373937.2012.763044.

Erdogan M, Graf S, Bau U, Lanzerath F, and Bardow A (2017). Simple two-step assessment of novel adsorbents for drying: The trade-off between adsorber size and drying time. Applied Thermal Engineering 125: 1075-1082. https://doi.org/10.1016/j.applthermaleng.2017.07.014

FAO Food and Agricultura Organization of the United Nations (2011). Grain Crop Drying , Handling and Storage. Rural Structures in the Tropics: Design and Development, 363–411.

Fraser B M (1980). Solargrain Drying in Canada: A Simulation Study. Canada. Can. Agric. Eng 22: 55–59. http://www.csbe-scgab.ca/docs/journal/22/22_1_55_ocr.pdf.

Gastón, Analía L, Rita M Abalone, and Sergio A Giner (2002). Wheat Drying Kinetics. Diffusivities for Sphere and Ellipsoid by Finite Elements. Journal of Food Engineering 52 (4): 313–22. doi:10.1016/S0260-8774(01)00121-2.

Mahmood M H, Sultan M, Miyazaki T, and Koyama S (2016). Desiccant air-conditioning system for storage of fruits and vegetables: Pakistan preview. Evergreen Joint Journal of Novel Carbon Resource Sciences and Green Asia Strategy 3(1):12-17.

Kang, Hyungmook, and Dae-Young Lee (2017). Experimental Investigation and Introduction of a Similarity Parameter for Characterizing the Heat and Mass Transfer in Polymer Desiccant Wheels. Energy 120. Elsevier Ltd: 705–17. doi:10.1016/j.energy.2016.11.122.

Kant K, Shukla A, Sharma A, Kumar A, and Jain A (2016). Thermal energy storage based solar drying systems: A review. Innovative Food Science & Emerging Technologies 34: 86-99. https://doi.org/10.1016/j.ifset.2016.01.007

Kozlowski, T. T. (1972). Insects, and Seed Collection, Storage, Testing, and Certification. Elsevier Science. 1972 PP: 435.

Marfil P HM, E M Santos and V R N Telis (2008). Ascorbic Acid Degradation Kinetics in Tomatoes at Different Drying Conditions. LWT - Food Science and Technology 41 (9): 1642–47. doi:10.1016/j.lwt.2007.11.003.

Mohapatra, Debabandya and P Srinivasa Rao (2005). A Thin Layer Drying Model of Parboiled Wheat. Journal of Food Engineering 66 (4): 513–18. doi:10.1016/j.jfoodeng.2004.04.023.

Molenda M, M D Montross, S G McNeill, and J Horabik (2005). Airflow Resistance of Seeds At Different Bulk Densities Using Ergun Equation. Transactions of the ASAE 48 (3): 1137–45. doi:10.13031/2013.18487.

Motevali Ali, Saeid Minaei, Ahmad Banakar, Barat Ghobadian, and Mohammad Hadi Khoshtaghaza (2014). Comparison of Energy Parameters in Various Dryers. Energy Conversion and Management 87. Elsevier Ltd: 711–25. doi:10.1016/j.enconman.2014.07.012.

Oberoi D P S and Sogi D S (2017). Moisture Sorption Characteristics of Dehydrated Watermelon (Citrullus lanatus Thunb) Pomace Wastes. Journal of Food Processing and Preservation, 41(2): 1-6. doi:10.1111/jfpp.12783

Sultan M, El-Sharkawy I I, Miyazaki T, Saha B B, and Koyama S (2015a). An overview of solid desiccant dehumidification and air conditioning systems. Renewable and Sustainable Energy Reviews 46: 16-29. https://doi.org/10.1016/j.rser.2015.02.038

Sultan M, El-Sharkawy I I, Miyazaki T, Saha B B, Koyama S, Maruyama T, Maeda S and Nakamura T (2015b). Insights of water vapor sorption onto polymer based sorbents. Adsorption 21(3): 205-215. https://doi.org/10.1007/s10450-015-9663-y

Sultan M, Miyazaki T, Saha B B, and Koyama S (2016a). Steady-state investigation of water vapor adsorption for thermally driven adsorption based greenhouse air-conditioning system. Renewable Energy 86: 785-795. https://doi.org/10.1016/j.renene.2015.09.015

Sultan M, El-Sharkawy I I, Miyazaki T, Saha B B, Koyama S, Maruyama T, Maeda S and Nakamura T (2016b). Water vapor sorption kinetics of polymer based sorbents: Theory and experiments. Applied Thermal Engineering 106: 192-202. https://doi.org/10.1016/j.applthermaleng.2016.05.192

Sultan M, Miyazaki T, Koyama S and Khan Z M (2017). Performance evaluation of hydrophilic organic polymer sorbents for desiccant air-conditioning applications. Adsorption Science & Technology 35(7):1-16. https://doi.org/10.1177/0263617417692338

Summers Claude M (1971). The Conversion of Energy. Scientific American 225 (3): 148–60. doi:10.1038/scientificamerican0971-148.

Sun B and Chakraborty A (2015). Thermodynamic frameworks of adsorption kinetics modeling: dynamic water uptakes on silica gel for adsorption cooling applications. Energy 84:296-302. https://doi.org/10.1016/j.energy.2015.02.101

Sun D W and Woods J L (1994). The selection of sorption isotherm equations for wheat based on the fitting of available data. Journal of Stored Products Research, 30(1): 27-43. https://doi.org/10.1016/0022-474X(94)90270-4

Torki-Harchegani, Mehdi, Davoud Ghanbarian, Abdollah Ghasemi Pirbalouti, and Morteza Sadeghi (2016). Dehydration Behaviour, Mathematical Modelling, Energy Efficiency and Essential Oil Yield of Peppermint Leaves Undergoing Microwave and Hot Air Treatments. Renewable and Sustainable Energy Reviews 58. Elsevier: 407–18. doi:10.1016/j.rser.2015.12.078.

Tsilingiris P T (2008). Thermophysical and Transport Properties of Humid Air at Temperature Range between 0 and 100 ºC. Energy Conversion and Management 49 (5): 1098–1110. doi:10.1016/j.enconman.2007.09.015.

Watts K C, W K Bilanski and D R Menzies (1987). Simulation of Adsorption Drying of Corn, Wheat, Barley and Oats Using Bentonite. Canadian Agricultural Engineering 29 (2): 173–78.

Whitaker Stephen (1972). Forced Convection Heat Transfer Correlations for Flow In Pipes, Past Flat Plates, Single. AIChE Journal 18 (2): 361–71. doi:10.1002/aic.690180219.

Whitesides Ralph E (1995). Home Storage of Wheat. All Archived Publications. Paper 638. 10 (June). http://digitalcommons.usu.edu/extension_histall/638.

Xia Z Z, Chen C J, Kiplagat J K, Wang R Z and Hu J Q (2008). Adsorption equilibrium of water on silica gel. Journal of Chemical & Engineering Data 53(10): 2462-2465. DOI: 10.1021/je800019u

Zhang L Z and J L Niu (2002). Performance Comparisons of Desiccant Wheels for Air Dehumidification and Enthalpy Recovery. Applied Thermal Engineering 22 (12): 1347–67.doi:10.1016/S1359-4311(02)00050-9.

CHAPTER 5

# EFFECT OF RELATIVE HUMIDITY ON THERMAL CONDUCTIVITY OF ZEOLITE BASED ADSORBENTS

# Chapter 5

# EFFECT OF RELATIVE HUMIDITY ON THERMAL CONDUCTIVITY OF ZEOLITE BASED ADSORBENTS

Effective thermal conductivity (ETC) of the adsorbent is an important parameter which influences the performance of the adsorption heat pump and adsorption cooling systems. Most of the adsorbents are porous in nature and therefore adsorption uptake is affected due to monolayer/multilayer configuration which results in different ETC at different operating conditions i.e. temperature and relative humidity (RH). Effect of temperature on ETC is somehow well-known in the literature; however, studies on RH effect are limited. Consequently, present study experimentally investigates the RH effect on the thermal conductivity of the commercially available zeolite-based adsorbents which are commercially named as: AQSOA-Z02 (zeolite-1) and AQSOA-Z05 (zeolite-2). The study is useful for the researcher who are working in the field of adsorption cooling, air-conditioning and desalination. In this regard, an experimental setup was developed by which the ETC was measured at different levels of RH. According to the results, the ETC of oven dried zeolite-1 and zeolite-2 was 0.060 W $m^{-1}$ $K^{-1}$ and 0.066 W $m^{-1}$ $K^{-1}$, respectively. With the increase in RH, the numerical value of ETC increases up to 0.090 W $m^{-1}$ $K^{-1}$ for zeolite-1 and 0.089 W $m^{-1}$ $K^{-1}$ zeolite-2. Moreover, the empirical relation is proposed which can estimate ETC at different levels of RH for both adsorbents. Dimensionless volumetric heat transfer coefficient for zeolite-1 varies from 7.86 to 7.91 whereas in case zeolite-2 it varies from 7.78 to 7.83.

## 5.1 Introduction

Adsorbent-adsorbate science and interactions have been extensively studies in last 2-3 decades in order to develop low-cost and sustainable thermally-driven adsorption cooling, air-conditioning and desalination systems. In this regard, thermal conductivity of the adsorbents is an important thermodynamic property by which the heat/mass transfer phenomena can be optimized (Sultan et al., 2017). Therefore, studies on effective thermal

conductivity (ETC) of adsorbents gradually seeks precedence (Zhu et al., 2017) as it is considered one of the important parameter to enhance the performance of the adsorption heat pump (AHP) and adsorption cooling systems (ACS) (Toe et al., 2017; Marlinda et al., 2010; Miyazaki et al., 2017). The importance of adsorption based systems is obvious due to energy shortage worldwide. In addition, increase in population and industrialization cause to increase the energy demand worldwide (Sultan et al., 2017) and its dependences on fossil fuels which results in environment hazardous emissions. Moreover, there is imbalance condition between demand and supply due to its speedy usage. To satisfy the demands of future for a sustainable environment, Kyoto protocol emphasis on utilization of renewable resources and precise use of heat energy i.e. re-use of exhaust and waste heat, storage of energy, etc (Aristov, 2007; Miyazaki et al., 2010). It emphasis the researchers worldwide to investigate the low-cost and energy-efficient cooling/air-conditioning systems which can be operated on waste heat. Consequently, studies have been reported on AHP (Umair et al., 2014), heat storage (Aristov, 2007), cooling and dehumidification systems (Sultan et al., 2018). From the prospective of development of optimum adsorption systems, it is important to establish/develop the appropriate adsorbent(s) whose thermal conductivity can be regulated according to the designed/designed heat and mass transfer. Therefore, the present study focuses the experimental evaluation of thermal conductivity at different relative humidity (RH) levels.

Recent studies on AHP and ACS make it possible to use the low temperature waste heat (Uyun et al., 2009). In addition, required characteristic of the adsorbent may be different under certain working range of AHP. Choice of the optimum absorbent as well as optimum designed working conditions are always essential in order to maximize the performance. It is usually desirable that the adsorbent adsorbs large amount of adsorbate for the small relative pressure range (Kakiuchi et al., 2009). Most of the studies available in the literature use the fixed value of ETC for the designing of AHP system. Whereas present work deal with the estimation of uptake effect on the effective thermal conductivity of adsorbent material at different relative humidity (Tong et al., 2009).

Thermal conductivity is one of the important characteristics of the absorbent material which describes its ability to transmit the heat. Absorbent materials having low thermal conductivity and low mass diffusivity are the main cause of reduction of the coefficient of performance (COP) and specific cooling power of the AHP and ACS system. Various

adsorbents have been developed to overcome such limitations which highlights its significance (De-Lang et al., 2015; Pal et al., 2017; El-Sharkawy et al., 2016). In addition, adsorption uptake of adsorbate onto adsorbents is usually determined by thermogravimetric technique (Sultan et al., 2016) This technique measures the change in adsorbed at controlled temperature and pressure without considering the thermal conductivity variation with respect to relative pressure.

There are numbers of techniques applied to measure the thermal conductivity of the material include a steady-state method, transient hot-wire method, laser flash diffusivity method, and transient plane (Pal et al., 2017; El-Sharkawy et al., 2016; Zhao et al., 2016). However, transient plane source method is based on simplicity and instant measurement of temperature. In present study, thermal conductivity has been experimentally measured using C-Therm TCi system (Pal et al., 2017; El-Sharkawy et al., 2016) which can also work on transient plane source method. According to the available literature, thermal conductivity of porous adsorbents show that ETC is not a constant quantity (Ould-Abbas et al., 2012; Rouhani and Bahrami, 2018; Rouhani et al., 2018). It depends on the interfacial contact between different constituent phases in a packed bed. In addition, due to coupling between fluid and solid particles ETC is considered as the function of porosity, pore structure of the media, water contents, saturation degree, phase change of water, and the temperature (Tong et al., 2009). In absorbent material, generally solid particles have higher thermal conductivity as compared to fluid (Calmidi and Mahajan, 1999). Heat transfer through the porous material in a packed bed is considered a combination of three mechanisms i.e. gas phase conductive and radioactive heat transfer, solid and gas phase conductive and radioactive heat transfer and within solid contact surface conductive heat transfer (Kunii and Smith, 1960).

In case of saturated adsorbents, all the pores are filled with fluid therefore, heat transfer is mainly due to conduction mechanism (Mendes et al., 2016). However, in some cases, convection and radiation type heat transfer may not be neglected. In addition, ETC depends on the solid and fluid property and porosity of the material; therefore, adsorbents from the same manufacturer could also result in a change in inherent material property (Mendes et al., 2016). Thermal conductivity becomes more sensitive when the porosity of materials reaches at saturation condition. It is because the porosity will be replaced by the adsorbate (Calmidi and Mahajan, 1999; Ye et al., 2015).

Effective thermal conductivity is an important transport property of the adsorbent material which has received incessant attention (Zhang et al., 2006). Many empirical and theoretical models have been presented to estimate the effective thermal conductivity for various materials. These models characterized by a single value and synchronous dependence of ETC on temperature, moisture and porosity are not considered in case of fully saturated or dry adsorbents (Tang et al., 2008). The operating conditions of adsorption-based open and close cycle cooling systems need to be optimized instantly in order to ensure the higher system COP. Consequently, the effect of a change in ETC due to change RH must be consider for the precise estimation of system COP. Its importance has been proven by many studies by means of sorption isotherm of adsorbent i.e. amount of moisture uptake is different at different RH or relative pressure (Pal et al., 2017; El-Sharkawy et al., 2016; Goldworthy, 2014). Similarly, the ETC of the adsorbents is supposed to be different at different RH or relative pressure.

The significance of this research is to determine the effect of relative humidity on the ETC of porous materials. Heat transfer mechanism through the porous material is very complex and the combination of conduction, convection, and radiation between fluid and solid phase. Increase in the porosity causes the decrease in effective thermal conductivity (Abuserwal et al., 2017). The knowledge of ETC is perquisite for the heat/mass transfer through the packed bed adsorbent. The objective of the present study is to measure the thermal conductivity of absorbents experimentally at different RH and compare the theoretical and modeled values of ETC. In addition, change in ETC is also determined at different moisture and uptake levels, consequently, empirical expressions are developed for the studies adsorbents.

## 5.2 Experimental section

### 5.2.1 Materials

In present study, two kinds of zeolite-based adsorbent are used which are commercially named as AQSOA-Z02 (zeolite-1) (Kakiuchi et al., 2005; Abuserwal et al., 2017; Shimooka et al., 2007; Intini et al., 2015) and AQSOA-Z05 (zeolite-2) (Goldworthy, 2014; Shimooka et al., 2007). These adsorbent materials can be regenerated at relatively low

temperatures as compared to those of conventional zeolites and silica gels (Wei-Benjamin-Teo et al., 2007). The main feature of these materials is an 'S' shaped water vapor adsorption isotherms that exhibits monolayer–multilayer adsorption stage at low partial pressure followed by micro pore filling at higher partial pressure (Shimooka et al., 2007). This leads to an extremely sharp increase in equilibrium moisture content over a narrow range of relative humidity as well as a much larger influence of temperature on the isotherm shape when plotted as a function of relative humidity. Zeolite-1 has structure type CHA and made of silico aluminophosphate gel with a pore size of 3.7 Å (Kakiuchi et al., 2009) and crystal density of 1.43 g m $L^{-1}$ (Structure Commission of the International Zeolite, 2017). Zeolite-2 has a AFI structure type and synthesized from aluminophosphate gel with a pore size of 7.4 Å (Shimooka et al., 2007) and crystal density of 1.75g m $L^{-1}$ determined from crystallographic structure (Abuserwal et al., 2017; Intini et al., 2015). In additions, key properties of adsorbents are given in Table 1 and scanning electron microscopy (SEM) images are shown in Figure 5.1.

**Table 5.1 Structural properties of adsorbent materials**

| Properties | Zeolite-1 | Zeolite-2 |
|---|---|---|
| Pore structure | 3-D * | 1-D * |
| Pore size [m] | $7.4\times10^{-10}$ (Kakiuchi et al., 2009) | $3.7\times10^{-10}$ (Shimooka et al., 2007) |
| Crystal density [kg $m^{-3}$] | 1430 * | 1750* |

*(Structure Commission of the International Zeolite, 2017)

### 5.2.2 Design and development of experimental setup

In the present study, an experimental setup has been developed to prepare an environment of various RH conditions. Consequently, thermal conductivities are measured by of C-Therm TCi system at different levels of RH. Figure 5.2 represents the schematic diagram of the experimental setup which consists of C-Therm TCi controller, C-Therm TCi sensor, control cell, evaporator, water circulators and sensors for temperature and relative humidity. C-Therm TCi sensor along with controller is used to measure the thermal conductivity of zeolite-1 and zeolite-2.

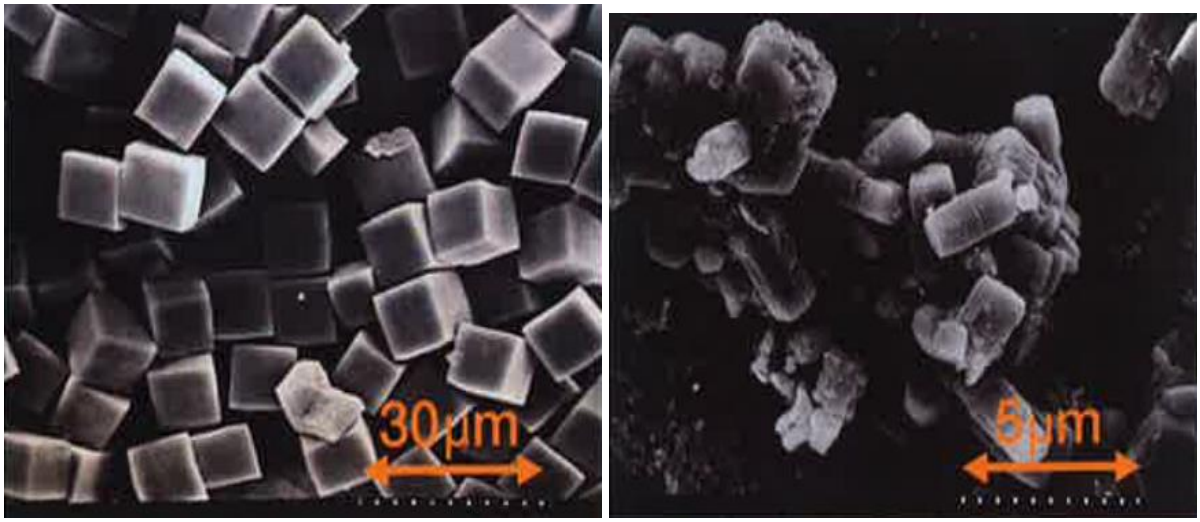


**Figure 5.1** SEM images: (a) Zeolite-1, (b) Zeolite-2 (MITSUBISHI PLASTICS).

In this system, control cells are used to develop the required experimental conditions with the help of evaporator and water circulator as explained in figure. A set of water evaporator with water circulator is used to control the humidity in the control cell whereas the temperature of the control cell is maintained by circulating the water. The temperature of the control cell is set at 25±0.1 ºC during the experiments. In the control cell, required RH is achieved by passing the 99.9% $N_2$ gas via evaporator. Two sensors are used to assure the development of required experimental conditions i.e. one for air passage and other for control cell. Hygroclip type sensor is used just before the entrance to control cell. The wireless type sensor is used to measure the RH and temperature inside the control cell with the accuracy of ±2% ±0.3%, respectively.

It is important to mention that the C-Therm TCi system uses the modified transient plane source technique which is founded the easiest method for accurately measuring the thermal conductivity within short duration of time (i.e. 0.8 sec) (Harris et al., 2014).

Figure 5.3 represents the C-Therm TCi system in which a constant amount of current is provided to central spiral shaped sensor that generates heat. The adsorbent absorbs some part of the generated heat itself and the remaining part is used to increase the temperature at the interface between sensor and sample.

Furthermore, spiral shape sensor is surrounded by a guard ring which also generates heat and makes the flow in one dimension.

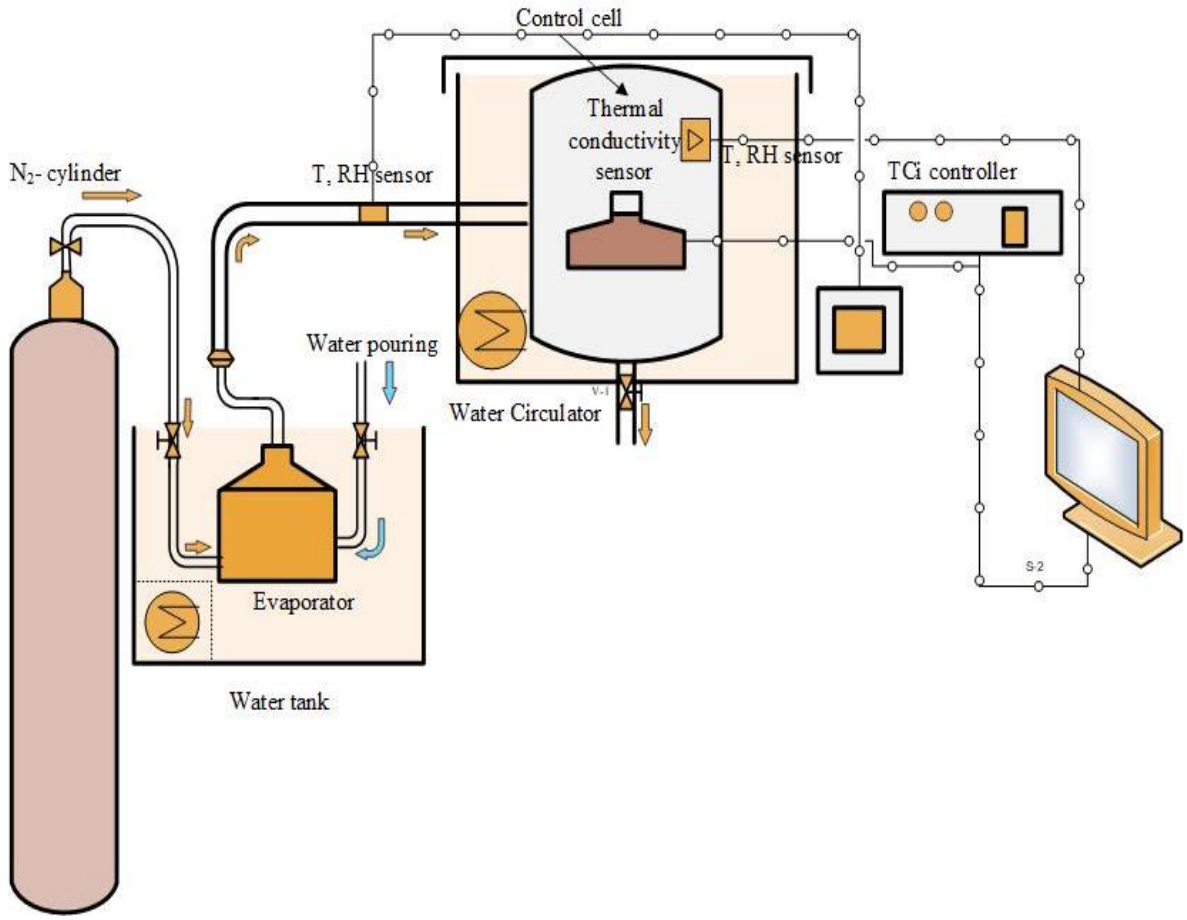


**Figure 5.2** Schematic diagram of thermal conductivity analyzer.

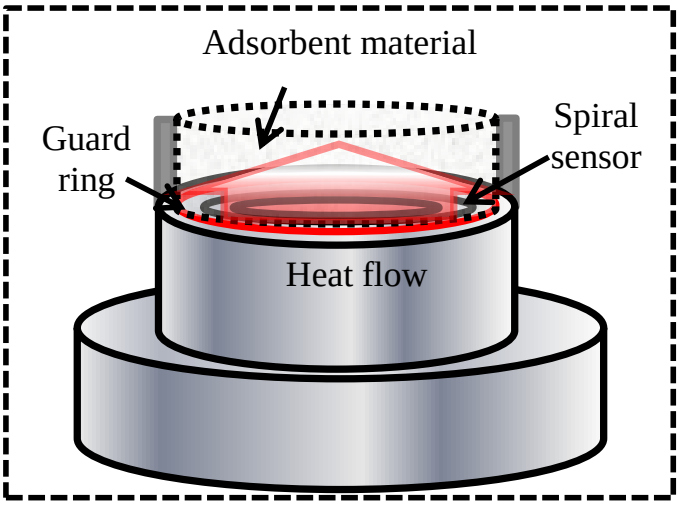


**Figure 5.3** C-Therm TCi sensor with sample material.

Eq. (5.1) describes the dynamics of temperature change and heat flow in one dimension (C-Therm technology, 2013) i.e.

$$\rho C_p \frac{\partial T}{\partial t} = k \frac{\partial^2 T}{\partial x^2} + G' \quad (5.1)$$

where $\rho$, $C_p$, $k$, $T$, $t$ *and* $x$ are the density [kg $m^{-3}$], specific heat capacity of sample material [kJ $kg^{-1}$ $K^{-1}$], thermal conductivity of the sample material [W $m^{-1}$ $K^{-1}$], temperature [K], time [s] and length flow parameter by heat [m], respectively. *G'* is the heat per unit volume [W $m^{-3}$]. The right-hand side of the quation represents the heat source *G'* and deviation of heat flux with respect to space through the medium. The left-hand side represents the change in temperature with time in the sample medium. The temperature change at the point of interface between sensor and sample material induce a resistance change of the sensor which results in a drop of voltage. Furthermore, voltage data is used for the estimation of effusively value and thermal conductivity of the adsorbent material.

## 5.3 Data reduction

Initially sample to be tested is dried in an oven for 24 hours at 80 ºC. Afterward sample is loaded on C-Therm TCi sensor via test cell which itself is attached with C-Therm TCi controller and computer. Control cell is made air tight and allowed the $N_2$ gas to pass through the control cell via evaporator according to the required experimental conditions. Once the required experimental conditions achieved, C-Therm TCi controller is turned on for reading. For each experimental conditions reading were taken at the intervals of 3hr for one day to make assure the development of equilibrium between the adsorbent sample and control cell. The average of the reading is used as ETC of material. According to the Fourier's law (Hua et al., 2018) heat applied to the adsorbent material is represented by Eq. (5.2)

$$Q = \frac{k_e A \Delta T}{L} \quad (5.2)$$

where $k_e$, $A$, and $L$ are the effective thermal conductivity [W $m^{-1}$ $K^{-1}$], contact area [$m^2$], temperature gradient and thickness of the adsorbent bed [m], respectively. Effective thermal conductivity of the porous material is a function of various parameters i.e.

$$k_e = f(k_s, k_g, E, T, D_p\ ) \quad (5.3a)$$

where $k_s$ and $k_g$ are the thermal conductivity of the solid particle and fluid, respectively. $E$ is the void fraction of packed adsorbent bed and $D_p$ is the average particle diameter. Model of Hayashi et al (Hayashi et al., 1987) is used to estimate the $k_s$ numerically. In this model solid particle of the adsorbent materials are considered as sphere and showed three types of heat transfer mechanisms as shown in Figure 5.4 i.e. (i) Conductive and radiative heat transfer in gas phase. (ii) Conductive and radiative heat transfer in gas and solid phase. (iii) Conductive heat transfer in connected solid particles.

$$k_e = \frac{1}{2}(3E-1)k_{g1} + \frac{\frac{3\beta\prime(1-E)(1-\delta)}{2\left(\phi+\frac{2\beta\lambda}{D_p}\right)}}{\frac{}{k_g}+\frac{(1-\phi)}{k_s}} + \frac{3}{2}(1-E)\delta k_s \quad (5.3b)$$

where $k_g$, $k_{g1}$, $k_s$, $\delta$, $\lambda$, $\beta'$ $D_p$ and $\phi$ are the thermal conductivity of fluid [W m $^{-1}$ K$^{-1}$], thermal conductivity of fluid in void space [W m $^{-1}$ K$^{-1}$], thermal conductivity of solid [W m $^{-1}$ K$^{-1}$], one contact point fractional area for heat flow, free path for fluid molecule [m], factor related to angle between the actual heat flow and parallel to the axis of solid particles (1.0 for loose packing, 0.9 for close packing), average particle diameter [m] and measure of the effective thickness of fluid between the solid particle [m], respectively. $\beta$ is calculated from (Hayashi et al., 1987) and its value found 0.7.

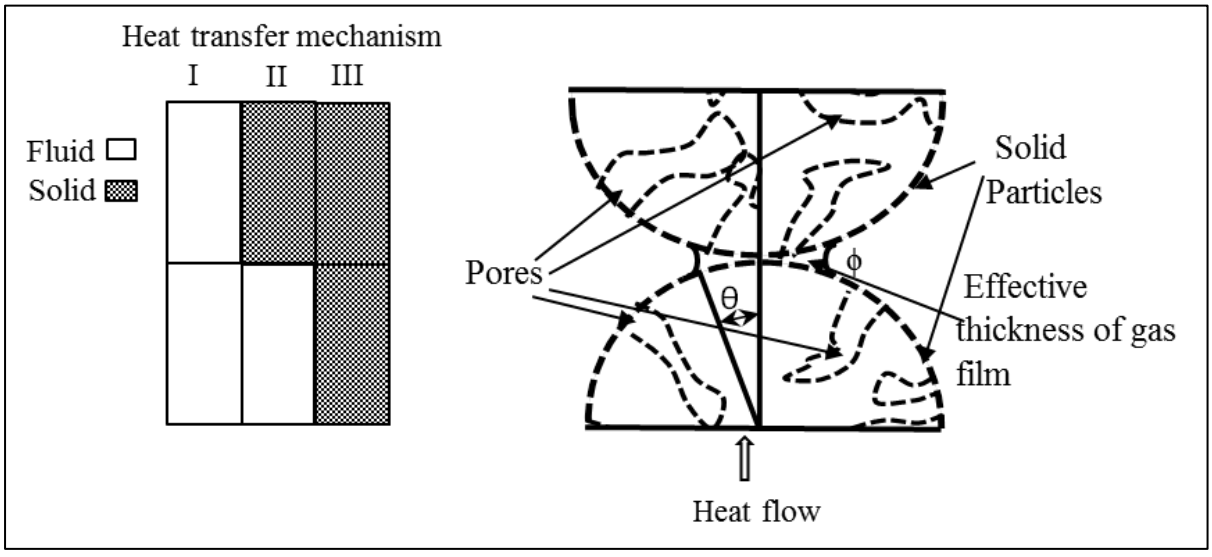


**Figure 5.4** Type of contact between two particles and heat transfer mechanism .

Thermal conductivity of fluid in voids is determined as (Hayashi et al., 1987).

$$k_{g1} = \frac{k_g}{1+\frac{2\beta\lambda}{D_e}} \tag{5.4}$$

where $D_e$ is the equivalent diameter for void space [m]. $\phi$ is calculated by using Equations. 5.5-5.8 simultaneously (Hayashi et al., 1987) as given by:

$$\phi = \phi_2 + \frac{(E-0.260)(\phi_1-\phi_2)}{0.476-0.260} \tag{5.5}$$

where $\phi_1$ and $\phi_2$ are the value of $\phi$ corresponding to the loose and close packing and calculated from Eq. (5.6) for angle corresponding to the boundary of heat flow area i.e. $\theta_1$= 90º and $\theta_2$= 41.15º.

$$\phi_{1,2} = \left(\frac{K^*}{K^*-1}\right)\left[\frac{0.5((K^*-1)sin\theta_{1,2}/K^*)^2}{\ln(K^*-(K^*-1)cos\theta_{1,2})-(K^*-1)(1-cos\theta_{1,2})/K^*} - \frac{1}{K^*}\right] \tag{5.6}$$

$$K^* = k_s/k_g^* \tag{5.7}$$

$$k_g^* = \frac{k_g}{1+(2\beta\lambda/\phi\ D_p)} \tag{5.8}$$

The value of $\phi$ was found 0.190 for zeolite-1and 0.183 for zeolite-2. Mean free path ( $\lambda$ ) is calculated by using Eq. (5.9) (Zhao and Shen, 2012).

$$\lambda = \frac{RT}{\sqrt{2}\pi d_a^2 N_A P} \tag{5.9}$$

where $R$, $N_A$, $P$ and $d_a$ are the universal gas constant [8.314510 J $K^{-1}$ $mole^{-1}$], Avogadro's number [6.0221367 × $10^{23}$ $mole^{-1}$], pressure [Pa] and pore size [m], respectively.

As adsorbent material's solid particles are itself porous in nature and cubical in shape in contrast of the model assumption, therefore, thermal conductivity of solid particle ($k_s$) also changes at different amount of moisture uptake at particular RH. So it is required to determine the change in thermal conductivity of solid particle ($k_s$) at different RH. Equation (5.10) is used to determine the thermal conductivity of the pore filling ($k_{pore}$).

$$k_s = \varepsilon\, k_{pore} + (1-\varepsilon)k_P \quad (5.10)$$

where $k_P$ is the thermal conductivity of particle and assumed 0.113 W $m^{-1}K^{-1}$ for both materials and porosity ($\varepsilon$) of zeolite-1is considered as 0.25 whereas in case of zeolite-2 it is 0.14 measured.

The increase in % ETC at different levels of RH was determined by using Equation (5.11)

$$\%\, ETC = \frac{k_{RH_i} - k_0}{k_0}.100 \quad (5.11)$$

Where $k_0$ is effective thermal conductivity of oven dry material (W $m^{-1}$ $K^{-1}$) and $k_{RH_i}$is the effective thermal conductivity of material at particular level of RH (W $m^{-1}$ $K^{-1}$).

Thermal conductivity of the desiccant material play important role in the performance of the desiccant dehumidification system. Increased in thermal conductivity of the material causes to increases the heat transfer and thermal diffusivity. On the contrary low thermal conductivity, suppress the overall performance. Many researches have been done to tackle the low heat transfer by introducing new materials or by using composite adsorbents (Wang et al., 2005).Temperature and relative humidity also causes to change in the effective thermal conductivity of the desiccant materials. Therefore change in thermal conductivity also affects the performance of the whole system. Equation (5.12) is used to measure the dimensionless heat transfer coefficient (Zhang and Huang, 2000) at different levels of RH.

$$H = \frac{8}{1+\frac{-2\ln(1-E)-2E-E^2}{\frac{k_s}{k_g}E^2}} \quad (5.12)$$

## 5.4 Results and discussion

The measured ETC of the adsorbent materials zeolite-1 and zeolite-2 are shown in Figure 5.5 at different RH at temperature 25 ºC. It is shown that by increasing the RH, ETC of the materials also increased. However increasing trend is different for both materials as they have different pore structure (Structure Commission of the International Zeolite, 2017). ETC value of the Zeolite-1 varies from 0.06 Wm-1K-1 to 0.09 Wm-1K-1 due to change in

RH from 0% to 100%, which is 50% increase from the initial value. Whereas in the case of Zeolite-2 it varies from 0.067 Wm-1K-1 to 0.089 Wm-1K-1 which is 35% increase from the initial value. The first values for each curve represented the ETC of the oven dry sample on thermal conductivity axis. Thereafter, RH increases correspondingly ETC also increases but follow a particular pattern for each material which has resemblance with adsorption uptake isotherm. In case of adsorbent material zeolite-1, ETC starts increasing from the beginning. The value of ETC increase very fast up to the range of RH 20%, however after this range increase in value is very small. Likewise adsorption isotherm of zeolite-1 at 25 ºC, maximum adsorbate uptake for a small range of relative pressure ratio (Shimooka et al., 2007).

Figure 5.6 represents some similar results in term of influence of the pressure on the thermal conductivity of the zeolite 13x reported in literature (Mori et al., 2000). Present study agrees well with the reported results in literature, the effect of pressure on the effective thermal conductivity of adsorbent material. In case of adsorbent material zeolite-2, no significant change observed in the start. However thereafter it start increasing and for a small range of RH which is due to isotherm type IV or V behavior (Sing, 1985) followed by zeolite-2. This lead to sharp increase in the amount of adsorbate uptake for a small range of RH changes (Goldworthy, 2014).

Figure 5.7 represents the ETC curves for both materials at different level of RH. It showed the discrepancy between the experimental data and empirical relation developed. Regression analysis has been performed to fit the appropriate empirical correlation to predict the ETC at different levels of RH. For both materials best fitted regression model found is sigmoidal with 4 parameters and represented by Eq. 5.13.

$$k_e = k_o + \frac{a\ RH^b}{c^b + RH^b} \quad (5.13)$$

where $k_e$ and $RH$ are the variables of equation and a, b, c are the coefficients of regression model and $k_o$ is the ETC of the oven dry material i.e. 0% RH.

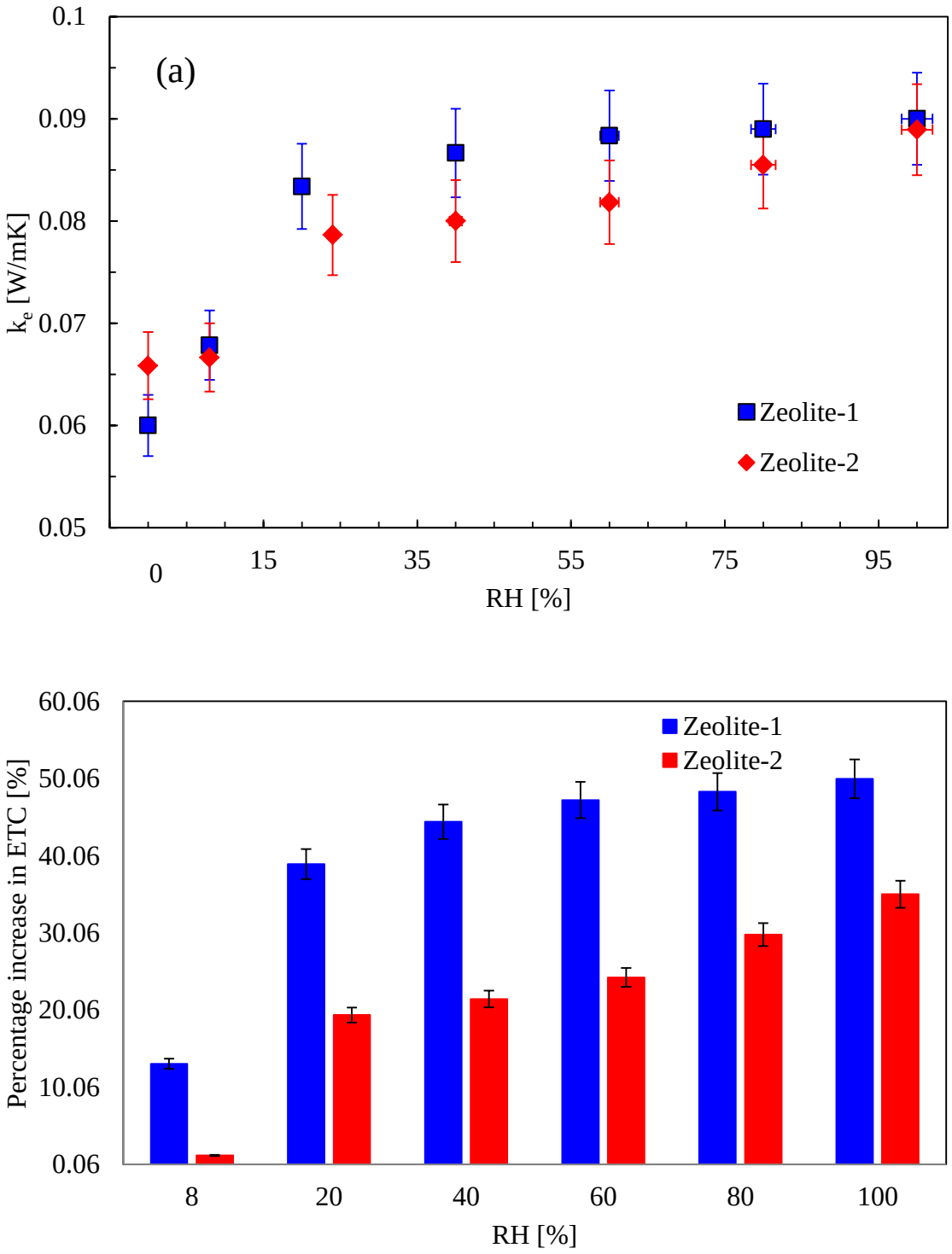


**Figure 5.5** (a) Experimental observed effective thermal conductivity of zeolite based adsorbent material at different levels of RH, (b) Percentage increase in ETC at different level of RH.

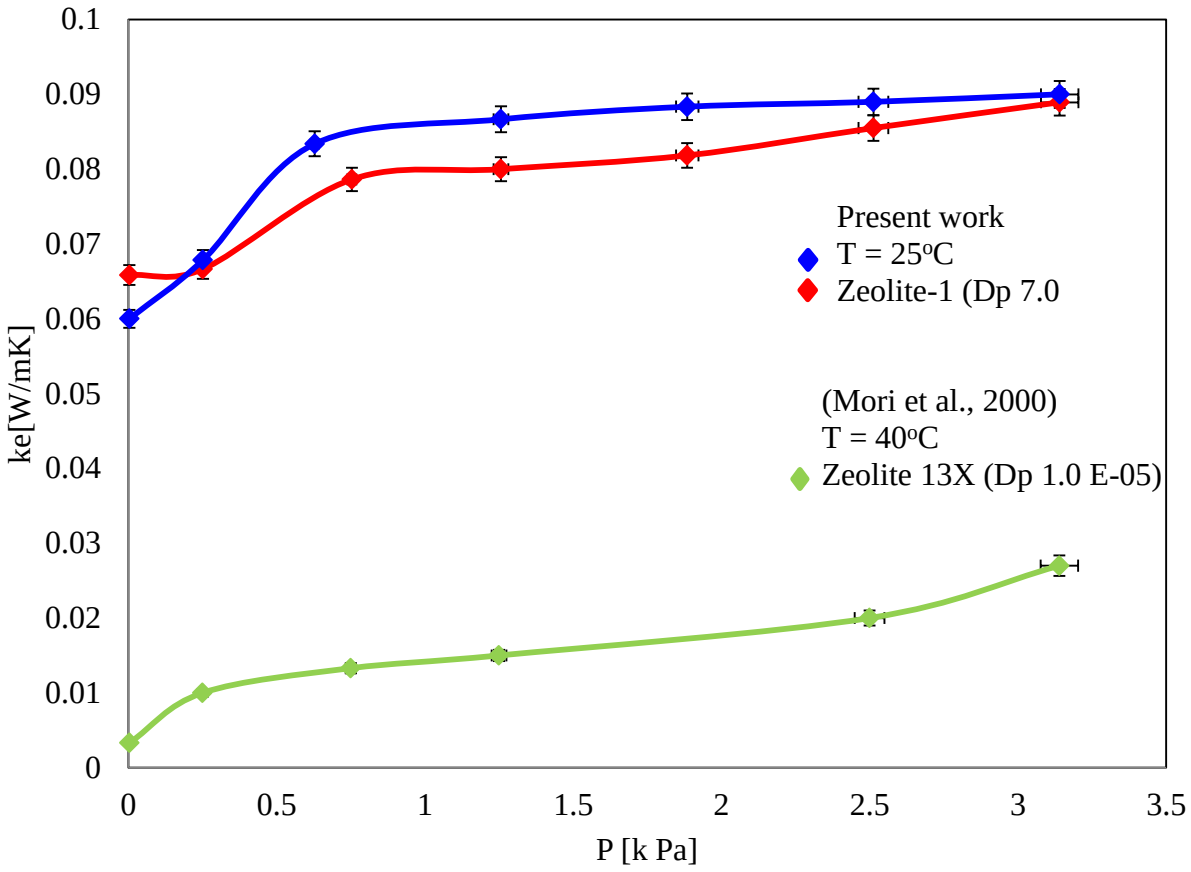


**Figure 5.6** Dependency of effective thermal conductivity on pressure.

The value of coefficients of regression and coefficient of determination ($R^2$) for both materials are given in the Table 5.2.

The reliability of the developed empirical relation is evaluated by comparing the experimental and predicted curves and standard error of estimate found were 0.000048 for both materials. The model fitted the results well as indicated by high values of $R^2$.

Figure 5.8 represents the change in ETC of zeolite-1 and zeolite-2 at different amount of moisture uptake. For the adsorption uptake data is taken from the literature (Shimooka et al., 2007) corresponding to the same level of RH. It showed that the value of ETC is increased cubically upward with the amount of uptake in the case of zeolite-1. Whereas in case of zeolite-2 it increased for a small range of moisture uptake thereafter showed some constant behavior. This behavior might be due to small porosity of zeolite-2 0.14 as compared to zeolite-1 which has 0.24.

**Table 5.2 Coefficient of determination ($R^2$) and Coefficients of regression model used in equation (5.11) for material zeolite-1 and zeolite-2**

| Material | Coefficient of determination ($R^2$) | Coefficient of regression | | | |
|---|---|---|---|---|---|
| | | $k^o$ | a | b | c |
| Zeolite-1 | 0.9990 | 0.0600 | 0.0282 | 2.7223 | 11.3036 |
| Zeolite-2 | 0.9952 | 0.0657 | 0.0156 | 3.7619 | 16.1460 |

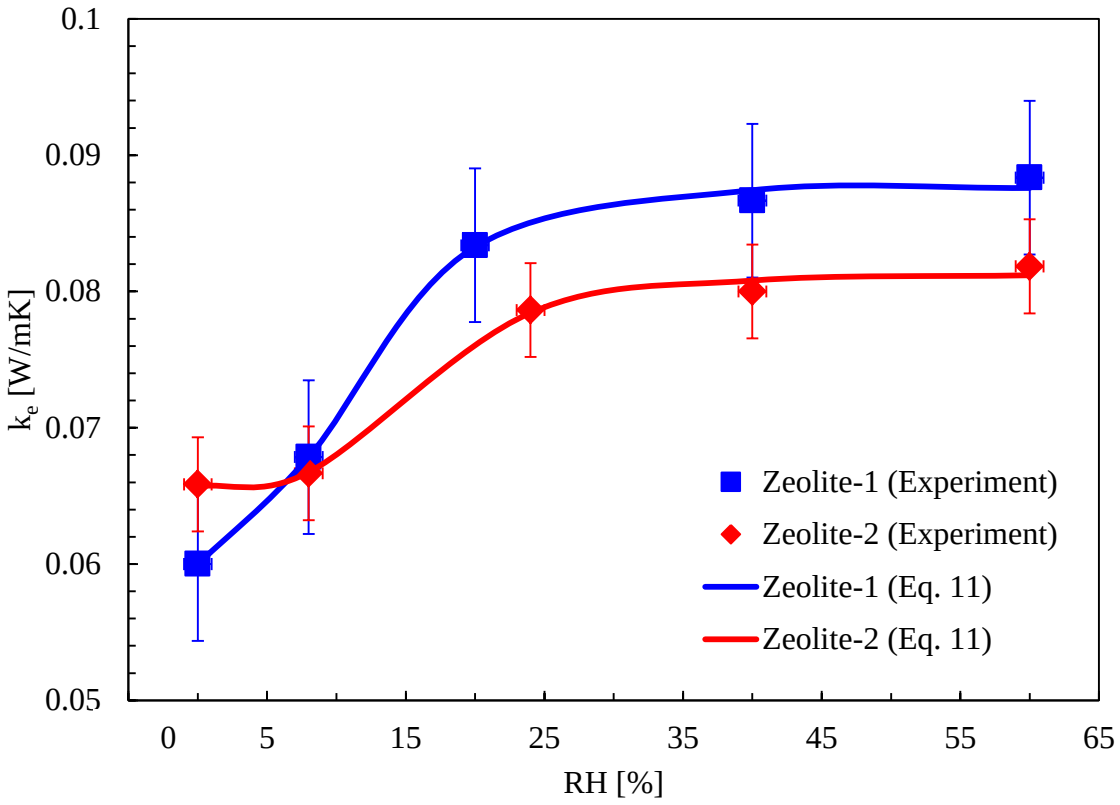


**Figure 5.7** Effect of relative humidity on the effective thermal conductivity of Zeolite-1 and Zeolite-2. Point represent the experimental data and line represent regression curves (i.e. 5.13)

Figure 5.9 showed the change in mean free path ( $\lambda$ ) by changing the RH on one axis and simultaneously changes in thermal conductivity of solid particle (ks) and pores (k pore)

on another axis. Mean free path is calculated from equation (10), whereas thermal conductivity of solid particle and pore filling is calculated by (Hayashi et al., 1987) and equation (10). Figure 5.9 represent that mean free path ( $\lambda$ ) decreases by increasing the RH and in the beginning decreasing trend is more prominent whereas later it reduced and followed constant line. The evidence of this decreasing trend is ascertained from the pore filling behavior of the both materials. Due to S shaped isotherm both materials exhibit monolayer adsorption at low partial pressure to multilayer adsorption at higher partial pressure (Sing, 1985).

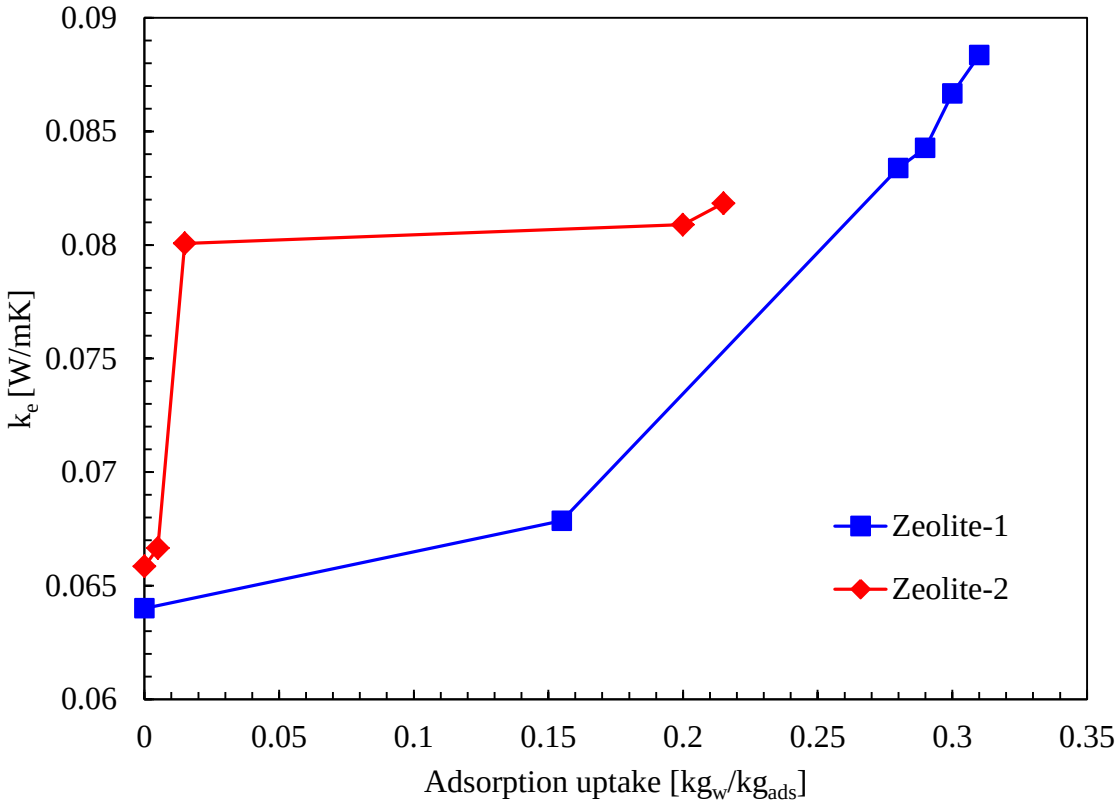


**Figure 5.8** Variation of ETC value with relation adsorption uptake.

In the case of adsorbent material zeolite-1 mean free path range from 27.75-2.22 µm at RH range 8-100%. Whereas in case of adsorbent material zeolite-2 it varies from 6.93-0.55 µm at RH range 8-100%. On the other hand inverse trend is observed in the change of thermal conductivity of pore (k pore) and thermal conductivity of solid particle ($k_s$). Thermal

conductivity of pores ($k_{pore}$) increases due to the phenomena of pores filling by adsorption as well as decrease in the mean free path by increase in RH.

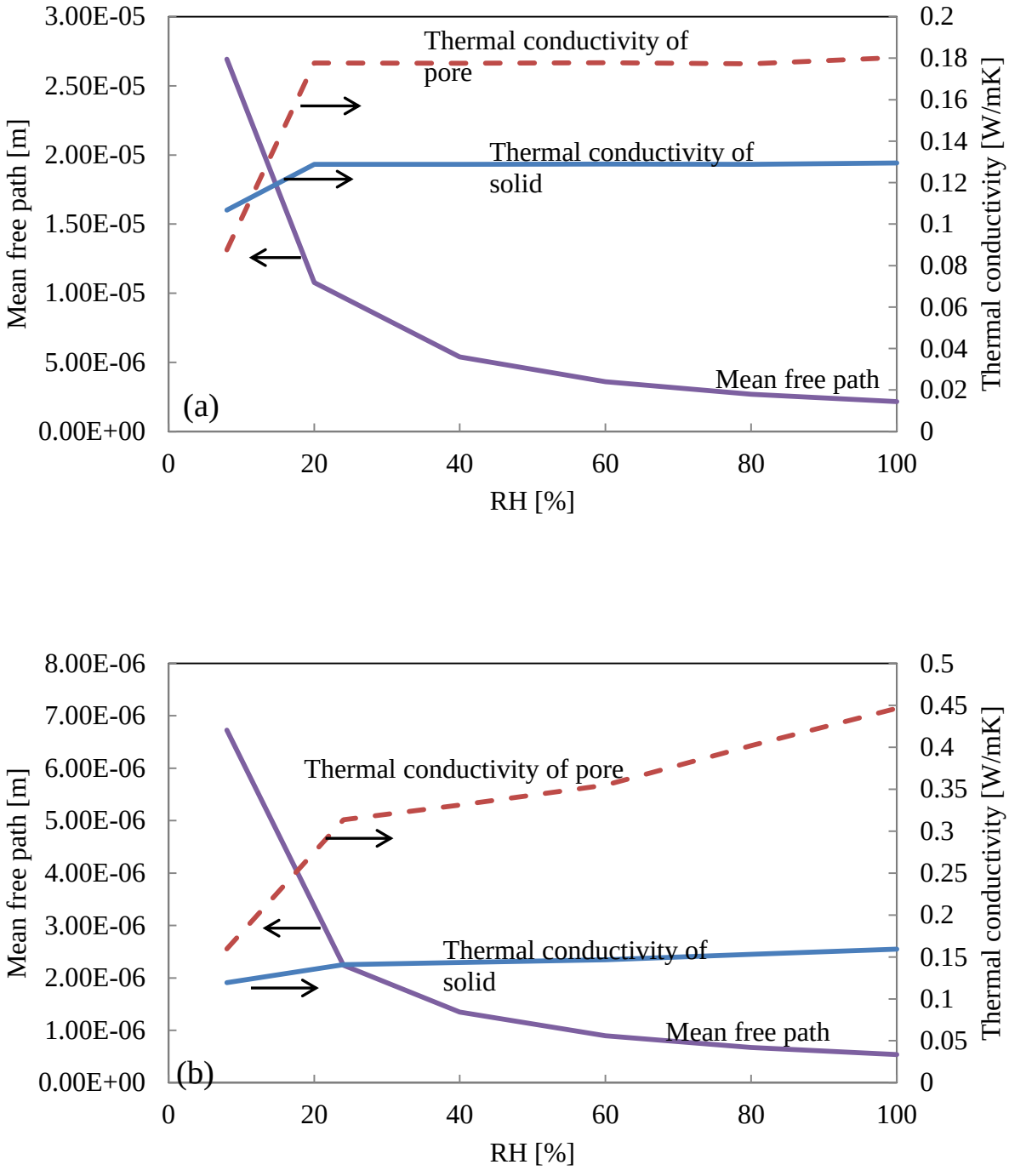


**Figure 5.9** Variation in mean free path, thermal conductivity of pores (k pore) and thermal conductivity of solid particle (ks): (a) Zeolite-1 (b) Zeolite-2.

This change in k pore persuades change in the thermal conductivity of solid particle ($k_s$). As in porous materials, solid particles itself have pores that's why thermal conductivity of the solid particle ($k_s$) also changes with the change in RH. In addition change in the thermal conductivity of the solids ($k_s$) and pore between the solids incorporate to change in the effective thermal conductivity of the packed bed.

Figure 5.10 represent the change in dimensionless volumetric heat transfer coefficient for both types of zeolite materials at different level of RH. In case of zeolite-1 its value varies from 7.86 to 7.91 whereas in case zeolite-2 it varies from 7.78 to 7.83.

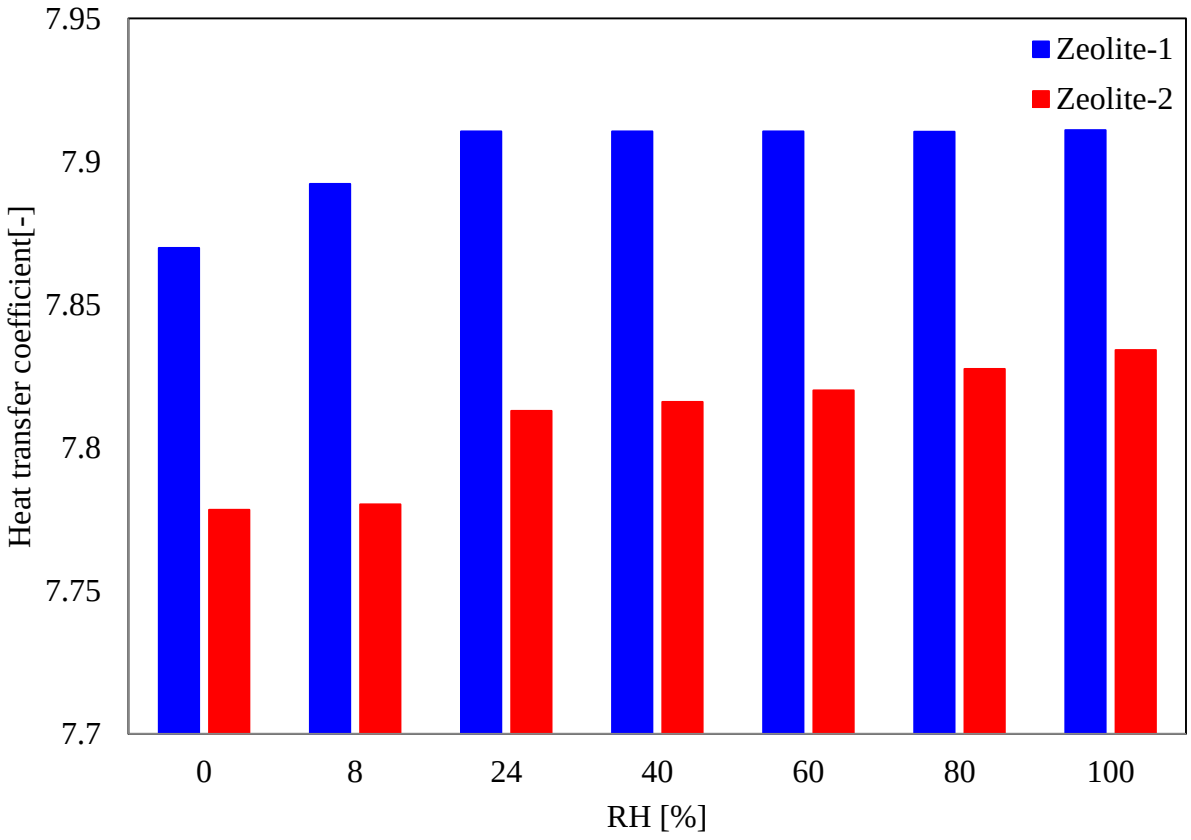


**Figure 5.10** Variation in heat transfer coefficient at different level of RH.

## 5.5 Conclusions

Present study experimentally investigates the effect of relative humidity (RH) on thermal conductivity of two kinds of zeolite-based adsorbents AQSOA-Z02 (zeolite-1) and AQSOA-Z05 (zeolite-2). In case of zeolite-1, effective thermal conductivity was found 0.060 W $m^{-1}$ $K^{-1}$ at over dried conditions (RH= 0%) which increases with the increase in RH and reaches up to 0.090 W $m^{-1}$ $K^{-1}$ at saturation conditions (RH= 100%). Similarly, the effective thermal conductivity of zeolite-2 is found 0.066 W $m^{-1}$ $K^{-1}$ at over dried conditions (RH= 0%) and increased up to 0.089 W $m^{-1}$ $K^{-1}$ at saturation conditions (RH= 100%). In addition, empirical relationships have been developed for both adsorbents in order to model the effective thermal conductivity at different RH levels. The developed empirical equations can successfully reproduce the numerical values of thermal conductivity at different levels of RH. Moreover, change in mean free path, thermal conductivity of solid particles and thermal conductivity of pores have been discussed in relation with change in RH. The porosity of the adsorbent material zeolite-1 and zeolite-2 was 0.25 and 0.14, respectively. Therefore, effective change in thermal conductivity trend of zeolite-2 has been resulted more complex as compared to the zeolite-1. In addition, the trend of effective thermal conductivity is quite resemblance with the adsorption uptake trend. Dimensionless volumetric heat transfer coefficient for both types of zeolite materials also changes with the change in RH. In case of zeolite-1 its value varies from 7.86 to 7.91 whereas in case zeolite-2 it varies from 7.78 to 7.83.

## 5.6 Nomenclature

| | |
|---|---|
| $C_p$ | Specific heat capacity [kJ kg $K^{-1}$] |
| $d_a$ | Pore size [m] |
| $D_p$ | Average particle diameter [m] |
| $D_e$ | Equivalent diameter for void space [m] |
| $E$ | Void fraction [-] |
| $G'$ | Heat source per unit volume [W $m^{-3}$] |
| $k$ | Thermal conductivity [W $m^{-1}$ $K^{-1}$] |
| $k_e$ | Effective thermal conductivity [W $m^{-1}$ $K^{-1}$] |
| $k_g$ | Thermal conductivity of fluid [W $m^{-1}$ $K^{-1}$] |

| | |
|---|---|
| $k_{g1}$ | Thermal conductivity of fluid in void space [W $m^{-1}$ $K^{-1}$] |
| $k_g^*$ | Thermal conductivity of fluid near solid–solid contact point [W $m^{-1}$ $K^{-1}$] |
| $k_p$ | Thermal conductivity of particle [W $m^{-1}$ $K^{-1}$] |
| $k_s$ | Thermal conductivity of solid [W $m^{-1}$ $K^{-1}$] |
| $K^*$ | Thermal conductivity ratio $k_s/k_{g*}$ [-] |
| $L$ | Thickness of bed [m] |
| $N_A$ | Avogadro's number [$6.0221367 \times 10^{23}$ $mole^{-1}$] |
| $Q$ | Heat flux [W] |
| $R$ | Universal gas constant [8.314510 J $K^{-1}mole^{-1}$] |
| $T$ | Dry bulb temperature [ºC] |
| $t$ | Time [s] |
| $\beta$ | Constant used in equation (3b) [0.7] |
| $\beta'$ | Constant used in equation (3b) [1.0 for loose packing, 0.9 for close packing] |
| $\delta$ | Fractional area corresponding to one contact point heat flow [] |
| $\lambda$ | Mean free path [m] |
| $\rho$ | Density [kg $m^{-3}$] |
| $\phi$ | Effective thickness of fluid between the solid particles [m] |
| $\phi_1$ | Value of $\phi$ corresponding to lose packing |
| $\phi_2$ | Value of $\phi$ corresponding to close packing |

## References

Sultan, M., Miyazaki, T., Koyama, S., & Khan, Z. M. Performance evaluation of hydrophilic organic polymer sorbents for desiccant air-conditioning applications. Adsorption Science & Technology, 2017, Vol. 36, No. 1-2; pp: 311-326. DOI: https://doi.org/10.1177/0263617417692338

Zhu, F.; Cui, S.; Gu, B. Fractal analysis for effective thermal conductivity of random fibrous porous materials. Phys. Lett. A, 2010, 374, 4411–4414. doi:10.1016/j.physleta.2010.08.075.

Teo, H. W. B.; Chakraborty, A.; Han, B. Water adsorption on CHA and AFI types zeolites: Modelling and investigation of adsorption chiller under static and dynamic conditions. Appl. Therm. Eng, 2017, 127, 35–45. doi:10.1016/j.applthermaleng. 2017, 08.014.

Marlinda; Uyun, A. S.; Miyazaki, T.; Ueda, Y.; Akisawa, A. Performance analysis of a double-effect adsorption refrigeration cycle with a silica gel/water working pair. Energies 2010, 3, 1704–1720. doi:10.3390/en3111704.

Miyazaki, T., Saha, B.B and Koyama, S. Analytical Model of a Combined Adsorption Cooling and Mechanical Vapor Compression Refrigeration System, Heat Transfer Engineering, 2017, 38 (4), 423–430. doi:10.1080/01457632.2016.1195135.

Aristov, Y. I. Novel Materials for Heat Pump and Storage: Screening and Nanotailoring of Sorption Properties. J. Chem. Eng. Japan, 2007, 40, 1242–1251.

Miyazaki, T., Akisawa, A & Saha, B.B.The Performance Analysis of a Novel Dual Evaporator Type Three-Bed Adsorption Chiller, International Journal of Refrigeration, 2010, 33 (2), 276–85. doi:10.1016/j.ijrefrig.2009.10.005.

Umair, M.; Akisawa, A.; Ueda, Y. Performance evaluation of a solar adsorption refrigeration system with a wing type compound parabolic concentrator. Energies 2014, 7, 1448–1466. doi:10.3390/en7031448.

Sultan, M.; Miyazaki, T.; Koyama, S. Optimization of adsorption isotherm types for desiccant air-conditioning applications. Renew. Energy, 2018, 121, 441–450. doi:10.1016/J.RENENE.2018.01.045.

Uyun, A. S.; Miyazaki, T.; Ueda, Y.; Akisawa, A. Experimental Investigation of a Three-Bed Adsorption Refrigeration Chiller Employing an Advanced Mass Recovery Cycle. Energies 2009, 2, 531–544. doi:10.3390/en20300531.

Kakiuchi, H.; Shimooka, S.; Iwade, M.; Oshima, K.; Yamazaki, M.; Terada, S.; Watanabe, H.; Takewaki, T. Water Vapor Adsorbent FAM-Z02 and Its Applicability to Adsorption Heat Pump. Kagaku Kogaku Ronbunshu 2005, 31, 273–277. doi:10.1252/kakoronbunshu.31.273.

Tong, F.; Jing, L.; Zimmerman, R. W. An effective thermal conductivity model of geological porous media for coupled thermo-hydro-mechanical systems with multiphase flow. Int. J. Rock Mech. Min. Sci. 2009, 46, 1358–1369. doi:10.1016/J.IJRMMS.2009.04.010.

De Lange, M. F.; Verouden, K. J. F. M.; Vlugt, T. J. H.; Gascon, J.; Kapteijn, F. Adsorption-Driven Heat Pumps: The Potential of Metal−Organic Frameworks. Chem. Rev. 2015, 115, 12205-12250. doi:10.1021/acs.chemrev.5b00059.

Pal, A., Thu, K., Mitra, S., El-Sharkawy, I.I., Saha, B.B., Kil, H.S., Yoon, S.H. and Miyawaki, J. Study on biomass derived activated carbons for adsorptive heat pump application. International Journal of Heat and Mass Transfer, 2017, 110, pp.7-19.

El-Sharkawy, I.I., Pal, A., Miyazaki, T., Saha, B.B. and Koyama, S. A study on consolidated composite adsorbents for cooling application. Applied Thermal Engineering, 2016, 98, pp.1214-1220.

Sultan, M., El-Sharkawy, I. I., Miyazaki, T., Saha, B. B., Koyama, S., Maruyama, T. & Nakamura, T. Water vapor sorption kinetics of polymer based sorbents: Theory and experiments. Applied Thermal Engineering, 2016, 106, 192-202.

Zhao, D.; Qian, X.; Gu, X.; Jajja, S. A.; Yang, R. Measurement Techniques for Thermal Conductivity and Interfacial Thermal Conductance of Bulk and Thin Film Materials. J. Electron. Packag. 2016, 138, 40802, doi:10.1115/1.4034605.

Ould-Abbas, A.; Bouchaour, M.; Chabane Sari, N.-E. Study of Thermal Conductivity of Porous Silicon Using the Micro-Raman Method. Open J. Phys. Chem. 2012, 2, 1–6, doi:10.4236/ojpc.2012.21001.

Rouhani, M.; Bahrami, M. Effective thermal conductivity of packed bed adsorbers: Part 2 Theoretical model. 2018, doi:10.1016/j.ijheatmasstransfer.2018.01.143.

Rouhani, M.; Huttema, W.; Bahrami, M. Effective thermal conductivity of packed bed adsorbers: Part 1 Experimental study. 2018, doi:10.1016/j.ijheatmasstransfer.2018.01.142.

Calmidi, V. V.; Mahajan, R. L. The Effective Thermal Conductivity of High Porosity Fibrous Metal Foams. J. Heat Transfer 1999, 121, 466, doi:10.1115/1.2826001.

Kunii, D.; Smith, J. M. Heat transfer characteristics of porous rocks. AIChE J. 1960, 6, 71–78, doi:10.1111/j.1365-2818.2010.03455.x.

Mendes, M. A. A.; Skibina, V.; Talukdar, P.; Wulf, R.; Gross, U.; Trimis, D.; Ray, S. Experimental validation of simplified conduction-radiation models for evaluation of Effective Thermal Conductivity of open-cell metal foams at high temperatures. Int. J. Heat Mass Transf. 2014, 78, 112–120. doi:10.1016/j.ijheatmasstransfer.2014.05.058.

Mendes, M. A. A.; Goetze, P.; Talukdar, P.; Werzner, E.; Demuth, C.; Rössger, P.; Wulf, R.; Gross, U.; Trimis, D.; Ray, S. Measurement and simplified numerical prediction of effective thermal conductivity of open-cell ceramic foams at high temperature. Int. J. Heat Mass Transf. 2016, 102, 396–406. doi:10.1016/J.IJHEATMASSTRANSFER.2016.06.022.

Ye, H.; Ma, M.; Ni, Q. An experimental study on mid-high temperature effective thermal conductivity of the closed-cell aluminum foam. Appl. Therm. Eng. 2015, 77, 127–133.doi:10.1016/j.applthermaleng.2014.12.029.

Zhang, H.-F.; Ge, X.-S.; Ye, H. Effective thermal conductivity of two-scale porous media Scaling laws for thermal conductivity of crystalline nanoporous silicon based on molecular dynamics simulations Effective thermal conductivity of two-scale porous media. Appl. Phys. Lett. 2006, 891, 81908–32905. doi:10.1063/1.2337274.

Tang, A.-M.; Cui, Y.-J.; Le, T.-T. A study on the thermal conductivity of compacted bentonites. Appl. Clay Sci. 2008, 41, 181–189. doi:10.1016/j.clay.2007.11.001.

Goldsworthy, M. J. Measurements of water vapour sorption isotherms for RD silica gel, AQSOA-Z01, AQSOA-Z02, AQSOA-Z05 and CECA zeolite 3A. Microporous Mesoporous Mater. 2014, 196, 59–67. doi:10.1016/j.micromeso.2014.04.046.

Wei Benjamin Teo, H.; Chakraborty, A.; Fan, W. Improved adsorption characteristics data for AQSOA types zeolites and water systems under static and dynamic conditions.

Microporous Mesoporous Mater. 2017, 242, 109–117, doi:10.1016/j.micromeso.2017.01.015.

Abuserwal, A. F.; Elizondo Luna, E. M.; Goodall, R.; Woolley, R. The effective thermal conductivity of open cell replicated aluminium metal sponges. Int. J. Heat Mass Transf. 2017, 108, 1439–1448. doi:10.1016/j.ijheatmasstransfer.2017.01.023.

Shimooka, S.; Oshima, K.; Hidaka, H.; Takewaki, T.; Kakiuchi, H.; Kodama, A.; Kubota, M.; Matsuda, H. The evaluation of direct cooling and heating desiccant device coated with FAM. J. Chem. Eng. Japan 2007, 40, 1330–1334. doi:10.1252/jcej.07WE193.

Intini, M.; Goldsworthy, M.; White, S.; Joppolo, C. M. Experimental analysis and numerical modelling of an AQSOA zeolite desiccant wheel. Appl. Therm. Eng. 2015, 80, 20–30. doi:10.1016/j.applthermaleng.2015.01.036.

Structure Commission of the International Zeolite Association-Database of Zeolite Structures Available online: http://www.iza-structure.org/databases/ (accessed on Dec 31, 2017).

MITSUBISHI PLASTICS, Zeolite, AQSOA, https://www.mpi.co.jp/english/products/industrial_materials/im010.html Google Scholar

Harris, A.; Kazachenko, S.; Bateman, R.; Nickerson, J.; Emanuel, M. Measuring the thermal conductivity of heat transfer fluids via the modified transient plane source (MTPS). J. Therm. Anal. Calorim. 2014, 116, 1309–1314. doi:10.1007/s10973-014-3811-6.

C-Therms Technologies Ltd. C therm TCi thermal conductivity User Manual; C-Therm Technologies Ltd. Canada., 2013

Hua, Y.-C.; Zhao, T.; Guo, Z.-Y. Irreversibility and Action of the Heat Conduction Process. Entropy 2018, 20, 206. doi:10.3390/e20030206.

Hayashi, S.; Kubota, K.; Masaki, H.; Shibata, Y.; Takahashi, K. A theoretical model for the estimation of the effective thermal conductivity of a packed bed of fine particles. Chem. Eng. J. 1987, 35, 51–60. doi:10.1016/0300-9467(87)80040-0.

Zhao, K.; Shen, A. Increasing ZnO Growth Rate by Modifying Oxygen Plasma Conditions in Plasma-Assisted Molecular Beam Epitaxy. World J. Condens. Matter Phys. 2012, 2, 160–164.

Wang, S.G., Wang, R.Z., Li, X.R., 2005. Research and development of consolidated adsorbent for adsorption systems, Renew. Energy 30 (9), 1425–1441.

Zhang, H.Y., and Huang, X.Y., 2000. Volumetric heat transfer coefficients in solid-fluid porous improvement with fluid flow. Int. J. of Heat and Mass Transfer, 43, 3417-3432.

Mori, H., Hamamoto, Y., and Yoshida, S., Effective thermal conductivity of adsorbent packed beds, Trans. Of the JSRAE, 17, 171-182. doi.org/10.11322/tjsrae.17.171

Sing, K. S. W. Reporting physisorption data for gas/solid systems with special reference to the determination of surface area and porosity (Recommendations 1984). Pure Appl. Chem. 1985, 57. doi:10.1351/pac198557040603.

CHAPTER 6

# CONCLUSIONS

# Chapter 6

# CONCLUSIONS

The main objective of the work presented in this thesis was to investigate the applicability of the desiccant drying system for the purpose of nutrient conservation and energy conservation by drying at low temperature. In this regards following work is carried out to cope the objectives and scope of the thesis

- Various factors and types of losses occur during drying and storage of agricultural produce is discussed in details especially drying air conditions i.e. Temperature and relative humidity. In addition complex structure of agricultural products and drying mechanism also explained.
- The motivation of desiccant drying system for agricultural product is ascertained from the drying chart developed for wheat, rice, corn and barley in relation with equilibrium moisture content (EMC) and temperature.
- A brief review about different drying technologies is made. Out of these freeze drying, microwave and vacuum drying technologies distinct by high energy and costs, thereby overall low efficiencies and sometime difficult to control the product temperature.
- Detail literature review about desiccant drying including rotor type, bed type and liquid desiccant type is made. In addition desiccant hybrid drying and aeration technologies are discussed to highlight the associated implication.
- A steady state investigation of desiccant drying system is made for agricultural applications especially for wheat, rice, barley and corn in order to find the optimum drying air conditions i.e. temperature and relative humidity for different crops.
- The effect of latent load control of drying air for the drying of wheat, rice corn and barley is determined.

- Combine effect of sensible and latent load control is also determined for the drying of agricultural products for commercial usage.
- Adsorption kinetics of desiccant drying for the drying of wheat is investigated.
- Comparison of desiccant drying and conventional hot air drying is made in term of allowable time for safe storage, total drying time and energy consumption.
- Effect of relative humidity on the effective thermal conductivity of the zeolite based desiccant materials is determined.
- Development of empirical relationship to predict the effective thermal conductivity of zeolite based desiccant materials at different relative humidity and constant temperature 25 $^{o}$C.
- Investigation of the variation of effective thermal conductivity value with relation to adsorption uptake.
- Determination of change in dimensionless volumetric heat transfer coefficient due to change in thermal conductivity by changing the relative humidity.

## 6.1 General conclusions

General conclusions from this thesis can be extracted as follows:

- Desiccant drying and aeration have been proposed for heat sensitive products. Usually, low temperature drying suffers from very low energy efficiencies but dehumidification of air by using adsorbents leads to a reduction in absolute humidity accompanied by the release of adsorption heat. The combined effect increases the capacity of the air to dry more efficiently without raising the temperatures. In addition hybrid drying system (integration of desiccant and other drying technologies) also gives better solution regarding the quality and quantity of drying product.
- Steady state desiccant drying for case I (drying at different regeneration temperature and correspondingly at different humidity ratio) showed that drying conditions are quite suitable for the drying of temperature sensitive products e.g. seed drying. It has been found that as the regeneration temperature increases from 50 ºC to 80ºC for both desiccant materials, Q also increases from 12.66-27.85kJ $s^{-1}$.

- Steady state desiccant drying for case II (drying at humidity ratio 0.010 kg $kg^{-1}$ and 0.008 kg $kg^{-1}$, drying air temperature 50 ºC to 60 ºC.) showed that it is feasible for commercial purpose drying as the drying air temperature is higher than the safe drying limit of temperature. It has been found that for desiccant material silica gel and LiCl, Q increases by increasing the drying air temperature from 13.65-17.7 kJ $s^{-1}$ for silica gel and 13.86-17.92 kJ $s^{-1}$for LiCl at humidity ratio 0.010kg/kgDA. Whereas for humidity ratio 0.008kg/kgDA, it varies from 16.72-20.77 kJ $s^{-1}$ for desiccant material silica gel and 17.50-21.55 kJ $s^{-1}$ for desiccant material LiCl.
- Adsorption kinetics of desiccant drying showed that the desiccant based drying process helps to provide relatively higher drying rate as compared to conventional drying and also provide low-temperature drying which assured the nutrient conservation too.
- It has been found that desiccant drying system is useful for domestic drying as well as industrial drying applications as it helps in overall energy saving as compared to conventional hot air drying system.
- The performance index of desiccant drying system is found higher than the conventional system at drying temperatures. It has been concluded that the desiccant based drying systems can provide low-cost and energy efficient drying.
- ETC value of the Zeolite-1 varies from 0.06 $Wm^{-1}K^{-1}$ to 0.09 $Wm^{-1}K^{-1}$ due to change in Rh from 0% to 100% RH, which is 50% increase from the initial value. Whereas in the case of Zeolite-2 it varies from 0.067 $Wm^{-1}K^{-1}$ to 0.089 $Wm^{-1}K^{-1}$ which is 35% increase from the initial value.
- The relation between the ETC and amount of uptake showed that the value of ETC is increased cubically upward with the amount of uptake in the case of zeolite-1. Whereas in case of zeolite-2 it increased for a small range of moisture uptake thereafter showed some constant behavior. This behavior might be due to small porosity of zeolite-2 0.14 as compared to zeolite-1 which has 0.24.
- Dimensionless volumetric heat transfer coefficient for both types of zeolite materials also changes with the change in RH.